FACULTY OF BIOSCIENCE ENGINEERING

CATALYTIC PYROLYSIS OF BIOMASS FOR THE PRODUCTION OF VALUABLE CHEMICALS

Number of words: 31.509

Thomas Detand
Student number: 01302737

Promotor: Prof. dr. ir. Frederik Ronsse
Tutor: M. Sc. Mehmet Pala

Master's Dissertation submitted to Ghent University in partial fulfilment of the requirements for the degree of Master of Science in Bioscience Engineering: Chemistry and Bioprocess Technology

Academic year: 2017 – 2018

GHENT UNIVERSITY

Ghent, June 8th, 2018

The promotor,

Prof. dr. ir. Frederik Ronsse

The tutor,

M. Sc. Mehmet Pala

The author,

Thomas Detand

Acknowledgements

While I'm writing this final part of my thesis, I start to realise that this is not only the end of my project I've worked on for almost a year, but also the end of my bioscience engineering studies. It makes me a little bit emotional to think about it. This is now the right moment to thank some people who stand close to me those last five years.

First of all I want to thank Prof. dr. ir. Frederik Ronsse. During his course of *Thermochemical conversion of biomass*, he woke up my interest in the field of fast pyrolysis. Whenever I had questions about my thesis, his door was always open to answer them. His insights, reasonable remarks and stimulating words made for sure my thesis better.

I'm also very thankful to my tutor, M.Sc. Mehmet Pala. We have stand a lot of time together in the lab but I never had the feeling that I must work for you. Maybe sometimes, my mood was below zero when the problems succeeded each other. You were also patient with my overload of questions or it doesn't matter for you if it was necessary to repeat some things to me. Your overviews of my thesis elevated for sure the quality of my thesis.

I also want to thank the members and the staff of the research unit Thermochemical Conversion of Biomass, and especially Stef, who were always willing to respond my questions or to help me in the lab whenever I had a problem.

Besides, I'm also very thankful to Jens, Lotte and Stein. When I was in my last year of high school, they convinced me to study bioscience engineering and I need to say now that I don't regret that choice. They also helped me a lot that summer with my herbarium so thanks for that!

For sure, I may not forget my parents. They also helped me with my study selection and they supported me during the exams. I'm also grateful for the sponsoring of my studies and to give me the chance to rent a student room in Ghent.

Finally also my friends I've met during my study career, I want to thank. I know for sure this isn't a goodbye after those five years but more a "see you next week!" or "when are we going to meet each other this month?" We could complain a lot of all our thesis troubles too each other and it felt good to share those with somebody.

Thomas Detand

Ghent, June 8th, 2018

Table of contents

List of abbreviations

Acronyms

AAEMs	Alkali and alkaline earth metals
aq. phase	Aqueous phase (bio-oil)
a.r.	As received basis
ASTM	American Society for Testing and Materials
BM/CAT	Biomass-to-catalyst ratio
CA	Citric acid
CFP	Catalytic fast pyrolysis
CO_x	$CO + CO_2$
d.b.	Dry basis
ESP	Electrostatic precipetator
FCC	Fluid catalytic cracking
GC/MS	Gas chromatography/mass spectrometry
HDO	Hydrodeoxygenation
HZSM-5	Acidic Zeolite Socony-Mobil 5
IH^2	Integrated hydropyrolysis and hydroconversion
IRR	Internal rate of return
KF	Karl Fischer (water content)
MAHs	Monoaromatic hydrocarbons
MP	Mini-plant
org. phase	Organic phase (bio-oil)
PAHs	Polyaromatic hydrocarbons
Py-GC/MS	Micropyrolysis-gas chromatography/mass spectrometry
SAR	SiO_2/Al_2O_3-ratio
SCB	Sugarcane bagasse
SCT	Sugarcane trash
WHSV	Weight hourly space velocity (h^{-1})

Symbols

ξ_o	Oxygen reduction
η_{ash}	Removed ash fraction after treatment
η_C	Carbon yield
η_{total}	Relative mass loss in pretreatment

Abstract

Catalytic fast pyrolysis with acidic zeolites enables the production of olefins (C_2-C_3) and aromatics from lignocellulosic biomass. However, there are some adverse properties linked to the use of acidic zeolite catalysts including the production of high amounts of CO_x (CO and CO_2) and water together with coke formation on the catalyst, resulting in its deactivation.

During this thesis, the influence of different biomass-to-catalyst ratios (BM/CAT) on catalytic fast pyrolysis process (CFP) is investigated by observing catalyst deactivation coupled with the evolution of the catalytic products. Bench-scale catalytic fast pyrolysis experiments with pine wood, and subsequently with model compound cellulose, were conducted in a continuously-fed fast pyrolysis system (with biomass feeding rate of 200 g/hour), enabling ex situ upgrading of pyrolysis vapours over a fixed-bed of catalyst (HZSM-5/Al_2O_3 extrudates, weight hourly space velocity (WHSV): 5 h^{-1}). Concerning the mass balances, when higher BM/CAT were applied, organic yields were increasing, while the yield of the gas, coke and water decreased. Over higher BM/CAT, less deoxygenation is observed, which was visualised in a oxygen content reduction (ξ_o) versus carbon yield (η_C) plot. Initially, a lot of aromatics are formed due to high catalyst activity but after deactivation, the product range changed more towards light oxygenates and anhydrosugars resembling non-catalytic pyroylsis oil composition. Physicochemically, The loss of activity could also be seen in a reduction of BET surface area, acidic capacity and pore volume. Cellulose had, compared to pine wood, a higher coking rate and a more narrow range of chemical functionality in the product bio-oil. Further analysis of the spent catalyst samples originating from cellulose catalytic fast pyrolysis needs to be conducted, to better understand the effects of catalyst deactivation.

As residues of agricultural industry, sugarcane trash (SCT) and sugarcane bagasse (SCB) are two low value biomass feedstocks that has the potential to be used for catalytic fast pyrolysis. Both feedstocks were subjected to non-catalytic and in-situ catalytic pyrolysis on analytical scale, making use of a micropyrolysis - gas chromatography/mass spectrometry (py-GC/MS) set-up. Due to the removal of the alkali and alkaline earth metals (AAEMs), there is a substantial increase of produced anhydrosugars together with (although for SCB) a decrease in light oxygenates during non-catalytic pyrolysis. Use of a catalyst resulted in more aromatics as was expected because of the low biomass-to-catalyst ratio employed. However, comparing catalytic pyrolysis of pretreated and untreated biomass, product composition was almost the same. This research must be extended with ex-situ experiments of SCB an SCT, just like similar experiments with levoglucosan.

Samenvatting

Katalytische snelle pyrolyse met zure zeolieten maakt het mogelijk om olefinen (C_2 – C_3) en aromaten te produceren uit biomassa. Echter zijn hier een paar nadelen aan verbonden: door de hoge deoxygenatiecapaciteit van dit type katalysator wordt er veel CO_x (CO en CO_2) en water gevormd. Dit gaat gepaard met de vorming van coke op de katalysator, wat uiteindelijk resulteert in zijn deactivatie.

Gedurende deze thesis is de invloed onderzocht van verschillende biomassa/katalysator-verhoudingen tijdens katalytische snelle pyrolyse door observatie van katalytische deactivatie gekoppeld met de evolutie van de door de katalysator beïnvloede reactieproducten. Katalytische snelle pyrolyse-experimenten werden uitgevoerd in een piloot-installatie. Eerst werd dennenhout gebruikt als biomassa, en vervolgens cellulose. In de installatie wordt snelle pyrolyse uitgevoerd in een continu gevoed systeem, aan een snelheid van van 200 g per uur. De pyrolysedampen worden ex situ geüpgraded over een vaste hoeveelheid katalysator (HZSM-5/Al_2O_3 extrudaten, WHSV: 5 h^{-1}). Wanneer hogere BM/CAT werden toegepast, steeg de opbrengst aan organische stoffen, terwijl de opbrengst aan gas, *coke* en water daalde. Met hogere ratio's wordt er minder deoxygenatie waargenomen, dewelke was gevisualiseerd in een plot van koolstofopbrengst t.o.v. zuurstofinhoudreductie. Initieel worden er veel aromaten gevormd door een hoge katalysator-activiteit maar wanneer er na bepaalde tijd deactivatie optreedt, verandert de productstroom meer naar lichte geoxygneerde verbindingen en anhydrosuikers. Zo lijkt de bio-olie (het vloeistofproduct van snelle pyrolyse) steeds meer op een niet-gekatalyseerde vloeistof. Fysicochemisch kan het verlies aan katalytische activiteit gezien worden in een reductie van BET-oppervlak, zure capaciteit en porievolume. Cellulose had ten opzichte van dennenhout een hogere *coke* vormingssnelheid en een nauwer spectrum aan gedetecteerde componenten. Analyses van de gebruikte en (deels) gedeactiveerde katalysatorstalen van cellulose moet in de toekomst nog worden uitgvoerd, om de effecten van deactivatie beter te begrijpen.

Suikerrietstro en suikerriet bagasse zijn twee laagwaardige bronnen van biomassa die het potentieel hebben om gevaloriseerd te worden in katalytische snelle pyrolyse. Beide grondstoffen werden zowel katalytisch als zonder katalysator gepyrolyseerd op analytische schaal, gebruik makende van een micropyrolyse eenheid gekoppeld aan een GC/MS apparaat. Door de verwijdering van alkali- en aardalkalimetalen is er een verhoogde productie aan anhydrosuikers gekoppeld met een afname (althans voor SCB) van de geoxygeneerde verbindingen tijdens niet-katalytische pyrolyse. Gebruik van een katalysator resulteert in meer aromaten zoals verwacht aangezien een lage biomassa/katalysator-verhouding werd gebruikt. Echter, productdistributie was echter niet sterk gewijzigd, indien onbehandelde en behandelde biomassa met elkaar worden vergeleken, in aanwezigheid van een katalysator. Dit onderzoek moet nog worden aangevuld met ex-situ experimenten van SCB en SCT, evenals gelijkaardige experimenten met levoglucosan.

1. Introduction

The finite supply of fossil fuels keeps on diminishing and within a certain time, they will not meet the demand of the continuously expanding world population. Consequently, changing towards sustainable energy alternatives is a booming business for the last decades. Solar and wind energy and hydropower are excellent natural resources. Nevertheless, those are rather dependent of meteorological or geographical conditions and it is hard to store that energy [1]. Biomass, on the other hand, can be utilised for heat, electricity, chemical and fuel production without the intermittency issue observed fro wind and solar energy. It comprises the biodegradable fraction of unvalorised agricultural residues (e.g. straw and bagasse), green waste, industrial waste (e.g. sawdust and black liquor), manure or wastewater treatment sludge. Those examples demonstrate its enormous diversity, which makes processing steps to convert it challenging. The use of those materials as resource has some advantages. Biomass is a renewable material interesting to use because its high availability and CO_2 neutrality [2].

The easiest way to obtain energy out of biomass, is to burn it. Other energy-rich products are obtained after a conversion technique. Biomass can be converted in either a biological or thermochemical way. Often, a physical pretreatment step like drying, milling or compressing is necessary to put it into a desired form. Fermentation and anaerobic digestion belong to biological processing, yielding e.g. biogas or short chain alcohols [1]. Whereas this process is rather slow (time span of days), thermochemical conversion can occur in a few seconds. Due to the rapid heating, the raw material is immediately converted into the desired product. When adjusting the temperature and vapour residence time, and in an environment with very little amounts of (or even without) oxygen, different pyrolysis processes can be distinguished. Fast pyrolysis is such a thermochemical process where biomass in an oxygen-free environment is transformed into mainly a liquid fraction (till 75 wt.%), but also a fraction of char and gas is formed. Char and gas production are favoured in respectively slow pyrolysis and gasification. The formed bio-oil in fast pyrolysis contains too much oxygen to be competitive with the petrochemical based fuels and chemicals. Catalysts could help here to selectively remove oxygen in the form of CO, CO_2 and H_2O. It is shown that deoxygenation could raise the yield of hydrocarbons like aromatics [2, 3].

The outline of this thesis is summarised in the next paragraphs. In the second chapter, principles of fast pyrolysis will be explained. First of all, an overview of the different pyrolysis reactors, applications and upgrading techniques are given in this literature review. Secondly, the catalytic fast pyrolysis process is explained with special attention on catalyst deactivation. After this study, the objectives for this thesis are explained in the third chapter. Chapter 4 describes the used installations and equipment during the experimental phase of this thesis.

The research and discussion part can be found in chapter 5, which consists of two main parts. In a first phase, deactivation of the catalyst is studied over different biomass-to-catalyst ratios. This series of experiments is conducted in the mini-plant installation of the Green Chemistry & Technology Department of the Ghent University. Pine wood and cellulose are pyrolysed in the reactor in order to obtain a high and qualitative liquid (yield). Analysis of the reaction products (gas, aqueous and organic phase of the liquid, char and catalyst) are done to get better insight in the occurring trends and mechanisms during deactivation.

Secondly, catalytic experiments were done in the micropyrolyser unit of this faculty. This device is coupled to a gas chromatograph and a mass spectrometer. Vapours formed during pyrolysis are immediately identified and integrated. In this experimental set-up, sugarcane bagasse and trash were used as feedstock. The effect of an acid pretreatment and the use of a catalyst are researched. In this set-up, sugarcane residues are mixed with catalyst in the sample cup (in-situ catalytic fast pyrolysis). Detected components are compared and some trends are observed and explained.

In chapter 6, most important results are summarised in this conclusion part. Chapter 7 comprises some current trends in the research of fast pyrolysis, which whether or not show some potential. This was supplemented with some own simple calculations to confirm or to reject these findings.

2. Literature review

2.1 Structure of biomass

Lignocellulosic biomass mainly consists of three fractions: cellulose, hemicellulose and lignin, supplemented with water, minerals and extractives. The share of each biopolymer is about 25 - 50, 15 - 40, and 10 - 40 wt.% respectively [4]. Cellulose $(C_6H_{10}H_5)_n$ is the most abundant biopolymer present. This typically crystalline homopolysaccharide consists of D-glucose units, linked with a β-1,4-glycosidic bond and it is mostly situated in the cell wall of the plant. Hemicellulose does not have such a defined structure. It consists of different hexoses (D-glucose, D-mannose, D-galactose…) and pentoses (D-xylose, L-arabinose…). Its average chemical formula is $(C_5H_{10}H_5)_n$ and this amorphous material is closely associated with cellulose in the cell wall, as well with lignin in the middle lamella. Lignin comprises a complex structure of aromatic compounds with a relatively low amount of oxygen in comparison with the two polysaccharides. Basically, three monomers, linked with alkyl and ether bonds make up the lignin structure. Those aromatic building blocks are coniferyl-, sinapyl- and coumaryl alcohol. Due to the large variability in the structure, it is not straightforward to process lignocellulosic biomass [1, 5].

To understand the thermochemical decomposition profile of these biopolymers, thermogravimetric studies have been conducted. When using a thermo-gravimetric analyser (TGA), the mass loss of a sample is determined while gradually heating. First, moisture must be removed (105 °C) and afterwards the sample is heated to a temperature far above the pyrolysis temperature, with a typical increase of 10 °C/min. This results in a graph giving the temperature and the corresponding mass percentage of the sample [1]. Such a degradation pattern is demonstrated in figure 1.

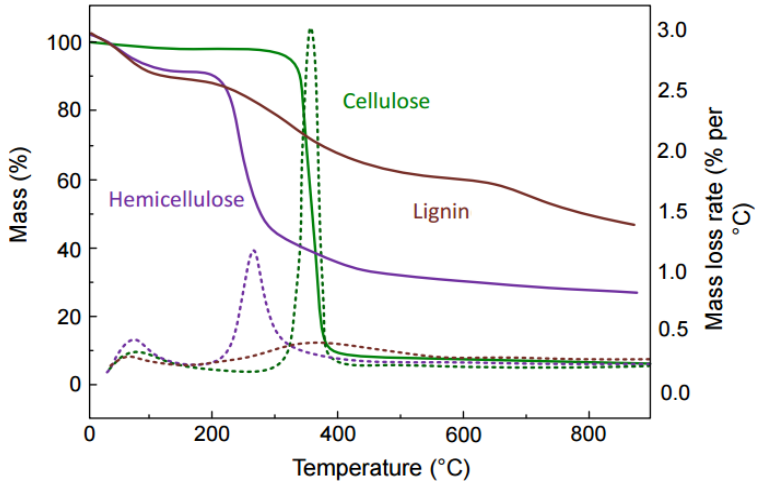

Figure 1: TGA of the cellulose, hemicellulose and lignin. The full lines are the TG (thermogravimetric) curves and correspond with the left axis, showing the residual mass percentages of all fractions at a certain temperature. The dotted lines give the DTG (derivative thermogravimetric) curves and correspond with the right axis, showing the mass loss rate (in % per °C) for each constituent [1].

Figure 1 illustrates that hemicellulose first decomposes at temperatures around 220 °C. When the largest amount of hemicellulose is already pyrolysed, the cellulose matrix starts to break up around 315 °C. Lignin does not give a sharp peak, meaning that the aromatic structure slowly dissociates over a wide temperature range [1, 4].

Several reaction models have been proposed for the degradation of cellulose. One of them assumes that in a first step, cellulose is converted to an active intermediate form, after which a depolymerisation and fragmentation step may occur [6]. The first reaction mainly forms anhydrosugars

like 1,6-anhydro-β-D-glucopyranose or levoglucosan. The latter reaction is a ring scission which mainly leads to acetol and hydroxyacetaldehyde [7 - 9].

2.2 Fast pyrolysis

2.2.1 Principles of fast pyrolysis

The conversion method used throughout this thesis, is fast pyrolysis. It is a thermal decomposition reaction of the feedstock material into a solid, liquid and gaseous phase. The solid fraction comprises char, while the liquid fraction, also called bio-oil or pyrolysis oil, is the collection of condensable compounds after cooling the hot vapours. The third fraction consists of those gases which do not condense. With fast pyrolysis, the aim is to maximise the production of the liquid from biomass, to yields up to 75 *wt*.%, as postulated by Bridgwater [10]. Fast pyrolysis is executed in the absence of oxygen, at atmospheric pressure and moderate temperatures of around 500 °C, within a very short reaction time of only a few seconds. Several requirements must be followed to obtain as much as possible liquid i.e. high heating (transfer) rates, short vapour residence times (1 – 2 sec.) and feed-stocks with small particle sizes (< 3 mm). Fast pyrolysis reactors are designed in such a way they fulfill these criteria [10, 11].

Figure 2 shows the different steps for the pyrolysis of wood. In a primary phase, decomposition of the macrobiopolymers within the biomass particles takes place resulting in char and vapours. Part of the primary vapours will 'condense' into the final bio-oil, but another fraction of the vapours can undergo additional cracking to non-condensable gases, heavy tars and/or char. The aim of fast pyrolysis is to maximise the quantity and optimise the quality of the pyrolysis oil [11].

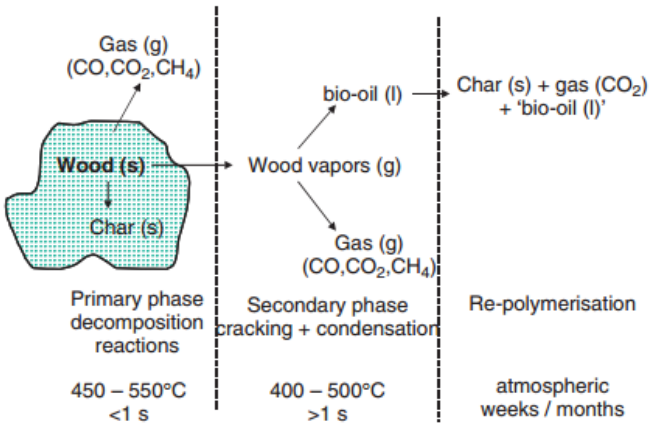

Figure 2: representation of the reaction paths for wood pyrolysis [11].

The type of feedstock is one of the most influencing parameters concerning the bio-oil yield. From an ecological and economical point of view, it is more interesting to use waste streams having (till now) no further use in already existing applications. Other conditions that may influence the amount of liquid are temperature, residence time of biomass and vapours, and pretreatment of the feedstock. With wood as used biomass, observed oil yields range from 55 to 70 wt.% (on dry-feed basis) [11]. Some articles report higher yields but those are rather exceptional and could only be produced in lab scale. Theoretically the share of the solid and gaseous phases account for 12 and 13 wt.% respectively. In practice, those values are higher because it is not always feasible to meet the required process conditions for fast pyrolysis. Mohan et al. (2006) stated that the yields of char and non-condensable gases are reported to be around 15 - 25 wt.% and 10 - 20 wt.%, respectively [12].

2.2.2 Fast pyrolysis reactor technology: state of the art

The reactor where fast pyrolysis is carried out is of utmost importance. Innovative technologies or adjustments to already existing techniques have been designed and implemented on small lab scale. On this scale, oil yields can be maximised because it is easier to reach all the requirements of fast pyrolysis. When operating on a bigger scale, it is not always feasible to achieve the required short vapour residence times, and this can unavoidably lead to secondary cracking [11]. About thirty years ago, the first steps were taken into research and development in the field of fast pyrolysis. Pilot plants were build, but a lot of them have been stopped and decommissioned nowadays. The most important reasons for their termination were legislative limitations and low efficiencies and yields that were obtained, so that the fast pyrolysis process could not compete to produce drop-in fuels or as a source of biochemicals. Table 1 gives an overview of the most important reactor technologies to perform fast pyrolysis.

Table 1: sketches and some characteristics of the most important reactor types. For each type, the industrial installation with the highest capacity is mentioned [10].

Ablative reactor [10, 11]	
- pressed biomass onto a hot rotating surface - heated by hot flue gas, obtained in two ways: combustion pyrolysis gases and/or produced char - small oil layer sticks on surface and vapourises, functions also as lubricant - heat transfer without inert gas, upscaling difficult due to surface heating - max. size industrial set-up: 250 kg/h (PyTec, Germany), not in use nowadays	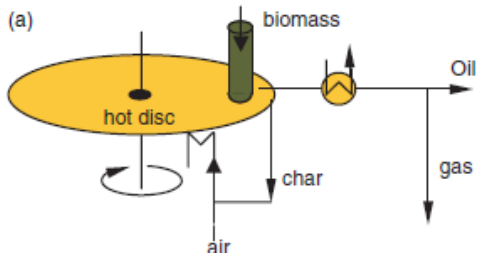
Bubbling fluid bed [10, 11, 13 - 15]	
- formed char is entrained with fluidising gas and separated with a cyclone - efficient heat transfer between sand and biomass - solid bed material can consist of sand, catalyst and char, not transported out of the reactor - heating: combustion pyrolysis gases or heating coils - residence times controlled by the fluidising gas - fine char in oil can lead to stability issues or sold as such: BioOil Plus - max. size industrial set-up: 8000 kg/h (Dynamotive, Canada), not in use nowadays	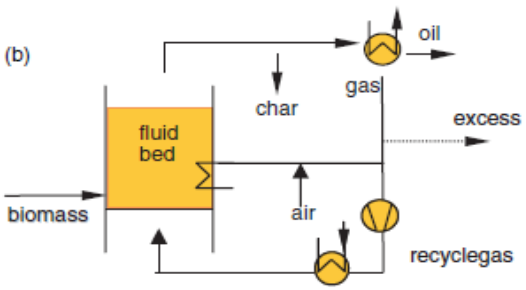
Circulating fluid bed [10, 16, 17]	
- direct heat supply to biomass via char combustion - sand and char separated from gas phase by cyclones - char is burned off in separate combustor - high gas flow rate, can be recycled - more flexible operation in terms of catalyst regeneration - max. size industrial set-up: 7000 kg/h (Fortum, Finland), in operation	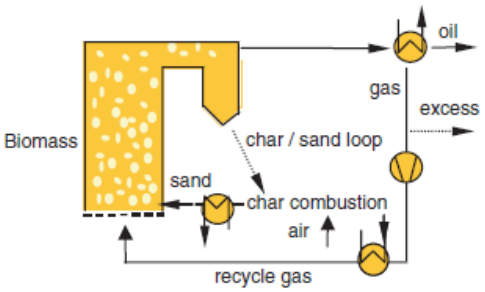

Rotating cone reactor [10, 11, 18]	
- pyrolysis due to mechanical mixing of sand and biomass without an inert gas - afterwards, sand and char are transported to a separate fluid bed where char is combusted - biomass is fed near the bottom of rotating cone - in combination with sand moving upwards along cone wall in spiral trajectory (centrifugal forces) - vapours pass a cyclone before condensation - max. size industrial set-up: 50 000 tonnes/yr (BTG, The Netherlands), in operation	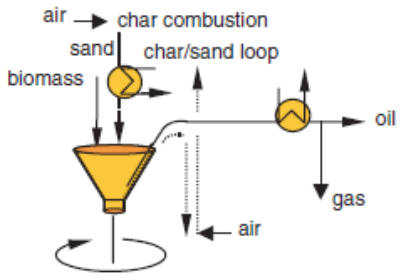
Auger reactor [11, 19 - 22]	
- biomass and sand contact each other in the heated screw - benefits: high heating rates when heated by an externally supplied heat carrier like sand, possibility to feed whole range of feedstocks, use of heterogeneous catalysts and low need of carrier gas (also possible without) - lower liquid yields - max. size industrial set-up: 500 kg/h (Bioliq, Germany), in operation	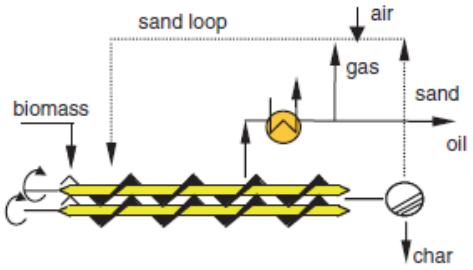

The final reactor described in Table 1 – the auger or screw – is the technology used in this thesis. Earlier doctoral research by Yildiz et al. (2013), has been performed with this type of reactor. They reported average liquid yields of 58.9 wt.%, and a gas, char and system carbon yield of 22.2, 15.9 and 2.6 wt.%, respectively (for non-catalytic experiments using pine wood as feedstock) [23]. For that study, they made use of the continuous fast pyrolysis mini-plant at the Ghent University's Green Chemistry and Technology Department (formerly within the Department of Biosystems Engineering). In paragraph 4.2.1, a full explanation of the installation is given there. In the MSc. thesis of Herregods-Van De Pontseele (2016), already a bio-oil yield of 64.9 wt.% was obtained, after some modifications were done at the same plant [3]. Brassard et al. give in their review paper an overview of bio-oil yields ranging from 30 (tyre rubber shred) to 70 (wood sawdust) wt.% [24]. During this research, the fast pyrolysis mini-plant is used to study catalyst deactivation during catalytic fast pyrolysis (CFP) of pine wood.

2.3 Bio-oil: properties and applications

2.3.1 Properties

The interesting product of fast pyrolysis is bio-oil. Although producing it with maximal yields is one of the purposes, the quality of the bio-oil predominates as the main aim of the fast pyrolysis. A critical factor in that regard is the amount of oxygen and its functionality in the bio-oil. Its relatively high oxygen content is one reason why it cannot be used as a direct substitute for heating fuels or for power production in boilers. Oxygen functionalities are present in more than 300 different compounds in the liquid as e.g. carboxylic acids, alcohols, ketones, aldehydes, ethers and esters. In that way, bio-oil may have some potential, but its complex composition makes it challenging to create a valuable and profitable product out of it [25, 26].

Table 2 gives an overview of the physicochemical properties of the bio-oil, compared with those of a conventional fuel oil. Typically, the liquid colour is deep brown [25]. Its elemental composition corresponds quite well with that of the original biomass. Bio-oil has a distinctive acid, smoky smell due

to the volatile, low molecular weight acids and aldehydes and it can irritate the eyes after prolonged exposure. The oil can corrode materials such as aluminum and carbon steel [27]. Polyolefins and stainless steel are more resistant to this liquid and should be used as such in handling and storing bio-oil. The low pH is resulting from the high concentration of organic acids such as formic and acetic acid in the bio-oil [28].

Another drawback is the relatively low higher heating value (HHV), as can be seen in table 2. A low HHV means that the product is less suited for fuel applications. As the produced oil contains water as well as organic compounds, phase separation may occur from a certain water/organic - ratio (from 50/50 till 70/30) [29]. At rather low water concentrations in bio-oil (between 15 – 25 %), water is usually miscible due to the presence of other polar hydrophilic constituents e.g. short alcohols, ketones or aldehydes. Water in bio-oil is partly derived from moisture in the feed material (usually feedstocks with a maximum moisture content of 15 wt.%) and dehydration reactions occurring during (catalytic) fast pyrolysis [30]. To remove all the water out of the pyrolysis oil, the liquid must be heated to at least 100 °C, which is also above the boiling point temperature of some light oxygenates in bio-oil. Sometimes, water is added to the bio-oil to reduce the viscosity and to improve the stability. Consequently, transportation of bio-oil may be facilitated [10].

Table 2: physical properties of bio-oil and a conventional light fuel oil [32].

Type of analysis	**Bio-oil**	**Light fuel oil**
Water content (wt.%)	20 - 30	0.03
Solid content (wt.%)	0.01 – 1.00	0
Ash content (wt.%)	0.01 – 0.20	0.01
N (wt.%)	0 – 0.40	0
S (wt.%)	0 – 0.05	0.20
Stability	unstable	stable
Viscosity (40 °C), mm^2/s	15 - 35	3.00 – 7.50
Density (15 °C), kg/dm^3	1.10 – 1.30	0.89
Flash point (°C)	40 - 110	60
Pour point (°C)	-36 to -9	-15
LHV (MJ/kg)	13 - 18	40.3
HHV (MJ/kg)	16 - 19	42 - 44
pH	2 - 3	neutral
Distillability	not distillable	160 – 400 °C

The properties of the liquid mixture can change over time. This process is known as aging and involves an increase of the viscosity and average molecular weight, possibly accompanied with a phase separation. When the bio-oil is held at room temperature instead of kept refrigerated, more secondary reactions (including polymerisation reactions) will appear, affecting the quality of the bio-oil. This can be controlled by adding alcohols (methanol or ethanol), that solubilise the less-soluble constituents and lower the reactivity of certain compounds in the bio-oil [28, 31].

2.3.2 Combined heat and power applications

In the last quarter of the past century, there was a growing interest in using bio-oil for its fuel applications [33]. Merits related to fuels based on biomass are their CO_2 neutrality and low sulfur content (see table 2). Biomass is converted to bio-oil via fast pyrolysis obtaining a more easily transportable and marketable product. Detrimental properties using bio-oil as a fuel are the high viscosity, poor volatility, coking, corrosiveness and variation in quality. For those reasons, it is hard to process it in boilers, gas turbines and other engines. Bio-oil upgrading (see section 2.4) is an option to overcome these issues.

Combustion of bio-oil in diesel engines is prone to some disadvantageous liquid properties. Solutions have to be found for the difficult ignition (caused by the low heating value and high water content), corrosiveness (acids) and coking (present thermally unstable compounds). Addition of alcohols, adjustments on the engine, acid feedstock pretreatment to leach the feedstock, staged condensation to decrease the acid and water content or hot-filtering of the bio-oil to remove the particulates present could solve some of these problems [33 - 35].

Diesel engines can withstand the presence of contaminants present in the pyrolysis oil [11, 33]. Normally, they are just designed to run on fuels with low acidity. Viscosity and stability are two issues that keep coming back in every application. To solve the problem that the liquid hydrocarbons and bio-oils are not miscible, surfactants can be added to emulsify both liquids with each other. Stable emulsions with several ratios of bio-oil in diesel have already been reached (from 10 % to 90 %) by CANMET (Canada) and the University of Florence (Italy). Detrimental effects of this technique are the cost of surfactants and the high amount of energy required to create those emulsions. Maybe more important was the appearance of corrosion and erosion spots in the engine. There is not much interest from engine manufacturers to combine bio-oil and petroleum fuels together [36, 37].

2.3.3 Chemicals

Due to the complex mixture of the bio-oil, it is hard to extract one single compound or group of chemicals. Important to note is that there are still some large, less severely cracked or de-/re-polymerised molecules in the oil not yet currently identified [11]. For that reason, it seems interesting to find industrial applications where the whole bio-oil or several easier separable fractions can be used instead, requiring less extensive isolation or bio-oil work-up [33].

Bio-oil can function as an alternative wood preservative or it can be used as a fungicide/insecticide due to the presence of some terpenoid and phenolic compounds [38, 39]. Another application of unfractionated bio-oil substituting an already existing product, are resins for MDF or OSB panels. It has been verified that bio-oil can replace partially the phenol-formaldehyde resins in those wood particleboards [40].

The water-soluble fraction of bio-oil includes e.g. those aldehydes responsible for the browning reaction of meat (glycolaldehyde). The isolation has been patented by Red Arrow Products [41] and RTI [42]. Besides, it contains phenolic constituents that give the typical smoky flavour. In the USA and Canada, Ensyn operates an entrained flow bed process with a yield of 1 ton/h to produce liquid smoke, a food flavour that can be sprayed on meat [11].

Levoglucosan and levoglucosenone are two detected sugars in bio-oil using gas chromatography (GC). Maximally 30 wt.% of the bio-oil are sugars, derived from (hemi)cellulose, and for conventional biomass. Amounts of aforementioned anhydrosugars are respectively 46 and 24 wt.%, using acid-pretreated cellulose [44]. The current market for those carbohydrates is rather small, however the prices are relatively high due to the difficult isolation. Levoglucosan can be used as a carbon source in fermentation and has potential in the synthesis of antibiotics, surfactants and biodegradable plastics. Levoglucosenone is a precursor e.g. in the synthesis of Cyrene™ (dihydrolevoglucosenone). This compound could replace less environmentally friendly solvents like DMF (dimethylfuran) and it also has been used in the synthesis of urea compounds (isocyanates and amines) [45, 46]. Further, it seems interesting to mention furfural and furfurylalcohol as carbohydrate-derived products that can be produced in amounts up to 30 wt.% [11, 33, 47].

2.3.4 Co-feeding in fluid catalytic cracking (FCC) unit

Next to the aformentioned applications, bio-oil can be fed into a fluid catalytic cracking unit of an existing petrorefinery. Feedstocks mixed with 10 % bio-oil result in as much as LPG (liquid petroleum gas) and gasoline compared if only feeding vacuum gas oil. In the past, problems arose concerning the immiscibility with hydrocarbons. A preceding HDO (hydrodeoxygenation, see section 2.4.1) step may overcome this drawback, but then a lot of hydrogen is necessary at elevated pressures. Pinho et al. made use of 150 kg/h demonstration-scale unit. In their research, the amount of renewable carbon content was determined by ^{14}C isotopic analysis and was around 2 % when feeding an FCC with 10 % bio-oil. They also introduced another parameter to demonstrate their efficacy namely the FCC carbon efficiency, which is the amount of carbon in bio-oil converted to carbon in total liquid product [48, 49].

2.4 (Catalytic) Bio-oil upgrading

Despite the advances made in the direct use of bio-oil in the applications described in the previous section, bio-oil upgrading has been investigated to obtain fuels and chemicals compatible with the current infrastructure. In general, three upgrading possibilities can be assumed namely a physical, chemical and catalytic upgrading of bio-oil. Hot vapour filtration, addition of short chain alcohols and emulsification are a few possibilities for physical upgrading [50, 51]. Chemical upgrading comprises supercritical CO_2 extraction, aqueous phase reforming, esterification and steam reforming [52 - 59]. Only catalytic upgrading techniques are described here in detail. Under this category, hydrotreating and catalyst (zeolite) cracking can be assumed.

2.4.1 Hydrotreating

Hydrotreating, and more specifically HDO can eliminate oxygen from bio-oil via dehydration, in the presence of high pressures of H_2 (up to 200 bar) and moderate temperatures (up to 400 °C). This hydrogen consuming upgrading technique is used to saturate alkenes and aromatics and to remove contaminative elements like oxygen, nitrogen, sulfur or metals. Actually not only HDO reactions occur, but also hydrodesulphurisation (HDS) and hydrodenitrification (HDN) steps can be completed [60 - 62]. Hydrotreating has the necessity for catalysts (sulfided CoMo or NiMo supported by alumina or aluminosilicates). The sulphided catalyst shows Brønsted acid sites (see section 2.5.2) with their H^+ and SH^- groups on the surface of the catalyst [55]. Sometimes, additional phosphorous containing compounds are added, in order to create new acid sites on the catalyst surface and to promote formation of more easily reducible and sulphidable compounds [63]. Problems occuring were related to the unstability of the catalyst supports in the highly aqueous pyrolysis oil and the fact that sulphur was stripped from the catalyst, so it was necessary to add sulfur continuously. Later, sulfur free catalysts have been developped for sustainability and economical reasons. Since noble catalysts have the possibility to easily activate hydrogen, they show better activity and stability compared to the aluminosilicates. Availability of the catalyst, cost and higher chance of poisoning due to Fe or S are the main drawbacks of this noble metal type [55].

Hydrotreating can be a part of a more complex process like described by the East China University of Science in Shangai, with an additional esterification and cracking step that takes place in supercritical ethanol [52 - 54]. The hardest property to make this process economically feasible, is the supply of hydrogen and the high pressure cost. About 80 % of the biomass needed for pyrolysis, would be necessary to provide hydrogen for this hydrotreating, e.g. via gasification. While only working with the organic phase from bio-oil, the aqueous phase can be used as hydrogen source for steam reforming. Eventually other options are more economic feasible instead of getting hydrogen out of biomass itself.

For example, sustainable electricity can be used to produce hydrogen via electrolysis. After hydrotreating, refining is mandatory but this can happen in a conventional refinery. Special reactors have been designed and are already on the market to perform HDO [55]. Hydrocracking is rather similar to hydrotreating, but it operates at higher temperatures while using noble metal catalysts like Pt and Pd on aluminosilicates [64].

2.4.2 Catalyst cracking

While hydrotreating was a dehydration reaction at high pressure, catalyst cracking occurs via decarboxylation and dehydration reactions at atmospheric pressure. Typically, the acidic and hydrophobic catalyst ZSM-5 (see section 2.5.2) is used for those type of reactions. The formed products are hydrocarbons, water and oil soluble organics, CO, CO_2 and coke. Due to the high temperatures, bonds in the larger molecules are cleaved and deoxygenation of the compounds takes place [55, 64].

General disadvantages of hydrotreating and catalytic cracking are the low yield of upgraded bio-oil and catalyst deactivation. This arises from the production of coke, char and tar [65]. This first issue can partially be solved by co-feeding hydrogen gas or hydrogen donors (methanol, tetralin or decalin) as well as modifications to the reactor systems themselves [64]. Catalyst deactivation and its approach to postpone it is more elaborated in section 2.5.5.

2.4.3 Integrated hydropyrolysis and hydroconversion (IH^2)

In the past, bio-oil upgrading using hydrogen gas was executed in pilot installations but these trials were done in short-time experiments with high pressures and low space velocities (so high amounts of catalyst compared to biomass) [66 - 68]. The hydrocarbon yield was between 26-30 wt.% of the starting biomass. Marker et al. proposed a direct route for producing fuels namely integrated hydropyrolysis and hydroconversion (IH^2). In the set-up from the Gas Technology Institute (GTI), biomass is sent to a bubbling fluidised bed of catalyst, with hydrogen pressures of 20 - 35 bar and temperatures of 350 - 480 °C. These pressures are much lower compared to those used for the upgrading of bio-oil [69, 71]. Initially a 1 µm hot sintered-metal barrier filter was put in the reactor so only vapours could pass through and char accumulated in the bed. Modifications were executed to separate the char and catalyst afterwards. The catalyst (specialty catalyst, supplied by their project partner CRI Catalyst Company) eliminates water, CO and CO_2, together with limiting the undesirable side-reactions (coking and acid catalysed polymerisation). In the hydropyrolysis reactor, most of the oxygen removal is carried out while a second reactor, namely the hydroconversion reactor primarily acts as a catalytic polishing reactor. The formed mixture of hydrocarbons can be further refined on the spot via hydrotreating or at an external refinery. The reformer receives the light gases (CO, CO_2 and C_1 – C_3 hydrocarbons) as they are converted in a product stream containing H_2 and CO_2, without CO. In a next step, CO_2 is evaporated and pure H_2 is sent back to the reactors for fluidisation. Concerning the capital costs of this process, they are comparable with those of pyrolysis. Other benefits are the floating of hydrocarbons on top of the water phase, which makes separation easier and the flexibility to process of a lot of different feedstocks. Marker et al. compared the atomic H/C-ratio of e.g. algae, bagasse, wood and corn stover based liquids, leading to the conclusion that using wood resulted in a lower liquid yield compared to algae (26.4 % vs. 46.3 %), but the wood pyrolysis oil had lower H/C-ratio [70]. While those results were reached in a 0.45 kg/hour semi-continuous pilot plant, further research was done with a 50 kg/day installation to demonstrate the operability and stability of the catalyst over the time. The same type of reactor (a fluidised bed reactor) was used. Organic liquid yields were around 26 wt.%, which were similar to those in bench-scale experiments [71, 72].

2.5 Catalytic fast pyrolysis (CFP)

Next to the (catalytic) post-treatment of bio-oil, the vapours of the pyrolysed biomass can be catalytically upgraded after their formation.

2.5.1 General aspects

The main reason to use catalysts in fast pyrolysis is to selectively remove oxygen prior to condensation of the gases to improve the oil quality [1]. This type of reaction is a heterogeneous catalysis, because it makes use of a solid catalyst facilitating its separation and recycling. It is claimed that CFP possess several interesting characteristics compared to other upgrading techniques. The possibility to execute the whole experiment in one single reactor (for in-situ mode), the use of relatively cheap and readily available catalysts like zeolites, the handling of an attractive range of feedstock biomass and the production of bio-oil blendable with current fuels are a few of them [73, 74].

In practice, there are two operating modes for CFP: in-situ and ex-situ catalysis. In the first type, biomass is pyrolysed in a reactor in which the heterogeneous catalyst is also present and vapours diffuse into the catalytic pores where they are reformed (figure 3a and 3b). In the ex-situ mode, created vapours come out of the pyrolysis reactor and contact with the catalyst in a second, separated reactor where the vapours are upgraded (figure 3c and 3d) [14].

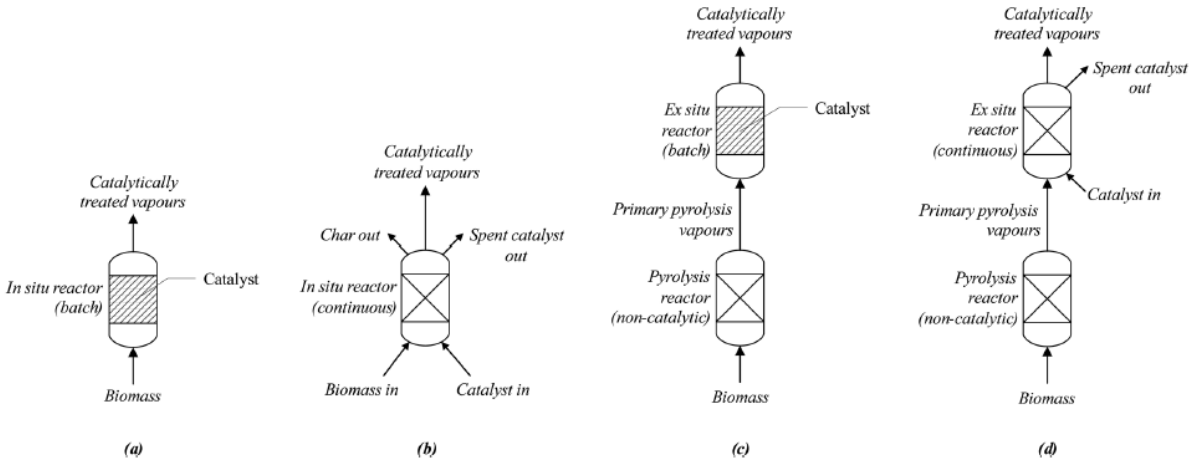

Figure 3: different options in operational mode of CFP: a: in situ (batch), b: in situ (continuous), c: ex situ (batch) and d: ex situ (continuous) [14].

The efficiency of a CFP system can depend on:

- operating temperature of the catalyst: determines the relative rate of the catalysed vapour phase reactions [75].
- heating rate and residence time of the feedstock: high biomass heating rates are essential to suppress coke formation [14].
- weight hourly space velocity (WHSV, h^{-1}) : ratio of mass flow rate of biomass to the mass of catalyst: higher values are preferable to lower the formation of coke and polycyclic aromatics as well as to improve process economics by reducing the amount of used catalyst [76].
- vapour residence time: must be minimised, heterogeneous coke is formed after secondary reactions on the catalyst surface, which is more frequent in the presence of alkali and alkaline earth metals [75, 77, 78].
- type of biomass: in catalytic experiments, high-lignin-low-ash-biomass like woody variants are preferred [79].

2.5.2 Choice of catalyst

In the search for the proper catalyst, some parameters must be considered. Catalysts keeping their activity and selectivity over an extended period, are favored. A stable catalyst will change very slowly over the course of time [73]. Porosity can also have a significant effect on catalytic properties [74]. Besides, the catalysts must be thermally and mechanically stable, robust and resistant against deactivation [12]. In this way, a lot of research has been performed with different types of catalysts e.g. metal oxides, mesoporous catalysts, transition metals or zeolites. Those latter are crystalline microporous silica based materials with a well-defined and ordered pore structure [80]. Zeolites are used in selective adsorbing, petroleum refining and purification processes [81]. In that category, the (H)ZSM-5 is the most well-known member. The secondary structure of ZSM-5 are pentasil units, as presented in figure 4a. These units are attached to each other to form pentasil chains, and ten pentasil units can form a 3D-structure, as shown in figure 4b. The created cavities have a size between 5.4 and 5.6 Å (10^{-10} m) [2, 80].

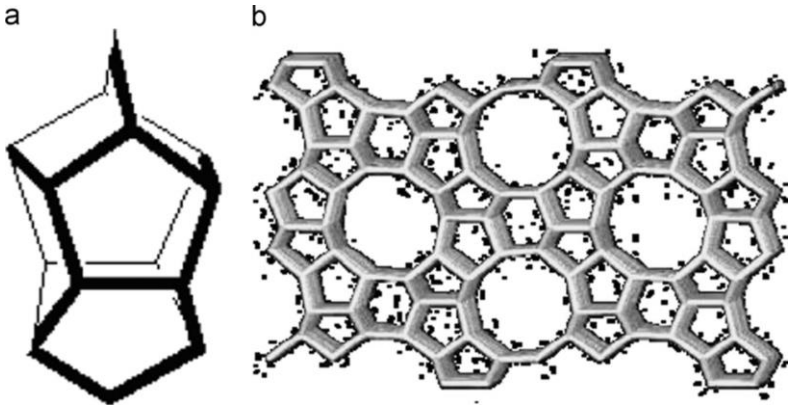

Figure 4a: structure of a pentasil unit. Figure 4b: 3D-structure of ZSM-5 [80].

This aluminosilicate material is built with units of SiO_4 and AlO_4, linked together with a common oxygen atom. The net negative charge is brought into an equilibrium by the presence of a cation [82]. Zeolites contain acid sites and have very small pore sizes so only small molecules will diffuse into [1]. Those sites can be Brønsted or Lewis type. The difference between them is shown in figure 5. They have an effect on promoting cracking reactions and selective deoxygenation of pyrolytic vapours, what results in more aromatisation reactions and a higher C/O ratio while keeping the C/H ratio acceptable [14]. Acid catalysts show excellent properties like tunable acidity, superior water tolerance and high thermal stability [83, 84].

The acidity of the catalyst, expressed as the SiO_2/Al_2O_3-ratio (SAR) has also its influence on the product selectivity. The more aluminum (III) oxide incorporated in the ZSM-5, the lower the ratio of Brønsted/Lewis acid sites. A higher SAR means a decrease in number of acid sites and apparently a lower total acidity. Engtrakul et al. investigated different ratios, ranging from a SAR of 23 to 280. With a higher acidity, more unsubstituted aromatics (e.g. benzene, naphthalene and anthracene) were created at the expense of alkylated aromatics (e.g. xylene, dimethylnaphtalene and methylanthracene). This is related to the relative cyclisation and alkylation rates within the zeolite. Within a more acidic catalyst, the acid sites are more concentrated to each other and additional cyclisation reactions occur at a higher rate than alkylations [83, 84].

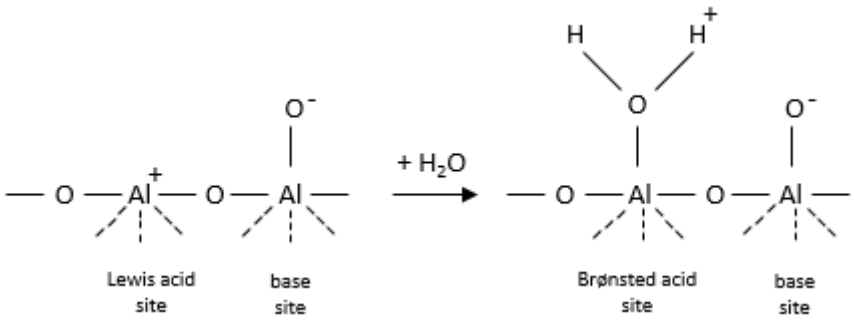

Figure 5: the Brønsted acid site contains an oxygen atom in its framework that is protonated, resulting in a hydroxyl group donating its hydrogen to the adsorbed molecule, while by the Lewis acid site, electron pairs are transferred from the adsorbed molecule to the solid surface [73, 80].

Zeolites with a lower acid site density tend to deactivate faster and generate more hydrocarbons (paraffins, olefins and aromatics) in total. A high SAR leads to the production of more aliphatic alkanes and alkenes, while more benzene containing compounds are produced with a lower ratio. A low SAR means high acid strength sites facilitating the dehydrocyclisation of alkanes/alkenes to aromatics [85].

2.5.3 Research on CFP

Experiments with catalysts have been performed on different scales: analytical (µg – mg), lab and pilot (g – kg) and commercial scale (kg – ton). An analytical set-up is ideal to establish a certain catalyst/biomass combination but it is not always feasible to scale up such an installation (e.g. heat and mass transfer limitations). The continuous supply of both biomass and catalyst makes it convenient to execute CFP with auger reactors on lab scale and larger. Several attempts to scale up CFP can be found in literature, but most of them failed because of insufficient oil yields [54].

Yildiz et al. carried out some experiments in the mini-plant of the faculty. The average liquid yield of catalytic experiments with HZSM-5 (protonated form of Zeolite Socony Mobil-5) and pine wood was significantly lower (50.3 and 50.1 wt.% for in-situ and ex-situ experiments respectively, compared to 58.9 wt.% for the non-catalytic conventional mode). Furthermore, the organic liquid yield is significantly lower for the catalytic experiments. The presence of a catalyst is responsible for the increase in dehydration reactions of the oxygenated species in the product vapours. Because of the formation of coke-on-catalyst, large losses in biomass carbon were observable and this also led to a lower share of organics in the bio-oil [19]. The composition of the liquid is of utmost importance. The use of catalysts led to a spectacular reduction in the amount of acids, aldehydes and detectable sugars. On the other hand, an increase in phenols and other aromatics could be observed. The catalyst is capable to stabilise part of the vapours of the aromatic monomers (who are originating from the lignin depolymerisation) before they can repolymerise into heavier and non-GC-detectable aromatic structures, also called pyrolytic lignin [12]. In general, zeolites lead to the formation of smaller compounds, due to cracking of high molecular weight molecules abundant in the primary pyrolysis vapours [86, 87]. Yildiz et al. also concluded that working in ex-situ mode requires less catalyst, but that the overall performance of in-situ catalysis in terms of oil quality is better. Although an important disadvantage that can occur with the in-situ set-up, is catalyst poisoning due to the direct contact of biomass originating minerals with the catalyst material [12, 19]. In the experimental work of this thesis, only ex-situ catalysis was applied.

A global reaction mechanism of CFP is shown in figure 6. Cellulose is converted into anhydrosugars like 1,6-anhydro-β-D-glucofuranose (AGF), 1,4:3,6-dianhydro-α-D-glucopyranose (DGP), levoglucosenone (LGO) and levoglucosan (LGA) due to the removal of water. Those intermediates can be transformed into furans by an acid catalysed dehydration or decarbonylation/decarboxylations steps. Furans are

also formed out of hemicellulose while losing water, and with the same reactions that occur during the conversion of anhydrosugars to furans, a pool of hydrocarbon compounds is created. When lignin is subjected to non-catalytic depolymerisation, monomeric phenols are created, which can be further converted into monoaromatics (MAHs) and eventually in a second phase to polyaromatic hydrocarbons (PAHs). From all those intermediates, heterogeneous coke can be formed on the catalyst [14].

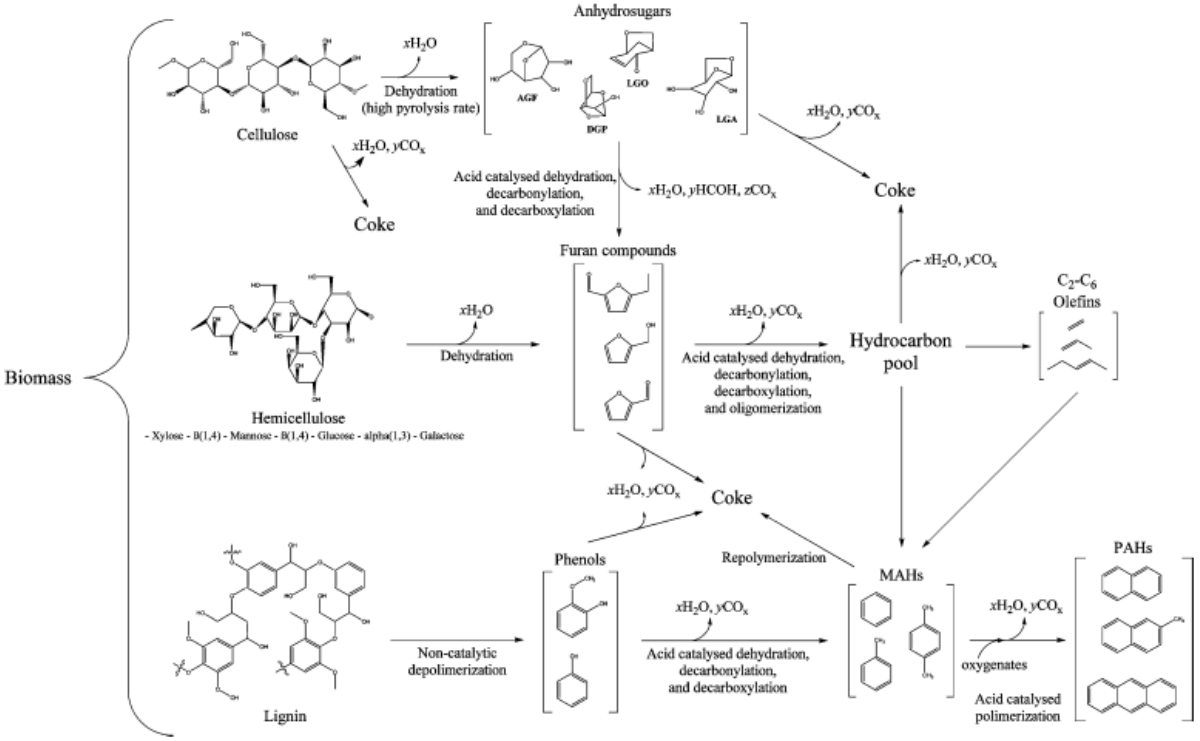

Figure 6: chemical conversion of cellulose, hemicellulose and lignin, with their mutual reactions [14].

To become competitive with the existing fuels, the oxygen content must be reduced while maintaining the carbon content as high as possible. Catalytic upgrading seems an excellent method to do this. Oxygen can be removed as CO (decarbonylation), CO_2 (decarboxylation) or H_2O (dehydration). Removal in the form of CO_2 is the most beneficial because two atoms of oxygen will leave with only one carbon atom. Dehydration reactions must be avoided to preserve the highly energetic C-H in the bio-oil and to keep the hydrogen in the oil for the catalysed hydrocarbon forming reactions [88]. In practice, decarbonylation reactions occur more frequently than decarboxylation for catalytic experiments [14].

2.5.4 Assessment of CFP bio-oils

The amount of carbon and oxygen originating from the biomass that ends up in the bio-oil, can tell something about the quality of the liquid. Venderbosch introduced two variables demonstrating the overall biomass-to-liquid carbon yield is directly related to the oxygen reduction. Eq. (2.1) and (2.2) were used to determine the oxygen reduction ξ_o and the carbon yield η_C.

$$oxygen\ reduction\ \xi_O = \left(1 - \frac{O_{oil,daf}}{O_{thermal\ oil,daf}}\right) . 100\ \% \qquad (2.1)$$

$$carbon\ yield\ \eta_C = \frac{n_{C,oil,daf}}{n_{C,feed,daf}} . 100\ \% \qquad (2.2)$$

Daf means on dry-ash-free basis. The fraction in the formula of ξ_o represents the ratio of the oxygen content in the CFP liquid over the oxygen content in the non-catalytic FP oil. η_C gives the moles of carbon in oil over the moles of carbon in the feed. Operating at high η_C and high ξ_o is preferable, corresponding with the upper right part of figure 7, with a low carbon loss and a high deoxygenation rate. Also in Figure 7, each data point represents the results (in terms of the two defined performance parameters) of a single study on CFP of lignocellulosic biomass. Almost all of these data points are located in the corner opposite to the preferred area, meaning that in practice, already a limited oxygen removal is associated with a high carbon loss. A desired oxygen removal finally happens when almost all carbon is already converted into less valuable products like gas and char meaning very little oil will be produced. In figure 7, two regions are delineated. In the first one, the carbon yield is strongly varying whereas the oxygen reduction is rather low. These conditions correspond with a mild deoxygenation. In the second box, more severe deoxygenation occurs. Some of the data only show the oxygen content in the organic phase of the liquid. The organics in the aqueous phase are neglected so this leads to a decrease in ξ_o and an underestimation of the η_C. In addition, Venderbosch introduced a third variable, the energetic yield η_E (Eq. (2.3)) and plotted also iso-energetic curves. As can be seen in the formula, maximising the ratio of HHV is desired, so the higher the η_E, the better the conversion. Similar plots were made to evaluate the quality of our produced bio-oils [89].

$$energetic\ yield\ \eta_E = \left(Y_{org.,oil,daf} \cdot \frac{HHV_{oil,daf}}{HHV_{feed,daf}}\right) . 100\ \% \qquad (2.3)$$

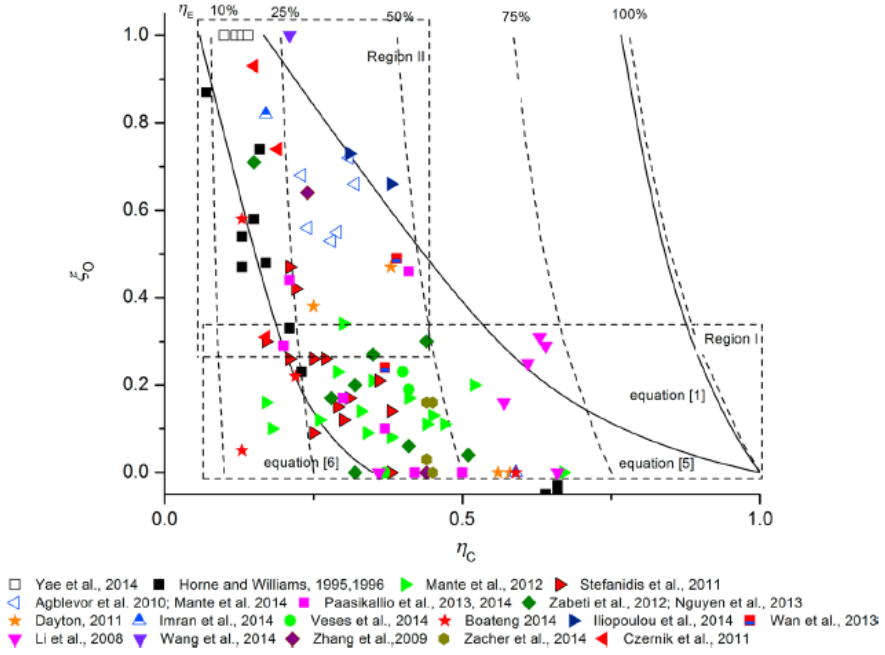

Figure 7: graph with carbon yield related to the oxygen reduction [89].

Venderbosch also stated that zeolites are too reactive to selectively convert oxygenated compounds. Two solutions are proposed, the first one is to lower the pyrolysis temperature. For biomass, at least 400 °C must be reached. The second solution is steam pyrolysis, in the presence of a catalyst. This option seemed better, with an acceptable carbon yield together with a serious deoxygenation. Although for this process, no remarkable difference was shown between catalytic and non-catalytic experiments. Unfortunately, dehydration was favoured, resulting in a high viscous and large molecular weight bio-oil [89].

If the residual oxygen content is around 10 wt.%, further refining is possible without substantial problems. According to current state in CFP as outlined in Figure 7, the carbon yield is only between 10 and 20 wt.%. This means that 80 % of carbon is converted into the gaseous or solid phase (as non-condensable gases (NCGs), char or coke).

Yildiz et al. also made a plot of the CO/CO_2 ratio from CFP experiments plotted against the water yields. Most data points in the graph showed a $(CO/CO_2)_{CFP}$ ratio higher than 1, meaning that less beneficial decarbonylation reactions appear more frequent than the decarboxylation reactions. This study also showed that the coke yield increased when the decarbonylation mechanism predominates. Yildiz et al. also revealed that for the higher amount of oxygen removal, the more catalyst will be consumed [14].

In that regard, they calculated different elemental yields from twelve leading studies and compared those results with each other. They designed two graphs (figure 8), with in the abscissa the ratio of the yield of CFP-oil over the yield of the non-catalytic FP-oil ($Y_{CFP\text{-}oil}/Y_{FP\text{-}oil}$) vs. in the ordinate the fraction of carbon/oxygen of the feed recovered in the organic liquid during a CFP experiment, over the feed recovered in the organic phase during a FP experiment (η_C) or (η_O), respectively Eq. (2.4) and (2.5).

$$carbon\ yield\ ratio\ \eta_C = \frac{\eta_{C,CFP}}{\eta_{C,FP}} = \frac{m_{C,CFP-oil} \cdot Y_{CFP-oil}}{m_{C,FP-oil} \cdot Y_{FP-oil}} \qquad (2.4)$$

$$oxygen\ yield\ ratio\ \eta_O = \frac{\eta_{O,CFP}}{\eta_{O,FP}} = \frac{m_{O,CFP-oil} \cdot Y_{CFP-oil}}{m_{O,FP-oil} \cdot Y_{FP-oil}} \qquad (2.5)$$

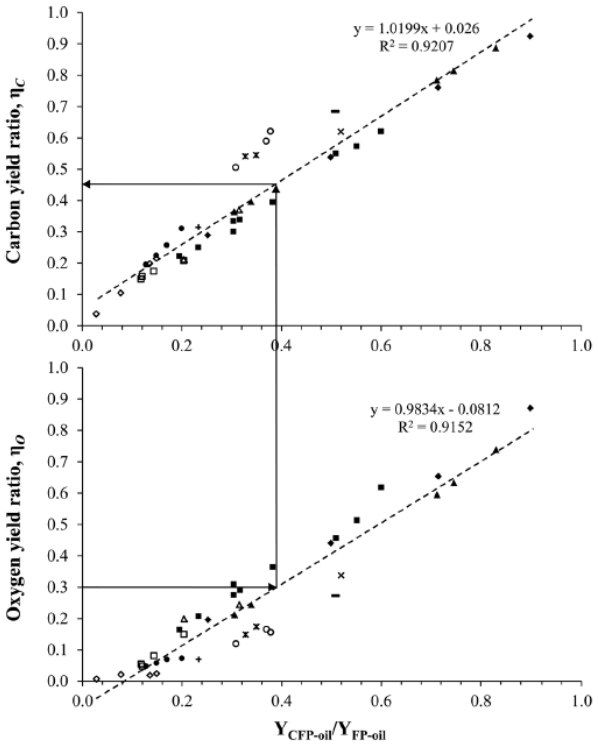

Figure 8: graph with carbon and oxygen yield ratios related to the liquid yield of a CFP experiment over the liquid yield of a similar FP experiment [14].

With CFP, a liquid low in oxygen is desired, so η_C must be maximised (value towards 1), whereas η_O must be as low as possible (value towards 0). Carbon and oxygen are always lower in the catalytic mode, so values above 1 are impossible. Since both trendlines have a rather similar gradient, a decrease in oxygen yield inevitably leads to a decrease of the carbon yield. For oxygen removal, low $Y_{CFP\text{-}oil}/Y_{FP\text{-}oil}$ ratios are preferable whereas for the carbon retention, high ratios are better so an

equilibrium must be found. Complete deoxygenation would result in only hydrocarbons, but the yield would be too low to economically compete with the current petrochemical production. In figure 8, an example is indicated with arrows: if the bio-oil yield of CFP is lowered by 61 % (x-axis) compared to a similar FP experiment, there is a decrease of 70 % in oxygen yield and 55 % in carbon yield (y-axis) [14].

2.5.5 Catalyst deactivation

Effects of ash and pretreatment steps

The main problem of CFP is the presence of ash that originates from the biomass, destroying and blocking the operation of the catalyst. This can be solved by indirect contact of the feedstock material and the catalyst, so in fact ex-situ CFP. In this way, only the vapours and not also the minerals can come into contact with the catalyst. Operating in ex-situ mode means that there are more parameters to select and to examine, but the lifetime of the catalyst will be extended.

Catalysts can be added to the biomass, but it already contains catalysts from itself. Alkali and alkaline earth metals (AAEMs) are the elements necessary for the biomass during its growing phase and are bound to hydroxyl and/or phenolic groups in the form of cations or as salts. Nevertheless, these metals form the ash [90]. Silicon and metals other than those of two first groups of the periodic table appear quite inactive. Sulfur and phosphorus-containing ammonium salts can affect the oil yields negatively in favour of the char production [91, 92]. AAEMs elevate the yield of char and water due to condensation and via fragmentation, the light organic fraction raises [93]. Already low ash feedstocks can lead to a phase-separated product in significantly lower yields. In that respect, feedstocks with a low ash content should be promoted to be used but unfortunately, the most interesting ones to work with (the low-valued residues like sugarcane straw), are known for their high amount of ash. An additional advantage from removing the ash from the feedstock by pretreatment, is the enhanced formation of levoglucosan, although till today, the demand for this anhydrosugar is still limited [10, 11, 92]. Section 2.5.6 goes more into detail about the pretreatment of sugarcane residues.

Pretreatment can be useful to elevate the biomass conversion efficiency. Four categories can be distinguished namely a physical, thermal, chemical and biological pretreatment. A combination of those four can also be applied [94]. Physical pretreatments are milling or grinding of the biomass to lower the particle size. Another option is extrusion under high pressure to create pellets. Just like bio-oil, pellets also have a large volumetric energy density and the water content is reduced [3, 95]. The second pretreatment technique can be a simple drying step but also more complicated like a torrefaction step, where biomass is treated at temperatures between 200 and 300 °C. In this way, water is completely removed and a significant amount of oxygen is already eliminated by hemicellulose removal. Several studies used this technology, leading to a lower yield but higher quality bio-oil. In steam explosion, the combination of elevated pressures and temperatures for a short period, with a subsequent depressurisation leads to an explosion of the biomass [96]. Due to this treatment, physico-chemical properties of the bio-oil will change in a positive way. Other unconventional thermal methods are ultrasound and microwave irradiation. The last category of pretreatment consumes less energy than the others, but it does not deliver always the desired effect [97].

Acids and water can be used to demineralise the feedstock, which is more explained in section 2.5.6. A new development is ionic liquids. Those materials, also called molten salts, contain only ionic species without any neutral molecule and having a low melting point [98]. Those solvents can be used for the dissolution of cellulose, hemicellulose and lignin. It has already been used to produce sugars from oil palm fronds [99].

Mechanisms of catalyst deactivation

The selected catalyst for CFP should promote the production of value-added compounds at the expense of unwanted highly oxygenated ones. In that regard, deactivation of the catalyst should be avoided. This is the physical, chemical, thermal and mechanical degradation of a catalyst with a loss of functionality. The loss of activity and/or selectivity of a catalyst can come from several reasons, shown in table 3 [100]. When executing CFP, coke and metal (ash) deposition on the catalyst are the most occurring problems. In this way, the active sites of zeolites are poisoned or the pores of the catalyst are blocked. Zeolites like ZSM-5 seem an appropriate solution for CFP, nevertheless a large amount of coke is formed. Some reaction products cannot enter the micropores of ZSM-5 and stick on the surface of the catalyst as coke [101 - 105]. In that way, several attempts to enlarge the pore size have already been executed as to accommodate larger molecules onto the active sites within the catalyst pores. Desilication leads to more mesopores, but most of the acid sites remain unaffected [106].

In FCC, the catalyst is subjected to an oxidative treatment at elevated temperatures to burn the coke and in this way to partially restore its activity [107] – a process also known as regeneration. With CFP, this process seems more complicated due the higher hydrogen and oxygen content in the coke. While recovering the catalyst in this way, an additional amount of CO_x and H_2O is formed. For zeolites, especially the water formation during regeneration leads to dealumination and loss of the active sites [107 - 109]. In practice, regeneration happens through a two-step (two-temperature) procedure (after the oxidative treatment in a first step, carbon is removed as CO_2 in a second phase). The condition of the catalyst (fresh, spent of regenerated) has also its effect on some important physicochemical properties of the catalyst itself. Specific area, pore volume and total acid sites lower along this order: fresh > regenerated > spent zeolite [110].

Table 3: mechanisms of catalyst deactivation [100].

Mechanism	Type	Description
Poisoning	Chemical	Strong chemisorption of reactants, products or impurities on catalytic sites, thereby blocking sites for catalytic reaction (physically blocking, inducing electronically modifications, restructuring the surface, preventing diffusion…)
Fouling	Mechanical	Physical deposition of species from fluid phase onto the catalytic surface and in catalyst pores. This includes the deposit of carbon and coke in porous catalysts.
Thermal degradation	Thermal	Thermally induced loss of catalytic surface area, support area, and active phase – support reactions
Vapour formation	Chemical	Reaction of gas with catalyst phase to produce volatile compounds
Vapour-solid and solid-solid reactions	Chemical	Reaction of fluid, support, or promoter with catalytic phase to produce inactive phase
Attrition/crushing	Mechanical	Loss of catalytic material due to abrasion and internal surface area due to mechanical-induced crushing of the catalyst particle

The ash can influence the vapour phase in different ways. Four hypothetical pathways can be distinguished, shown in figure 9 [111].

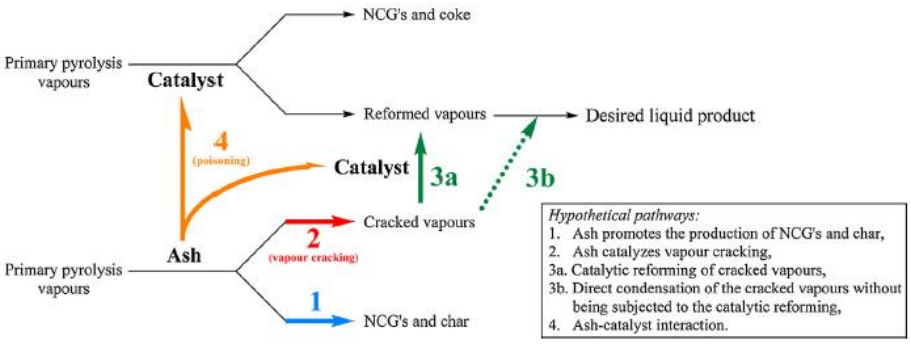

Figure 9: effect of ash on the catalyst and end products [111].

Effects of catalyst deactivation

Three types of coke exist: the toxic coke captured inside micropores, external coke of the outside of a catalyst particle and coke precursors deposited in the mesopores. Those three types vary with the biomass-to-catalyst ratio (BM/CAT). External coke is formed because the supply on the external surface is bigger than the diffusion into the catalyst. Jia et al. examined the coke produced on two types of catalyst, an original HZSM-5 and a hierarchical zeolite, created by desilication with NaOH. They observed an increase in the selective production of monoaromatics with the treated catalyst. Till a BM/CAT of 0.85, the sum of all quantified MAHs was 6.2 wt.% and 4.4 wt.% respectively for the hierarchical zeolite and the parent one. Towards a ratio of 1.7, both fractions decrease to 5.0 wt.% and 2.0 wt.% respectively. Intra-crystal open mesopores are formed, enhancing the diffusion of biomass originating volatiles with a consequently higher yield in desired products (see figure 10). Although the parent catalyst possesses more Brønsted sites, those becoming inaccessible after coke clogging the micropores. In the parent zeolite, there is formation of toxic catalytic coke in the micropores, which is not present in the hierarchical HZSM-5. The opposite applies for the non-toxic coke precursors [112].

The field of hierarchical catalysts gets more and more interest. With this catalyst modification, diffusion limitations can be overcome, so larger compounds (e.g. PAHs) can more easily diffuse through the porous catalyst. Hierarchisation can occur via desilication or dealumination. This can affect the SAR and mitigate the deactivation of the catalyst. Desilication leads to a higher mesoporous surface area and more active sites are accessible. Due to this higher pore width, coke precursors can pass more easily through the pores without sticking on the catalyst's surface [106].

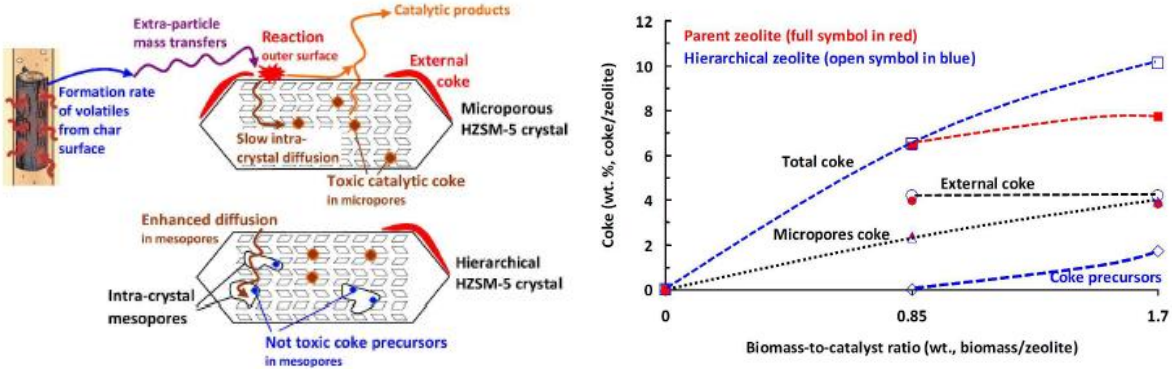

Figure 10a: possible ways of coke formation on a microporous zeolite and hierarchical zeolite. Figure 10b: attribution of each type of coke with their catalyst, also varying with the BM/CAT [112].

In the study of Mukarakate et al., the deactivation of HZSM-5 was followed during upgrading of pine pyrolysis vapours, using a small laboratory reactor. Deactivation of the catalyst was presumably occurring by coking. It initially started at the outside of the catalyst, without affecting the micropores.

The amount of oxygen in the upgraded bio-oil gives an indication of the level of deactivation. The coking rate is influenced by the reaction temperature. Higher temperatures result in lower coking rates, but more cracking happens, also with the formation of NCGs [113]. The researchers plotted the BM/CAT over the resulting oxygen in the oil in wt.%, as can be seen in figure 11. An asymptotic regression was obtained. Starting with a lot of catalyst, compared to biomass, will lead to a serious reduction of oxygen. With higher BM/CAT, this diminution becomes less distinct [114]. In this graph, around a BM/CAT of 4, the catalyst seemed completely deactivated. The oxygen content does not differ anymore compared to a non-catalysed pyrolysis oil.

Figure 12 shows the spectra of various stages during the CFP. The lower spectrum has the least number of peaks. In that stadium, the catalyst is still fresh and only olefins and aromatics are formed. During this process, the catalyst becomes more and more deactivated and more (oxygenated) compounds can be detected in run 12 and especially in run 47. They concluded that the compound range may differ with the amount of coke deposited on the zeolite. Some of those compounds that arise after a while may be first held up, due to their higher affinity for the catalyst [114].

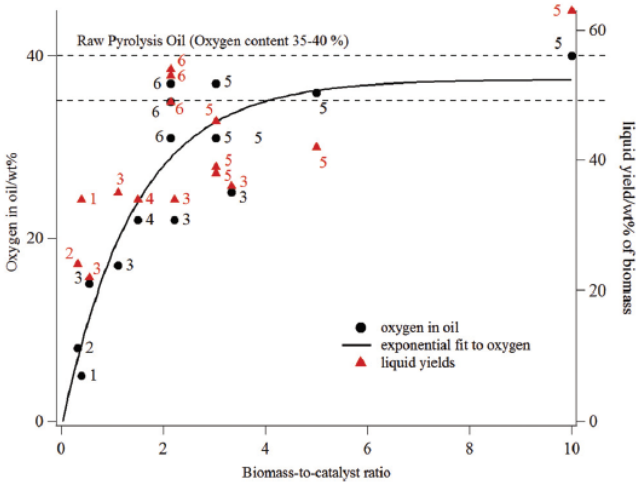

Figure 11: graph representing the BM/CAT over the oxygen content in the oil (left axis) and the total liquid yield (right axis). The line potted through the data is an exponential fit [114].

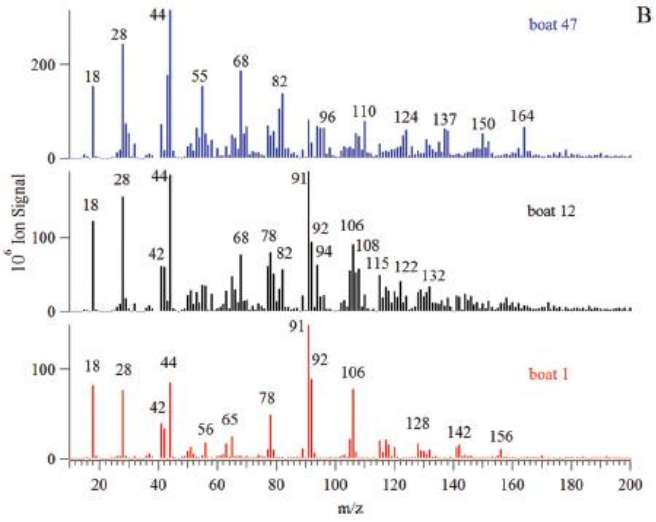

Figure 12: mass spectra of three boats (each containing 50 mg of pine) during CFP over 1 g of HZSM-5. In their set-up, 50 quartz boats, each with 50 mg of pine were pyrolysed one by one. Pyrolysis vapours pass over a catalyst bed of 1 g of HZSM-5. The more boats encountered the catalyst, the more deactivated the catalyst becomes. Boat 12 and 47 are recorded after already respectively 0.6 g and 2.35 g of pine vapours have come into contact with the zeolite. [114].

The pore size of this zeolite is around 5 Å, so heavy primary vapours need sufficient catalytic cracking on the macrosurface to create lighter species that can pass through. Those lighter compounds deoxygenate and polymerise to form olefins. The smallest compounds can escape from the micropores. Olefins retained in the micropores undergo further reactions to form aromatic hydrocarbons by alkylation, isomerisation and oligomerisation [115 - 119]. At the same time, coke formation starts. Polymerisation of aromatic hydrocarbons results in large aromatic complexes that can plug the micropores of the catalyst, with a consequently increasing coke formation.

In another experiment with a comparable set-up, chromatograms were obtained with a continuously raising BM/CAT. Where in the first chromatogram (ratio 0.1) mainly aromatic hydrocarbons like BTX-derivatives, indene and naphthalene were detected, the amount of observed oxygenated products increased with the increasing BM/CAT ratio. Methyl furan, cresol and phenol starts to appear around 0.6. Furthermore, with a ratio of 1.3, lignin primary vapours (2-methoxy-phenol, 4-methylguaiacol) can be recognised in the spectra.

Mukakarate et al. also analysed the catalyst during deactivation. In total four samples were taken, respectively with a BM/CAT of 0.4, 1, 1.7 and 5. In this sequence, coke build up increases with a higher ratio. The more deactivated the catalyst, the higher the surface carbon content but the less rough the catalyst become. N_2 physisorption was executed to research if any coke was formed inside the micropores. All four samples showed a type IV hysteresis, meaning that meso- and micropores are present. If one compares the results of 0.4 and 1, the latter has a lower adsorption capacity over the entire range of pressures, indicating a decrease in pore size uniformity. A higher BM/CAT (like for 1.7 and 5) also leads to a decrease in surface area.

TGA analysis was done to determine the amount of carbon retention on the catalyst. They also differentiate the coke inside the micropores and the coke formed on the mesopores. Till a BM/CAT of 1.7, a linear trend can be deduced. Then, around 6 % of the original biomass was converted into coke. Later, this fraction lowers to 2.5 %. Zeolites quickly lose their water till temperatures of 175 °C. 250 °C is the temperature where the coke starts to oxidise. Out of the DTG curve, two zones of coke combustion can be found: the first one between 500 and 525 °C with the highest rate of combustion and a second one between 575 and 675 °C, which is a not completely separated peak against the first one. Coke with a lot of hydrogen, also called soft coke or type I coke burns at low temperature and contains typically multiple aromatics. Hard coke or type II burns at higher temperatures (around 425 °C) [114].

Zhang and co-workers characterised the coke deposition after CFP of furan, a main intermediate in the pyrolysis process. They extracted the organics of the catalyst and analysed them by HPLC to determine the chemical composition of the coke. The researchers came also to the conclusion that loss of catalyst activity is related to the coke-on-catalyst. Furthermore, the coking rate seems to be dependent of the furan conversion. Around the start of the reaction when more furan was reacting, higher coking rates were observable. Zhang et al. also observed that the product distribution changed over time: in the first 2 minutes, more olefins and aromatic hydrocarbons were obtained, while when the reaction is halfway, product distribution moves more to the aromatic hydrocarbons and aromatic oxygenates [120].

2.5.6 Effect of biomass pretreatment on CFP

Das et al. analysed different leaching procedures to pretreat biomass feedstocks originating from sugarcane (*Saccharum officinarum*) [121]. Sugarcane bagasse and trash (respectively SCB and SCT) seem at first sight excellent input materials for fast pyrolysis. The first type is the remaining solid fibrous material after extraction of the sugar solution. Trash (sometimes also referred to as straw) is mainly left on the field or unvalorised in a cleaning station after harvesting the sugarcane [122, 123].

Leaching agents are used in the first place to reduce the AAEMs, that are capable to disturb the production of levoglucosan and favor the creation of light oxygenates off lesser value (ketones, aldehydes, acids…) [124]. Moreover, as these group I and II elements are present within the char particles, some of them can be transferred by the fluidising gas and end up in the oil, where those elements behave like catalysts that can change the oil quality over a longer period (ageing) [121, 124, 125].

Negative aspects linked to those leaching solutions are a high mass removal (in case of HCl) or environmental issues with HF, HCl or H_2SO_4. Acid pretreatment causes hydrolysis of (hemi)cellulose, resulting in smaller and potentially extractable molecules [121, 126, 127]. Furthermore, nitric acid (HNO_3) can alter chemical interactions between the biomass and its native inorganics [128].

Das and co-workers treated SCB respectively with water, hydrogen chloride (HCl) and hydrofluoric acid (HF). The use of HCl led to a higher ash content after the pretreatment, but that phenomenon was caused by the higher removal of organic components in bagasse compared to the removal of the minerals. The elemental composition of ash was determined with ICP-AES (inductively coupled plasma atomic emission spectroscopy). Alkali metals like Na and K are leached by water, while 5M HCl led to the further removal of Mg, Ca and Al. HF was the best solution as almost all the ash elements were removed with apparently a higher liquid yield. During ash elimination of the feedstock and the subsequent fast pyrolysis thereof, the number of volatiles increase. They undergo a secondary cracking step and form in this way a sooty deposit on the char. As earlier declared, the oil primarily comprises the condensates of the primary pyrolysis vapours. This yield is increased when there is secondary oil cracking to form lighter organic compounds [121].

Rodríguez Machín et al. have done research in the use of SCB and SCT. Before both feedstocks were used, they were subjected to different pretreatment steps to reduce the ash and mineral content. Both types of biomass were treated with HCl, sulfuric acid (H_2SO_4) and citric acid (CA), as well with demineralised water. ICP-OES demonstrated clear reductions of Al, Fe, Si, K, Mg and Na. Ash removal efficiencies of all treatment steps were calculated with Eq. (2.6) and Eq. (2.7):

$$\eta_{ash} = \frac{m_{untr.}.C_{ash,untr.} - m_{tr.}.C_{ash,tr.}}{m_{untr.}.C_{ash,untr.}} . 100\ \% \qquad (2.6)$$

$$\eta_{total} = \frac{m_{untr.} - m_{tr.}}{m_{untr.}} . 100\ \% \qquad (2.7)$$

η_{ash} is the removed ash fraction. η_{total} is the relative mass loss in pretreatment (because not only inorganic elements but also organic compounds can be removed during the leaching process). $m_{untr.}$ en $m_{tr.}$ are respectively the masses of the untreated and treated samples, while $C_{ash,untr.}$ and $C_{ash,tr.}$ are respectively the ash mass fractions in the untreated and treated samples. CA scores the best in that context for SCB, with the total mass loss closest to that of water washing. This acid can be inexpensively produced by fermentation, is less harmful to the environment and can also act as a chelating agent [129, 130]. This effect compensates its weaker acidic nature compared to stronger mineral acids [123].

Furthermore, H_2SO_4 and HCl led to a larger removal of extractives and hydrolysed cell wall compounds which reduced the oil yield in the subsequent fast pyrolysis process, and hence is undesirable. Fast pyrolysis experiments were here performed in the batch operating PY-reactor of the Ghent University's Department of Green Chemistry and Technology and bio-oil percentages are summarised in table 4. There was a significant raise of the oil yield when applying an acid pretreatment step, for both feedstocks. As the ash is removed, the catalytic activity also disappears. While examining the acid pretreated pyrolysis oil, there was a relatively large raise in the share of sugars. The fragmentation of sugars to alcohols, acids or ketones is slower due to the removal of the ash [131]. The amount of phenols and aromatics are very low, so to elevate that portion, CFP can be applied.

Table 4: bio-oil yields of all pretreatment steps for SCB and SCT (every concentration in wt.%) [3].

SCB pretreatment step	**Untreated**	**Water**	**HCl**	**H_2SO_4**	**CA**
Bio-oil yield	54.4	55.0	60.6	60.8	61.3
Oil yield	25.2	29.0	41.0	41.2	42.0
Water yield	29.2	26.0	19.6	19.6	19.3
SCT pretreatment step	**Untreated**	**Water**	**HCl**	**H_2SO_4**	**CA**
Bio-oil yield	45.6	47.9	55.5	60.6	60.3
Oil yield	18.7	17.1	34.8	42.7	42.7
Water yield	26.9	30.8	20.7	17.9	17.5

3. Objectives

Catalytic fast pyrolysis (in short CFP) of biomass holds promise in that it enables the production of aromatics and olefins from biomass. However, previous attempts of the commercialisation of this process have met little success because of the technical challenges CFP needs to overcome. The main problem is the deactivation of the catalyst over time when high amounts of biomass derived pyrolytic vapours are passing over the catalyst. In that respect, the BM/CAT (i.e. biomass-to-catalyst ratio) is a very important variable. With an increase of this ratio, product yields and bio-oil composition will converge back to those obtained under non-catalytic conditions.

There is still more need for insights in how catalyst deactivation can be detected over time. After acquiring those missing links, it will become feasible to make consequent and explicable choices in the future to adapt properties or variables of the pyrolysis set-up, leading to a reduction in catalyst deactivation. To this end, CFP experiments are performed with pine wood in a bench-scale reactor employing different BM/CAT. Analysis of the reaction products (gas, aqueous and organic phase of the liquid, char and catalyst) are executed to get better insight in the occurring trends. Those trends can be whether or not correlated to the deactivation of the catalyst.

Deactivation is mainly originating from coke precursors. Furthermore, it needs to be researched which type of biopolymer(s) are mainly responsible for these coking reactions. Research papers stated that cellulose is the most promising type of biopolymer to produce aromatics. In a subsequent step, pure cellulose was used as feedstock material to pyrolyse in the same set-up and similar BM/CAT were used. In that respect, the specific contribution of cellulose to the coke formation and catalyst deactivation as opposed to the more generic feedstocks like pine wood, can be deduced.

It should be emphasised that the experiments were done on bench-scale, as opposed to a lot of other published studies with similar research goals in which the experiments were carried out in an analytical set-up on a microgram scale. A bench-scale reactor like the mini-plant in this thesis gives a better overview if pyrolysis is met with scaling problems to industrial scale set-ups.

Another issue that can disturb the working and effectiveness of the catalyst, is the presence of mineral matter in the feedstock. These minerals – more specifically those containing alkali and alkaline earth metals (AAEMs) – can change the reaction chemistry in pyrolysis, subsequently altering the yield and the composition of the pyrolysis vapours, resulting in the production of a whole bunch of less desirable products in the pyrolysis oil. Previous research at the Ghent University focused on the removal of those AAEMs from the biomass. It needs to be questioned if the combined effect of a low BM/CAT, pretreatment (demineralisation) and catalyst presence will overcome catalyst deactivation. For that reason, in-situ py-GC/MS experiments were executed with two mineral-rich feedstocks and their demineralised counterparts, namely SCB (sugarcane bagasse) and SCT (sugarcane trash).

4. Materials and methods

4.1. Materials

4.1.1 Biomass

Three types of biomass (pine wood, sugarcane bagasse (SCB) and sugarcane trash (SCT)) and one model compound (cellulose) were used for fast pyrolysis experiments during this research. For the catalytic and non-catalytic fast pyrolysis experiments in the mini-plant (MP), pine wood was delivered by Bemap Houtmeel B.V. (Bemmel, The Netherlands). To introduce this feedstock in the reactor, the particle size must be reduced to between 1 and 2 mm. To obtain this fraction, the pine chips were grinded by UGent Woodlab using a cutting mill (Retsch SM 200). Subsequently, this batch was sorted according their size (> 2 mm, 1 – 2 mm and < 1 mm) with an automatic sieve shaker (Retsch AS 200). Afterwards, proximate and ultimate analyses were conducted to characterise the biomass. Results are shown in table 5. Explanation of each analytical technique is given in section 4.2.2.

Table 5: determination of the pine wood composition and ultimate analysis of cellulose (d.b.: dry basis, a.r.: as received).

Proximate analysis	pine wood	Ultimate analysis	pine wood	cellulose
Volatile matter (g/g d.b.)	0.8591 (± 0.0034)	**C (g/g, d.b.)**	0.5256 (± 0.0052)	0.04232 (± 0.0003)
Fixed carbon (g/g, d.b.)	0.1393 (± 0.0027)	**H (g/g, d.b.)**	0.0609 (± 0.0018)	0.0662 (± 0.0002)
Ash (g/g, d.b.)	0.0016 (± 0.0008)	**N (g/g, d.b.)**	0.0019 (± 0.0008)	0.0000
Moisture (g/g, a.r.)	0.0830 (± 0.0010)	**O* (g/g, d.b.)**	0.4101	0.5106

*Determined by difference, assuming that pine wood and cellulose only consists of ash, C,H, N and O (no S was detected).

In the py-GC/MS experimental procedure, the effect of catalysis and pretreatment on SCB and SCT is explored. Both feedstocks were obtained by Rodríguez Machín from the sugar mill "Ifraín Alfonso" in Villa Clara, Cuba [123]. After drying and milling, a certain amount of both feedstocks was treated with different acids in different concentrations as part of earlier research. Treatment with 0.5 M citric acid for 1 hour at 25 °C seemed to be a promising solution in terms of ash removal and subsequent fast pyrolysis oil yield (see section 2.5.6) [123, 132].

The last material used throughout this thesis experiments, is cellulose. In the MP, small beads (Cellets® 1000, Pharmatrans Sanaq AG, diameter ± 1 mm) of this biopolymer are used. To fill up the dead volume of the biomass hopper (see section 4.2.1), small plastic inert and coloured beads (> 4 mm) were used, covered with a fine sieve to prevent mixing of both solid products. Table 6 gives an overview of all analysis that were done over the biomass and all obtained different reaction products from pyrolysis.

Table 6: overview of the analysis with the different reaction products.

biomass	aqueous fraction (bio-oil)	organic fraction (bio-oil)	catalyst	NCGs
ultimate analysis	elemental analysis	elemental analysis	elemental analysis	μ-GC
proximate analysis	water content	water content	BET surface area	
	GC/MS	GC/MS	TPD-NH_3	
			pore volume	

Moisture content and all other proximate analysis is done in triplicate. This first determination is done according ASTM (American Society for Testing and Materials) procedure E871 and calculated with Eq. (4.1). $m_{BM,initial}$ is the weight of biomass on the plate before putting it into the drying furnace at 105 °C, $m_{BM,final}$ is the remaining biomass weight after drying.

$$water\ content\ [\%] = \frac{m_{BM,initial} - m_{BM,final}}{m_{BM,initial}} . 100\ \% \qquad (4.1)$$

Ash content is performed according to ASTM procedure E1755, with use of Eq. (4.2). m_{ash} is the crucible weight after analysis, and $m_{water\ content\ BM}$ is the biomass weight, multiplied by the water content [%].

$$ash\ content\ [\%] = \frac{m_{ash} - m_{emtpy\ crucible}}{m_{BM} - m_{water\ content\ BM} - m_{emtpy\ crucible}} . 100\ \% \qquad (4.2)$$

Volatile matter of the feedstock can be estimated with ASTM procedure E872 and following Eq. (4.3) and Eq. (4.4). $m_{crucible\ +\ BM,initial}$ and $m_{crucible\ +\ ash,final}$ are respectively the weights of the crucible filled with biomass before and after putting into the muffle furnace at 950 °C for 7 – 8 minutes.

$$loss\ of\ weight\ [\%] = \frac{m_{crucible\ +BM,initial} - m_{crucible\ +\ ash,final}}{m_{crucible\ +BM,initial} - m_{emtpy\ crucible}} . 100\ \% \qquad (4.3)$$

$$volatile\ matter\ [\%] = loss\ of\ weight - ash\ content - water\ content \qquad (4.4)$$

The amount of C, H and N is determined with the elemental analyser (Flash 2000 Organic Elemental Analyser from Thermo Scientific), while the oxygen content is calculated by difference Eq. (4.5). Elemental analysis is used to characterise the elemental composition of the feedstock (pine) and in the aqueous as well as the organic fraction of the bio-oil.

$$O_{content}\ [\%] = 100\ \% - C_{content} - H_{content} - N_{content} \qquad (4.5)$$

Prior to those elemental analyses, ten samples with BBOT standard (2,5-bis(5-ter-butyl-benzoxazol-2-yl)-thiophene), with known elemental composition, must be run to define a calibration curve. Moreover, some blank, piston and baseline runs are obliged before the actual samples can be examined. Afterwards, the sample is prepared in a similar way. A few mg of biomass is weighted with the micro-balance and a tin container is filled with this material prior to introduction into the elemental analyser.

4.1.2 Catalyst

During the literature review, it has become clear that already a lot of research has been conducted with zeolites. The catalyst extrudates used in this thesis are prepared as such: alumina powder (binder), water, an aqueous acid solution and ZSM-5 powder are mixed in a kneader for about 60 minutes at room temperature. Afterwards, the obtained paste is passed through an extruder to obtain long chains of extrudates. Before they are crushed into 1-2 mm sized particles, the catalyst is dried overnight at room temperature. Finally, a calcination step occurs for 32 h, first half of that time at 350 °C and subsequently at 600 °C. Some properties of this type of catalyst are given in table 7.

Table 7: properties of the HZSM-5 catalyst extrudates used throughout this thesis.

SiO_2/Al_2O_3-ratio	23
BET surface area (m^2/g)	307
V_{micro} (cm^3/g)	0.08
V_{total} (cm^3/g)	0.44
Total acidity (mmol NH_3/g catalyst)	0.65 (at 230 °C) 0.27 (at 432 °C)

4.2 Mini-plant experiments

4.2.1 Description of the reactor set-up

During this thesis, fast pyrolysis experiments were executed in a fully controlled mini-plant. The Biomass Technology Group (Enschede, The Netherlands) was responsible for the design and construction of this installation. The plant uses auger reactor technology (see section 2.2.2), so pyrolysis takes place in the screw itself. Up to 500 g biomass can be handled per hour, but usually it was set up that only 200 g/h of biomass was pyrolysed into char, bio-oil and non-condensable gases. Three types of pyrolysis could be performed with this installation: non-catalytic experiments, where only sand is used as heat carrier material. Besides also catalytic experiments are possible. When the reactor operates in the in-situ mode, the catalyst is mixed with sand before it contacts the biomass. In ex-situ catalytic experiments, the principle of vapour phase upgrading is carried out. In this way, the contact of biomass-originating ash and catalyst is avoided [111]. Vapours are moving through a fixed catalytic bed. An additional positive effect is that the temperatures of both reactors can be controlled, which is helpful in controlling the selectivity and product distribution [133].

In figure 13a, a drawing is given of the whole installation. Figure 13b is a picture of the mini-plant. The operating mode for non-catalytic experiments is almost completely the same as for ex-situ catalytic experiments. The only difference is that with ex-situ catalytic mode, the catalytic tube (11) is filled with catalyst extrudates, in non-catalytic experiments, this catalytic tube is bypassed.

An overview of a typical fast pyrolysis experiment in the mini-plant is given here. The biomass (in case of pine usually 2 kg) is fed to its storage hopper (1). The biomass conveyor (5) sends the feedstock to the reactor conveyor (6) where they will be mixed with the hot sand. To make sure the biomass will not decompose before contacting the heated sand, a cooling jacket is placed in front of the first furnace. The sand is stored in a separate hopper (2). The sand conveyor (3 & 4) is heated in the first zone at 520 °C and in the second at 580 °C. The zone after which the biomass reached the reactor conveyor (or auger screw) is heated to a temperature of 545 °C. At the end of this screw, the biomass and the hot sand are mixed intensively with a very short residence time (time span of seconds). At the end of this reactor screw, the content is poured into the in-situ reactor (7) where the sand and biomass are still into contact for a short period. After that period, the pyrolysis vapours pass through the first knock-out vessel (10) where fine char and sand particles are trapped in steel wool present in this part.

Subsequently, the gases leave the first furnace and go over to the second. They move through another steel wool containing knock-out vessel and in case of ex-situ catalysis, also through a tube filled with catalyst (11). At the end of the second furnace, the vapours go to the electrostatic precipitator (ESP, 12), which is cooled with water. The inlet line of the condenser is heated to prevent tar accumulation and therefore also to prevent a lower gas throughput. In the ESP, the remaining dust and aerosol particles in the gas/vapour stream are removed due to electrostatic attraction. The gases are cooled down and condense into a liquid, the so-called bio-oil (13). Some of the condensable gases are not yet completely condensed. These go subsequently to a spiral glass condenser (14) and a cotton wool filter (15). The remaining gases flow into a drum type wet gas flow meter (Ritter TG 3/6, flow rate 300 l/h, 16) and leave the installation via the exhaust system (17). At a junction of the exhaust pipe, a gas sample can be taken for GC-analysis of non-condensable gases (18). Next to the produced gas and oil, there is still a solid phase present in the set-up. The mixture of sand and char formed in the in-situ reactor is periodically discharged in the solid collection vessel (9). The rate of discharge can be controlled by the sluice system (8) situated underneath the reactor. This system has been introduced a few years ago to ensure complete biomass devolatilisation by increasing the solid residence time in the reactor.

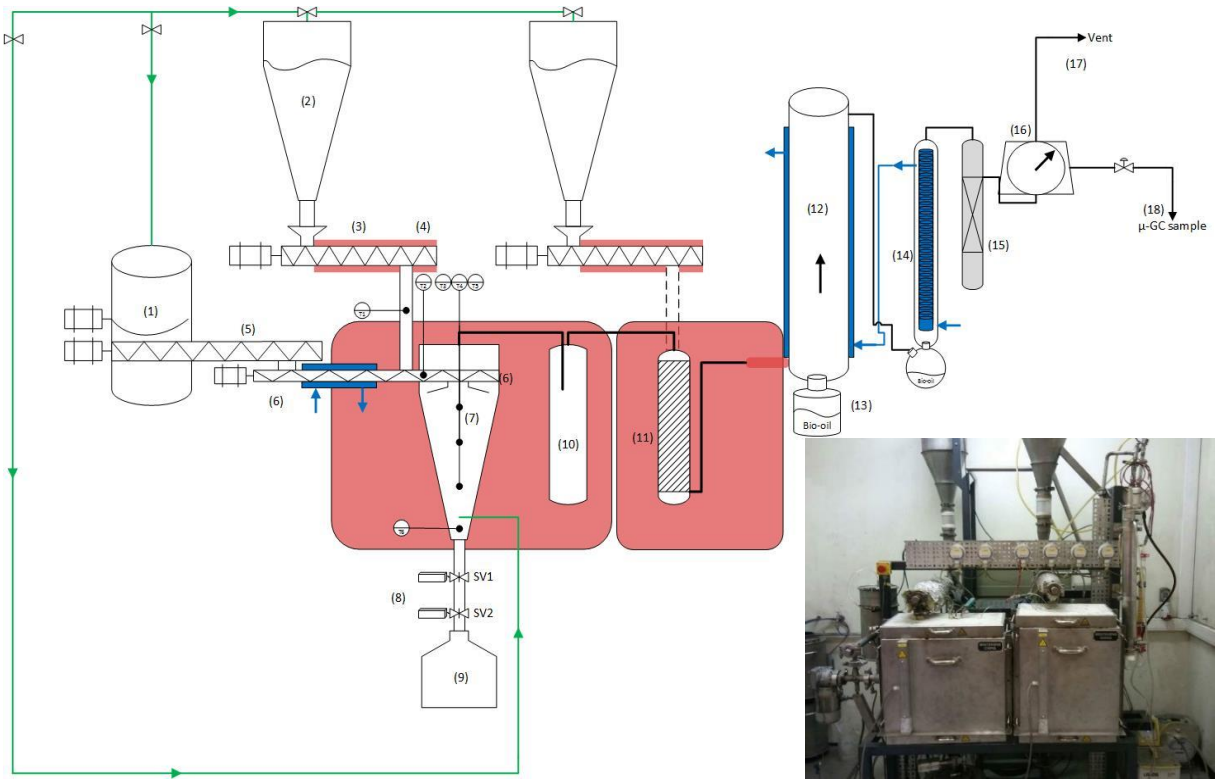

Figure 13a: schematic overview of the MP. (1) biomass hopper; (2) sand hopper; (3) and (4) sand conveyor; (5) biomass conveyor; (6) reactor conveyor with cooling jacket; (7) in-situ reactor; (8) sluices; (9) solid collection vessel; (10) first knock-out vessel; (11) second knock-out vessel or catalytic tube; (12) ESP; (13) liquid collection vessel; (14) glass condensor; (15) cotton wool filter; (16) gas meter; (17) exhaust system; (18) µ-GC sample port
Figure 13b: picture of the fast pyrolysis MP.

Figure 14a gives an overview of the sluices that were installed to overcome the problem that the biomass was not pyrolysed completely. The residence time of the bed material must be controlled carefully. The reactor is equipped with four thermocouples (respectively TI-303, TI-303A, TI-303B and TI-303C), of which their temperature profile can be followed in the software program ADAMView Builder. The sluices may open and close manually or automatically, with a timer that counts the interval time between the opening and closing of the sluices. Especially the temperature of thermocouple TI-303A and TI-303C must be kept constant. Figure 14b shows a typical temperature profile of the pyrolysis reactor under steady-state operation. If the temperature is rising, it means that the bed level is decreasing, so the interval time of the sluices must be lowered to achieve the same bed level. When the temperature starts to decrease, so to react on the bed level that increase in height, the interval time must be increased. After finishing an experiment, the solid collection vessel may not be decoupled immediately, because the formed char is pyrophoric. In contact with air and still being hot, it can easily catch fire. So, after cooling and disconnection, the vessel is sealed with a special cap and clamp [3, 19].

Nitrogen can be purged near the sluices and through both storage hoppers to purge the vapours out of the hot reactor zone, thereby helping to reduce the vapour residence time. Evidentially, nitrogen purging creates an oxygen-free environment which is essential in pyrolysis.

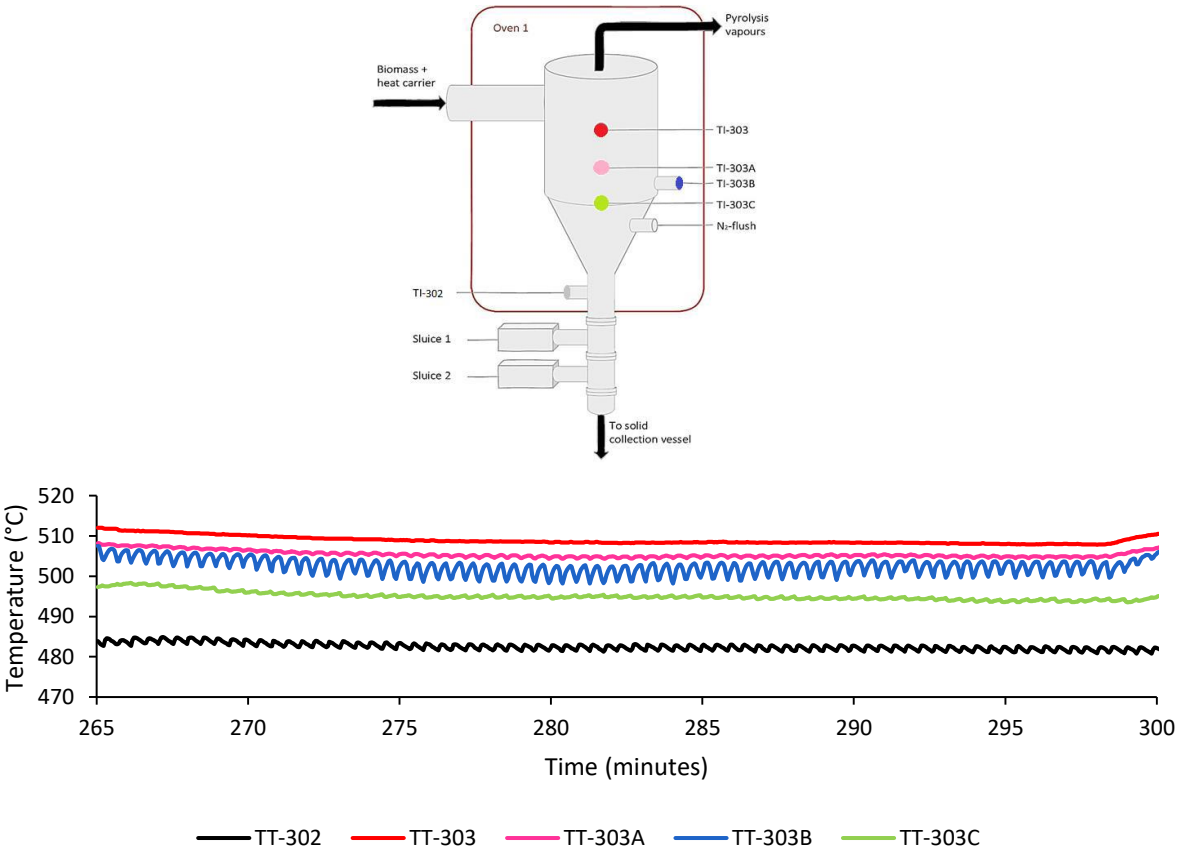

Figure 14a: reactor with the thermocouples and the sluices. Figure 14b: typical temperature profile measured by multiple thermocouples with stable oscillating temperatures around the fast pyrolysis temperature of 500 °C.

4.2.2 Experimental procedure

This paragraph describes the operation of the MP. First, both hoppers must be filled. The biomass and sand are weighted carefully with a balance (Sartorius Combics CW1P1, ± 2 g). Usually 2.0 – 2.5 kg milled and sieved pine and 10 – 15 kg sand are fed to their corresponding hopper. Dried quartz sand is used, with a mean diameter of 250 µm and solid density of 2650 kg/m³ (Compaktuna).

The liquid collection vessel must be tared separately (with balance Kern FCB 3K0.1, ± 0.1 g) together with the ESP and attaching parts, before being mounted outside of the second furnace. During CFP, the catalytic tube is filled with 40 g of fresh catalyst. With a chosen screw frequency of 8.5 Hz, around 200 g/h of pine is fed so a WHSV of around 4 h^{-1} is obtained. For cellulose, this frequency was lowered to 7.5 Hz. It is quite clear that every part of the MP has to be cleaned and no oil residues from a previous runs is still sticking on any recipient attached to the plant before the experiment. Before starting an experiment, the installation must be leak free. To check this requirement, a pressure is build up in the reactor by flushing nitrogen through the hoppers and the sand collector (N_2, Air Liquide, purity ≥ 99.9 %). In the software, it can be followed if the pressure rises very steeply to 50 mbar (chosen set point). If that value is not reached within a considerable time, there is a leak present in the system. To find that spot, every connection must be sprayed with a soap solution and if there are bubbles appearing, it means that there is a leak at that position and the closure must be checked again. During pyrolysis, the nitrogen flow is still on but at a lower level.

When the whole system is leak free, heating elements and the reactor conveyor can be turned on. Every 5 minutes, the sand conveyor is running for 10 seconds to prevent blockages that may occur due to thermal expansion. With opening and closing the sluices, the sand can be discharged from time to

time. When the reactor is completely warmed up (usually after 75 minutes) and the gas flow passing through the gas meter is constant, pyrolysis can start. During the experiment, not only the gas flow but also the gas composition is determined. Its composition can be determined with a micro-GC (see paragraph 4.2.3.2).

At the end of the pyrolysis run, the furnaces are turned off and the installation is allowed to cool down. The biomass is taken out and weighted. By difference, it can be determined how much biomass was pyrolysed within a certain time. The liquid collection vessel must also be reweighted, together with ESP (according Eq. (4.11), see further). In that way, the bio-yield is determined (on weight percentage). If a catalyst is used, it should be taken out of the catalytic tube, sieved and weighted again to have an idea about how much coke was formed (the 'official' coke determination is explained in section 4.2.3.4). After a while when the system is at room temperature, the solid collection vessel can be disconnected and the sand and char mixture are removed out of it.

4.2.3 Analysis of mini-plant fast pyrolysis products

For each MP experiment, a mass balance is made. Usually, this balance needs to be closed as good as possible but a value above 90 wt. % is already acceptable. The biomass in the MP is converted into a solid (char and coke), liquid (aqueous and organic phase of the bio-oil) and gaseous product (non-condensable gases), as can be seen in Eq. (4.6). Yields of every product are marked according $Y_{product}$.

$$Y_{total}\ [wt.\%] = Y_{char} + Y_{NCG} + Y_{aq.\ phase\ liquid} + Y_{org.\ phase\ liquid} + Y_{coke} \qquad (4.6)$$

4.2.3.1 Char yield

Char is burnt off from the char/sand mixture in a muffle furnace at 600 °C for at least 6 hours. The metal tray is weighted before and after and in this way, the char yield (Eq. (4.7)) can be determined. Due to the large amounts of sand and char mixture produced over all MP experiments and the small capacity of the muffle furnace, 1 kg of char/sand mixture could be placed into the oven each time. Because of this elaborate procedure, char yield was only determined for two pine wood and two cellulose experiments. For pine wood, a value of 16.51 wt.% was obtained, while cellulose had a char production of around 12.80 wt.%. Those values for char yields were used in every mass balance of the other experiments in which a direct char yield determination had not been performed.

$$Y_{char}\ [wt.\%] = \frac{\sum_i^n (m_{i,sand\,+\,char} - m_{i,sand})}{m_{feed}} \qquad (4.7)$$

With i corresponding to every tray of 1 kg char/sand mixture put into the furnace and n the total amount of trays. $m_{i,sand\,+\,char}$ is the weight of the tray with sand and char, and $m_{i,sand}$ is the weight of the sand in the tray after burning-off the char.

4.2.3.2 Gas yield

During the heating-up of the reactor, nitrogen is purged. The volume of this inert gas in a certain time is measured with the Ritter gas flow meter. During the reaction, nitrogen and the formed non-condensable gases (NCG) pass combined through this meter. It is possible to calculate the average net

NCG flow rate $\Phi_{g,avg}$ (l/hour) by the difference of the total gas flow rate (first part of Eq. (4.8)) with the nitrogen gas flow determination during heating of the reactor (second part of Eq. (4.8)).

$$\Phi_{\mathbf{g,avg},\,N_2\,\text{free}}\left[\frac{m^3}{s} = \frac{1000\,l}{\frac{1}{3600}\,h}\right] = \left.\frac{\boldsymbol{readout_{final} - readout_{initial}}}{\boldsymbol{t_{final} - t_{initial}}}\right|_{\boldsymbol{total\ gas}} - \left.\frac{readout_{final} - readout_{initial}}{t_{final} - t_{initial}}\right|_{N_2} \tag{4.8}$$

During feeding of the biomass, gas samples are taken with a syringe at the gas meter outlet. Usually, this happens every 5 minutes in the first half hour and afterwards every 10 minutes. Samples can be analysed directly in a micro GC (Varian Micro-GC 490-GC) with two analytical columns: 10 m Molesieve 5A (with backflush) and 10 m PPQ with thermal conductivity detectors (TCD), using helium and argon as carrier gases. Eight different gases can be detected with this GC. In the first column and detector, H_2, O_2, N_2, CH_4 and CO are detected (in order of occurrence of the peaks) and for the second column and detector CO_2, C_2H_4, C_2H_6 and C_3H_6/C_3H_8. The volume percentage and retention time of every of those gases except the carrier gas N_2 is determined. The weight percentage of each gas (m_i) is calculated with Eq. (4.9):

$$\mathrm{m_i}[wt.\%] = \frac{m.\%_i}{m.\%_{total}}.100\,\% = \frac{MW_i \cdot \frac{vol.\%_i}{vol.\%_{total}} \cdot t_{BM} \cdot \Phi_{\mathrm{g,avg,N_2\,free}}}{22{,}41\,l \,.\, 60} \cdot \frac{100\,\%}{m.\%_{total}} \tag{4.9}$$

t_{BM} stands for the time that the biomass was fed. 22,41 l is the volume of gas under standard conditions (273,15 K and 1 atm). MW_i is the molecular weigth of gas i. The total gas yield, without nitrogen is determined with Eq. (4.10):

$$\mathrm{Y}_{gas}[wt.\%] = \frac{m.\%_{total} \cdot \frac{60\,min}{h}}{t_{BM}} \cdot \frac{1}{m_{feed}} \tag{4.10}$$

m_{feed} is the difference between the amount of biomass that was put in the biomass hopper before the experiment and the amount that still is present in that hopper when the process is finished.

4.2.3.3 Liquid yield and separation of the bio-oil

For the determination of the amount of bio-oil, Eq. (4.11) can be applied.

$$\mathrm{Y}_{liquid}\,[wt.\%] = \frac{m_{ESP,out} - m_{ESP,in}}{m_{feed}} \tag{4.11}$$

$m_{ESP,in}$ and $m_{ESP,out}$ are the weights of the ESP (without cooling water), with electrode, liquid collection vessel, brown cap and two clamps before and after an experiment. The difference is the amount of bio-oil produced in the liquid collection vessel and the resting (tarry and sticky) material in the ESP. It is possible to make this calculation based on the difference in weight of the liquid collection vessel, which will be slightly lower than the yield calculated by Eq. (4.11) because then, the oil sticking on the inside wall of the ESP will be ignored. Bio-oil samples were transferred to small Eppendorf tubes and separated with a micro centrifuge for 90 seconds at 7000 rpm. After centrifugation of pine wood bio-oils, the clear top layer consists of the aqueous phase while at the bottom of an Eppendorf the organic phase adheres. There is also a very small amount of water still present in the darker organic layer. For

cellulose pyrolysis oils, it is the opposite: the organic phase is on top of the aqueous phase, so this will contain now lower-density compounds.

4.2.3.4 Coke yield

This last term can be defined in two ways. The first and quick method is to sieve the coked catalyst with a 1 mm sieve to remove the dust between the particles and then the catalyst is weighted again. A more accurate determination is based on the loss on ignition according to Yildiz et al [131]. This is also the used determination to complete the mass balance. A fraction of the catalyst is put into the muffle furnace and goes through a selected temperature profile:

1) From 25 °C tot 250 °C with an increase of 4,5 °C min^{-1} (50 min).
2) Kept isothermal at 250 °C for 40 minutes.
3) From 250 °C to 600 °C with an increase of 6 °C min^{-1} (58 min and 20 sec.).
4) Kept isothermal at 600 °C for 5 hours.
5) Cool down to 105 °C

After this selected temperature profile, the catalyst is weighted again and the difference ($m_{cat,in}$ – $m_{cat,out}$) can be used for determining the coke yield (Eq. (4.12)). m_{cat} stands for the weight of catalyst initially put into the crucible.

$$Y_{coke}\,[wt.\%] = \frac{m_{cat,in} - m_{cat,out}}{m_{cat}} . \frac{40\ g}{m_{feed}} \qquad (4.12)$$

4.2.3.5 Elemental analysis

This procedure is already explained in section 4.1.1. For catalyst samples, the same procedure is used. The only difference is that the catalyst is crushed with mortar and pestle before being added to the sample tin container. For the aqueous and organic phase of the liquid, another type of tin container is used and folded with the available sealing device.

4.2.3.6 Water content

As well for the aqueous as for the organic phase of liquid samples, the water content is determined volumetrically. This is done by an automatic Karl Fischer (KF) titrator (Mettle Toledo V20, 5 ml buret, electrode: DM 143-SC, reagent: Merck Combi Titrant 5 Keto and solvent: Merck Combi Solvent 5 Ketp). This titration is based on following reaction, Eq. (4.13):

$$I_2 + SO_2 + 2\,H_2O \Leftrightarrow 2\,HI + H_2SO_4 \qquad (4.13)$$

In the presence of water originating from the sample, iodine can oxidise sulphur dioxide (both in the aqueous-free KF solvent) resulting in two acids. To keep this reaction in an equilibrium, a base must be added. Two or three drops of the bio-oil sample, with known weight, are added to the reactor and the water content is measured. To know the total water fraction of the bio-oil, Eq. (4.14) must be used.

$$Y_{water} = Y_{aq.} . water\ content_{aq.\ phase} + Y_{org.} . water\ content_{org.\ phase} \qquad (4.14)$$

4.2.3.7 GC/MS

To identify which compounds are present in the produced bio-oil, GC/MS analysis of both phases was executed. In an Eppendorf, 0.20 – 0.25 g of oil, 100 µl of internal standard (fluoranthene (2.5 wt.%) in acetonitrile) and circa 5 g acetonitrile is added and mixed. 2 ml of this tube is taken out with a syringe, filtered through a 45 µm micropore filter and injected into a vial. Subsequently, this mixture is injected in the GC and components are analysed and integrated. The GC, the MS, the column and the operational parameters are the same as used in the micropyrolysis set-up, which are described in following section.

4.3 Micropyrolysis experiments

4.3.1 Description of the micropyrolysis set-up

With this apparatus, fast pyrolysis experiments can be carried out on micro-scale (100 – 500 µg). The micro-pyrolyser (FrontierLab Multi-shot pyrolyser EGA/PY-3030D) is coupled to a gas chromatograph connected to a mass spectrometer (Thermo Fisher Scientific Trace GC Ultra and Thermo ISQ MS), as is shown in figure 15 [134]. This first part incorporates a sampler, a stainless steel pyrolysis tube that can be heated to the chosen temperature (in this case to 500 °C), a heated interface and a deactivated needle directly inserted into the injector of the GC. For GC/MS analysis of liquid samples only, the pyrolyser and catalytic reactor are disconnected and the liquid sample can be injected directly in the injector. The vapours are directly arriving in the GC using a split/splitless injection port with split ratio of 1:100. Created vapours are directly separated in the GC (Rtx-1707 column, 60 m length x 0.25 mm internal diameter x 0.25 µm df), consisting of 14 % cyanopropylphenyl and 86 % dimethyl polysiloxane and the helium carrier gas flow was held at 1ml/min. The GC furnace goes through a predefined temperature profile, starting at 40 °C for 3 minutes, followed by a steady increase up to 280 °C at 5 °C/min. Like the MP set-up, also here three operation modes can be used, as shown in figure 16. After analysis, peak areas are obtained out of a total ion current chromatogram (TIC) and were identified with the NIST MS library. In this thesis, in-situ catalytic experiments of both sugarcane residues was applied. For the ex-situ catalytic pyrolysis, this installation is extended with a secondary small tube quartz furnace (Frontier Tandem Pyrolyser, inner diameter: 5 mm), mounted between the pyrolyser and the GC and containing the powdered catalyst [135], as can be seen in figure 16.

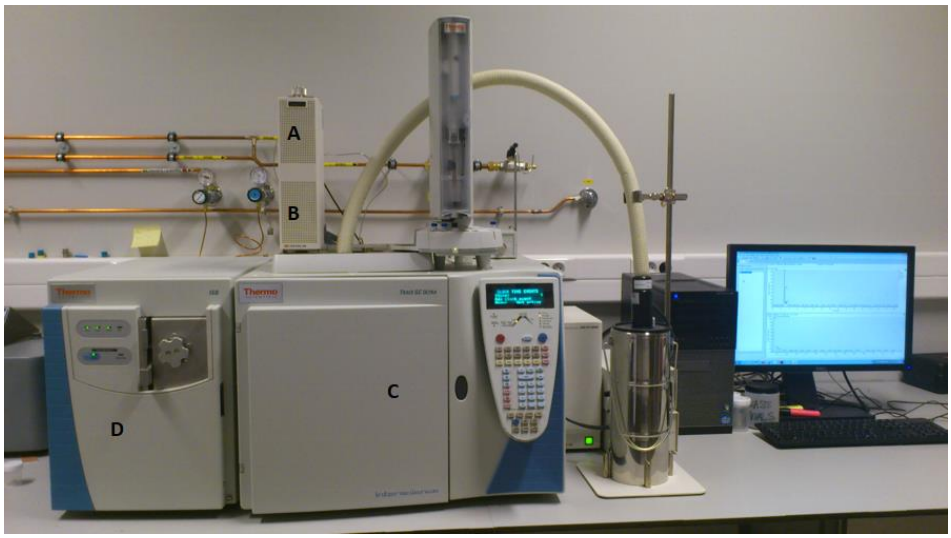

Figure 15: picture of the py-GC/MS set-up in ex-situ mode: (a) pyrolyser, (b) catalytic reactor, (c) GC with split/splitless injection port, (d) ISQ Single Quadrupole MS [134].

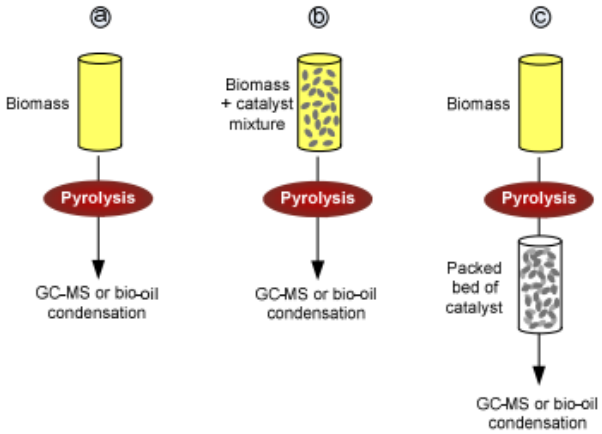

Figure 16a: py-GC/MS without catalyst. Figure 16b: py-GC/MS with catalyst and biomass together mixed in the sample cup (in-situ mode). Figure 16c: py-GC/MS with biomass vapours passing through the packed bed of catalyst (ex-situ mode) [135].

4.3.2 Experimental procedure

For the in-situ experiments, sample cups are filled with the SCB or SCT and, in case of CFP, together with crushed H-ZSM 5. Initial tests demonstrated that a BM/CAT of 1/5 (300 µg BM/1500 µg catalyst) was sufficient for the catalyst's effectiveness. To prevent loss of the sample during micropyrolysis (i.e. the sample cup is dropped into the micropyrolyser) out of the cup, deactivated wool was placed on top of the sample. Using a hook, the sample cup is hung onto the sample holder, which is mounted on top of the micropyrolyser and in this location, the sample cup is held at room temperature. To start the pyrolysis, the sample cup is dropped in the tubular furnace of the micrpyrolyser. Processing of the results occurs in the same way as for the liquid samples analysed on GC/MS.

4.3.3 Data collection and analysis

MP experiments were done twice and the analysis of products in triplicate. Average and standard deviation are the only statistics used for processing the data. Error bars, which demonstrate the average value ± standard deviation, are used in graphs.

Results obtained from py-GC/MS are processed in such a way that the 75 components with highest relative peak area are selected, with for each retention time the three compounds with highest probability of occurrence. Here, every experiment is done in triplicate. Detected compounds are grouped according to chemical functionality. These groups are CO_2, light oxygenates (carboxylic acids, aldehydes, ketones and alcohols), furans, phenols, anhydrosugars, aromatics (mono- and polyaromatic hydrocarbons) and others like N-components, ethers or esters. The cumulative peak area of each group is calculated, and is normalised for all three repetitions to their biomass' weight. Average and standard deviation are determined and graphs are made.

For GC/MS, an internal standard is used. With Eq. (4.15), the amount of a certain compound in the organic or aqueous phase can be calculated, corrected for changes in the response of the internal standard. A_x and A_{IS} are the peak area corresponding respectively to compound x and to the internal standard. C_x and C_{IS} are their corresponding concentrations in wt.%. Prior to analysis, a calibration curve is made of a mixture of possible detectable compounds. When a response factor for each standardised compound is set, the concentrations (in wt.%) of those can be calculated by reformulating Eq. (4.15).

$$Response\ factor\ RF = \frac{A_x . C_{IS}}{A_{IS} . C_x} \rightarrow C_x = \frac{A_x . C_{IS}}{A_{IS} . RF} \qquad (4.15)$$

5 Results and discussion

This section firstly describes the deactivation of the catalyst over an increasing biomass-to-catalyst ratio (BM/CAT), by investigating the evolution of the catalytic reaction products (gas, bio-oil, and coke) in terms of both quantity and quality. The used feedstock for this first series of experiments was pine wood, and in a second phase the model compound cellulose was used.

In a final and more separate part, catalytic py-GC/MS experiments were executed for two types of sugarcane residues :where the effect of an earlier optimised pretreatment method and the effect of catalyst was researched, in order to look under which conditions the most desired valuable and competitive chemicals are created.

5.1 Catalytic fast pyrolysis of pine wood in the mini-plant

5.1.1 Mass balances and product yields

The main goal of this first set of experiments was to examine the influence of an increasing BM/CAT over time in the catalytic pyrolysis process. With higher time-on-stream (TOS), more biomass was fed over a fixed amount of catalyst (40 g). The mentioned times in figure 17 correspond to a particular BM/CAT. For instance, in case of the 20 min. experiment (BM/CAT of 1.6), 64 g of pine wood was fed to the reactor over 40 g of catalyst. The majority of biomass (ca. 85 wt.%) was converted to pyrolysis vapours (condensable and permanent) in the pyrolysis reactor which were then passed over the fixed bed of catalyst. Only the char is discharged before contacting the catalyst into the solid collection vessel. In total, fourteen successful mini-plant experiments were completed, with pine wood as feedstock material. Five experiments in duplicate (10, 15, 20, 40 and 60 min.), and two with higher TOS (120 and 180 min.) were done once, due to high pressure build-up in the reactor. The 180 min. experiment was conducted over two days of 90 min. each, due to this aforementioned issue. Between those two runs, all pipes were cleaned and feeding hoppers were refilled, but the catalyst was not replaced between these runs. Finally, two non-catalytic pyrolysis experiments (both 120 min. long) were also performed, to have benchmark values to compare to the catalytic pyrolysis experiments. During this pine wood study, the biomass conveyor has a fixed frequency of 8.5 Hz, which feeds approximately 200 g pine wood per hour. In that way, the WHSV (mass flow rate of biomass over mass of catalyst) is set to be around 5. In practice with increasing BM/CAT, the WHSV is often found to be between 5 and 6, due to the higher loading of the biomass hopper for the longer experiments.

Figure 17 demonstrates the mass balances of all experiments. All mass balance closures vary between 91.7 wt.% and 101.9 wt.%, which are rather satisfactory values compared to previous mini-plant experiments and other scientific research on this scale [23, 137, 138]. The catalyst facilitates dehydration reactions leading to excessive formation of reaction water and phase separation of the liquid fraction into an aqueous phase and an organic phase. Both phases are a mixture of water and organic compounds. The organic phase is heavier than the aqueous one and sticks on the bottom of the liquid collection vessel. Addendum A.1 shows their concentration in both phases. With higher BM/CAT, the share of liquid yield (water and organics) increases significantly, from 45.75 to 54.20 wt.%. This is due to the quick increase of organics that overcompensate the slow decrease in water with increasing time-on-stream.

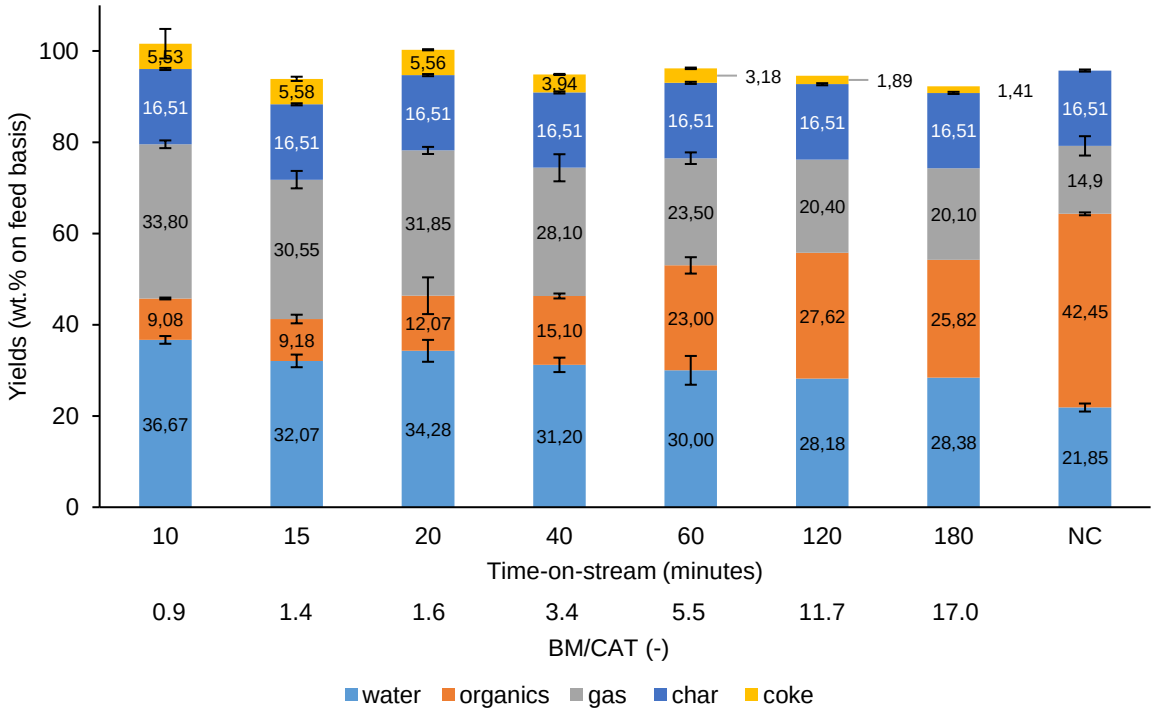

Figure 17: mass balances of the different (catalytic) fast pyrolysis experiments with pine wood in the mini-plant. NC stands for non-catalytic experiment (120 min). Water and organics are present in the aqueous phase as well as in the organic phase.

The general trend of rising organic compound yield is related to the increase in organic constituents in organic as well as in the aqueous phase, as can be seen in addendum A.1. In the bio-oil after 10 min. of time-on-stream, 2.44 wt.% of the aqueous phase consists of organic constituents, whereas this share increases over time to 43.28 wt.% (at 180 min.) with the remainder 56.72 wt.% being water in that phase. There is also a visual difference: the colour of the aqueous phase changes from yellowish orange (10 min.) to a dark brown/black liquid (180 min.). It can be concluded that with the increasing duration of a pyrolysis, this phase tends to a more organic-rich liquid, which makes it harder to separate from the organic phase. This increase in organics and also the general increase in liquid over time starts to resemble more a non-catalytic bio-oil, with an average liquid yield of 64.3 wt.% in the NC run. These observations give a first indication the catalyst is losing its effect over time.

Next to the rise in liquid yields, the yields of non-condensable gases (NCG) decrease with higher BM/CAT. As can be seen in Eq. (4.8) – Eq. (4.10), gas yield is correlated with the flow rate passing through the gas meter. Addendum A.2 gives the wt. % of each NCG. All gases follow the same general decreasing trend. The gas flow that pass the gas meter quickly rises till 10/15 min. of experiment, but after that a maximum is reached, the gas flow rate slowly converges back towards the initial flow rate when only nitrogen gas was purged through the reactor. For short experiments (10/15/20 min.), the average flow rate will be high, because the average is taken over the initial higher flow rates. For longer experiments (60/120/180 min.), the average flow rate is lower, because it also considers the lower flow rates after that peak flow rate around 10 min. The gas yield and composition also converge for higher BM/CAT towards non-catalytic conditions, which gives already a second confirmation about the activity loss of the catalyst.

As stated already in section 4.2.3.1, the char yield does not change a lot with varying BM/CAT as char formation is not influenced by the downstream catalyst. For that reason, the char yield was only determined for two catalytic experiments and its value amounted to 16.51 (± 0.23) wt.% of the total

mass balance. Hence, this char yield value was adopted for the mass balance of all other experiments in which a direct char yield determination was not conducted. This value is higher than the theoretical char yield in fast pyrolysis, which is 12 wt.% but our established value is around the experimental yield of earlier mini-plant research which was 15.70 (± 0.97) wt.% for ex-situ catalytic and 15.90 (± 1.11) wt.% for non-catalytic experiments [2, 23]. Because these values do not change significantly from each other, similar char yields for catalytic as well for non-catalytic experiments were assumed. Higher char yields may be due to higher vapour residence times promoting repolymerisation reactions of primary pyrolysis vapours and possible deviations from heating rate requirements of typical fast pyrolysis conditions [4, 11, 131].

Besides after 20 min., the coke yield starts to decrease. Although more coke-on-catalyst is measured after burning-off the coke for every higher BM/CAT, the additional amount of deposited coke does not increase linearly with the additional amount of biomass pyrolysis vapours that were passing over the catalyst (and the latter is directly proportional to the amount of biomass fed to the reactor). The initially higher coke yield is partially responsible for the low organic liquid yield. At lower BM/CAT, more desired products (aromatics and olefins) are formed, but part of them can undergo secondary reactions on the catalyst surface leading to additional coke formation. Severe deoxygenation conditions are dominating in that time frame (high acidic nature of the catalyst with a SAR of 23 and a low BM/CAT still results in a very active catalyst). This results in a very low organic yield, and a lot of hydrogen is consumed for the dehydration of the primary pyrolysis vapours. For higher run times, there is a coke saturation effect on the catalyst that plays an important role, which explains the non-linear response of the amount of coke-on-catalyst versus the amount of biomass fed to the pyrolysis reactor. A visual difference can be seen when the obtained catalysts are ordered according their BM/CAT: the colour changes from lighter gray to completely black. Also in their paper of catalyst regeneration, Yildiz et al. found a decreasing coke yield after the catalyst had become less active over successive pyrolysis experiments [131]. All those observations agree with the statement of Venderbosch in his critical review of catalytic fast pyrolysis (CFP): he stated that in the beginning of the reaction, reactive pyrolysis intermediates are mostly converted into gas, water and coke and rather to a limited amount of desired organic products (being mainly aromatics) [89]. Making use of lower BM/CAT enhanced the cracking capacity of the catalyst. In that way, more gases, water and coke were produced, together with a consequent reduction in the yield of organics [139].

Hernando et al. researched fixed bed CFP (with a SAR of catalyst is 42) of wheat straw, with a slightly different biopolymer composition compared to pine. They tested eight different BM/CAT, namely 1.4, 2, 2.5, 3.3, 4, 5, 6.7 and 10. With declining quantity of catalyst (the amount of biomass was kept constant here), the bio-oil yield on water-free basis increased almost linearly from ca. 21 wt.% to 52 wt.%. This was accompanied by a decreasing gas yield from ca. 28 wt.% to 10 wt.%, a lowering coke yield of ca. 7 wt.% to 1 wt.%. and a slowly diminishing water yield from ca. 21 wt.% to 18 wt.%. All these pyrolysis products follow the same trend as found in this research, but higher differences in product yields were obtained in Hernando et al. This can be due to several reasons. Firstly, there is a considerable difference in scale: only 4 g of wheat straw was fed, which is more lab-scale instead of the pilot scale of the mini-plant. They also used fixed-bed reactor technology for pyrolysis, which can have its influence on product yield. Besides, the temperature of the catalytic zone was 400 °C, which resulted to a 10 wt.% higher catalytic bio-oil yield compared to when the catalytic tube was held at 500 °C [140].

5.1.2 Deoxygenation of the bio-oil

The catalyst's main function is to reject oxygen out of the pyrolytic compounds that ultimately end up in the bio-oil, in order to obtain a more valuable product. Deoxygenation can be completed via three possible ways: through removal via CO (decarbonylation), CO_2 (decarboxylation) and H_2O (dehydration). Large amounts of water are responsible for the inhomogeneity of CFP bio-oils. A biphasic system arises, which must be separated [2]. In figure 18, the extent to which each deoxygenation mechanism of the catalyst took place, is shown and expressed as CO, CO_2 and water yield in wt.%. These results are presented on a dry feed basis, in that way eliminating the contribution of moisture present in the original pine wood and to only consider the water that was chemically formed during the pyrolysis and subsequent catalysis. The gas composition was considered as an average over the whole TOS indicated, so e.g. the CO and CO_2 yields with an indicated TOS of 20 min. were calculated based on the results of four different gas samples analysed by the micro-GC, samples which were taken every 5 min. of the experiment.

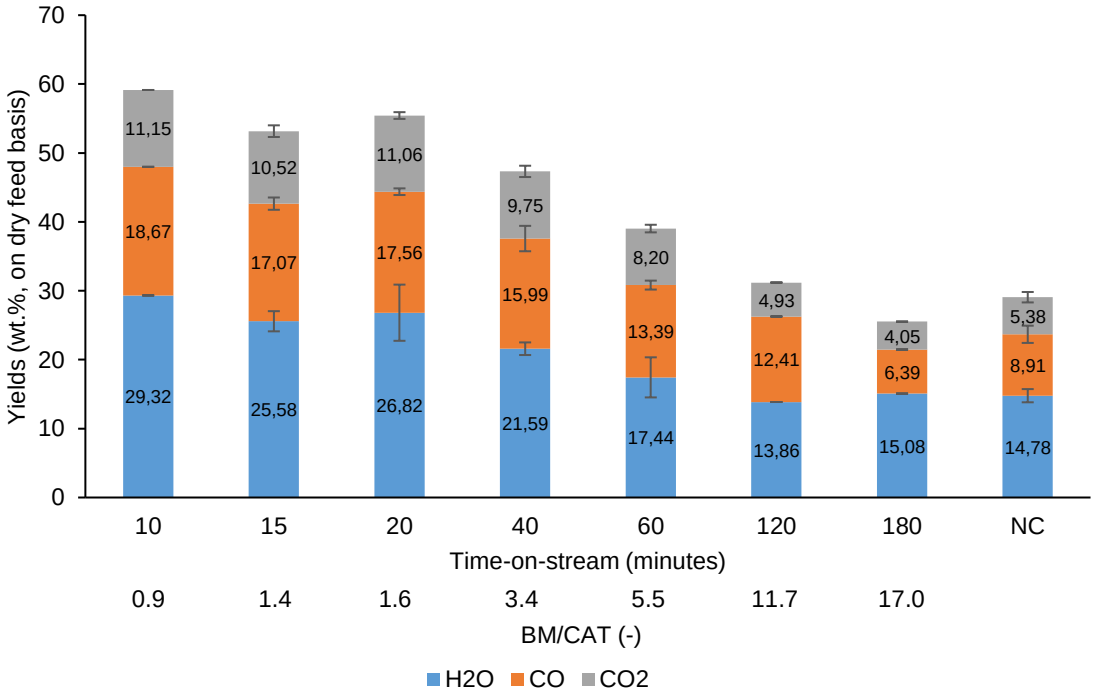

Figure 18: yields of deoxygenation products of the different (catalytic) fast pyrolysis experiments with pine wood in the mini-plant.

In general, oxygen removal decreases with higher run times. Initially, when the zeolite has still a high activity, the deoxygenation capacity is rather high. Figure 18 shows that oxygen removal mainly occurs via dehydration, so a lot of water is formed for the lowest BM/CAT. Wang et al. also reported this trend [136]. This is in accordance with the high share of water for the lowest BM/CAT which could be noticed in figure 17. As the catalyst becomes deactivated, oxygen removal will decrease and will converge to the results obtained without catalyst. In fact, for the 60, 120 and 180 min. experiment, there was no appreciable difference in water yield compared to the non-catalytic result. There is even a small increase from 120 to 180 min. in yield of water, which can be noticed in figure 17, figure 18 and in addendum A.1 (see further). Because the aforementioned experiments were not repeated and the difference is almost negligible, the data is not sufficient for a definitive conclusion. Since the 180 min. experiment was done in two sequential batches, the experimental error might be higher compared to the other sets of experiments. The amount of light oxygenates in the organic phase (see addendum

A.4), which rose substantially for these higher BM/CAT, can also support the decreasing deoxygenation trend.

The reduction of deoxygenation capacity over time is not only evident from the yield in water, but also from the yield in CO_x. Oxygen rejection via CO_2 instead of CO is preferred because in that respect, per carbon atom, twice as much oxygen is removed. Loss of hydrogen is also undesired, because they contribute significantly in the hydrocarbon structure. For all BM/CAT, oxygen removal occurs according this order: dehydration > decarbonylation > decarboxylation. In addendum A.2, a remarkable decrease can be seen in CO and CO_2 over time, respectively from 17.19 to 10.99 wt.% and from 10.63 to 7.15 wt.%. Iisa et al. and Wang et al. also noticed that decarbonylation is favoured over decarboxylation [136, 137]. Together with the high coke content for the lower BM/CAT, the energy efficiency (i.e. chemical energy in the liquid product versus the energy contained in the feedstock) for short time experiments will be reduced drastically.

5.1.3 Assessment of the bio-oil quality

As already explained in the literature review, Venderbosch proposed a way of presenting pyrolysis liquids in a graph by plotting the oxygen reduction (ξ_O, Eq. (2.1)) over the carbon yield (η_C, Eq. (2.2)). In that respect, something can be said about the energetic efficiency of the bio-oil and CFP in a broader context. Here, a similar graph was constructed in figure 19, based on the data of water content determination and elemental analysis, which are listed in table 8 and 9. ξ_O and η_C are both determined on dry feed basis and are listed in addendum A.3. This was done for the organic phases as well as for the complete bio-oil. Nevertheless, for the complete liquids, outliers were obtained and those were only mentioned in addendum A.3, but not represented in Figure 19. The high water content in the whole bio-oil could have interfered in the elemental analysis. A better solution is to determine the TOC (total organic carbon) content via a TOC analyser where presence of water does not interfere with carbon content determination. But, this was not done during this thesis due to the lack of time and the absence of this device in the lab.

In general, because of the severe deoxygenation, it was expected that the oxygen content of the organic phase would be low for low BM/CAT. With increasing oxygen content of the organic phase, the catalyst becomes more and more deactivated. Figure 18 already demonstrated that deoxygenation capacity remarkably decreases with higher run times. Less oxygen is removed and oxygen will end up in the organic phase, resulting in a rise of oxygen content over higher run times. The opposite effect could be predicted for the aqueous phase. As deoxygenation is diminished over time, less water, CO and CO_2 will be formed. Those trends were visible in addendum A.2 and table 8.

Elemental analysis of the organic phases resulted in rather high standard deviations between experiments with equal BM/CAT, and even the standard deviation in three repetitions of one sample can be rather high. This may be due to the fact that preparing those samples was not straightforward. The sample cups must be filled enough and no oil may stick on the outside during sealing. However, regarding the lowest and highest BM/CAT results, the results were more or less as expected. Concerning the elemental yields of N, C, H and O in the aqueous phase, the trend could be more clearly deduced. With increasing BM/CAT, the carbon yield is significantly rising, which approved supported the aforementioned hypothesis. Addendum A.1 also showed a higher share of carbon-containing organics for those higher BM/CAT. Consequently, their oxygen content decrease and converge slowly towards non-catalytic conditions.

Table 8: elemental analysis of all the organic phases and some of the aqueous phases of the (catalytic) pine wood bio-oils. The duplicates for each BM/CAT are presented separately. By the lack of time, not all elemental yields of the aqueous phase could be determined.

		Organic phase, average (± stdev.), on dry basis				Aqueous phase, average (± stdev.), as received basis*			
BM/CAT	**TOS (min.)**	**N**	**C**	**H**	**O****	**N**	**C**	**H**	**O****
0.9	10	0.51 (± 0.44)	76.41 (± 1.51)	6.79 (± 0.21)	16.29				
		0.02 (± 0.04)	77.88 (± 0.58)	6.59 (± 0.08)	15.51				
1.4	15	0.72 (± 0.05)	82.76 (± 0.80)	6.50 (± 0.13)	10.03				
		0.42 (± 0.34)	80.24 (± 1.84)	6.68 (± 0.48)	12.67				
1.6	20	3.18 (± 0.00)	82.79 (± 2.85)	6.28 (± 0.53)	7.75	0.00	3.68 (± 0.49)	3.18 (± 2.63)	93.14
		3.62 (± 0.31)	73.62 (± 0.96)	6.22 (± 0.54)	16.54				
3.4	40	1.32 (± 1.05)	70.63 (± 2.51)	6.32 (± 0.72)	21.72	0.00	11.68 (± 0.29)	6.32 (± 0.58)	82.01
		0.76 (± 0.06)	73.59 (± 1.94)	6.78 (± 0.34)	18.87				
5.5	60	1.85 (± 0.41)	64.13 (± 6.88)	6.98 (± 0.44)	27.04	0.00	14.90 (± 0.13)	7.03 (± 1.70)	78.07
		3.38 (± 0.13)	69.03 (± 1.23)	5.08 (± 0.25)	22.50				
11.7	120	1.99 (± 0.20)	54.38 (± 1.08)	7.30 (± 0.07)	36.34	0.33 (± 0.57)	23.89 (± 0.56)	9.17 (± 0.35)	66.61
17.0	180 (2x 90)	0.71 (± 0.09)	65.24 (± 1.14)	6.77 (± 0.10)	27.28	0.00	20.39 (± 0.92)	8.05 (± 2.60)	71.56
NC***	120	1.74 (± 0.24)	58.40 (± 0.34)	6.52 (± 0.05)	33.34				

*Some aqueous phase analysis could not be completed due to lack of time in this thesis.
**Oxygen content is determined based on difference: O (wt.%) = 100 % - N (wt.%) – C (wt.%) – H (wt.%).
***This non-catalytic bio-oil is single-phase, so elemental analysis (on dry basis) of the whole liquid is presented in table 8.

The results in table 9 match with the lowering water content for higher BM/CAT, which was already deduced in figure 17 and 18. The more abundant (see addendum A.1) aqueous phase is rich in water, and as this phase contains more and more organics over time, its water content decreases and converges slowly to that of a non-catalysed bio-oil. This effect overcompensates the small water increase in the organic phase. Iisa et al. stated that the water content in the organic phase is determined by the miscibility of water within the oil [137]. Most probably, the reason for this unexpected behavior at 180 min. is due to injecting a sample in the Karl Fischer titrator that was not a representative sample of the aqueous phase for that TOS.

Table 9: water content of both phases of the (catalytic) pine wood bio-oils.

BM/CAT	TOS (min.)	Org. phase	Aq. phase
0.9	10		97.55 (± 0.77)
1.4*	15	9.57 (± 1.74) 6.52	96.47 (± 0.38) 97.01 (± 0.78)
1.6	20	12.64 5.00 (± 0.23)	95.55 (± 1.52) 90.56 (± 0.86)
3.4	40	8.14 (± 1.25) 9.29 (± 1.17)	84.90 (± 4.87) 86.90 (± 2.85)
5.5	60	8.96 (± 0.23) 8.63 (± 0.21)	74.47 (± 2.68) 73.92 (± 1.29)
11.7	120	11.81 (± 0.08)	62.98 (± 0.28)
17.0	180 (2x 90)	14.99 (± 0.75)	64.34 (± 2.25)
NC	120	34.35 (± 0.94)	

*From experiment MP (mini-plant)186-2, there was too less oil left to analyse the water content.
**From those short experiments, the amount of water in the organic phase could only be determined once.
***This non-catalytic bio-oil is single-phase, so the water content of the whole liquid is presented in table 9.

Carbon yields over oxygen reductions are plotted in figure 19, and the values are listed in addendum A.3. For the BM/CAT of 1.4, deoxygenation was the highest at all (ξ_O of 97.83), but it was not significantly differing from the experiment a ratio of 0.9, which had an ξ_O of 97.83. Low BM/CAT organic phases have a high deoxygenation capacity, which was already seen in table 9 and addendum A.1. On the other hand, lower deoxygenations are observed for the complete bio-oil, because the high share of water which needs to be taken into account for the calculation. Short time experiments result in the lowest carbon yields, as well for the organic phase as for the complete bio-oil. In the beginning of CFP, high carbon losses are inevitable due to higher formation of NCGs. Besides, also coking rate is higher in the beginning of the reaction [89].

When focusing on the data in the upper left corner of figure 19, a trend can be seen there: for higher BM/CAT, oxygen reduction is decreasing and while the carbon yield is decreasing. The highest oxygen reduction can be attained for lower BM/CAT, but is at the expense of carbon yield. Higher BM/CAT will retain more carbon in the organic liquid phase, but that will lead to a lower degree of deoxygenation. Plotting a linear trendline through those five data points results in a R^2 of 0.95 and a slope of -1.17. The latter means that when the carbon yield increases with 1 %, the oxygen reduction decreases with 1.17 %, although it is risky to extend this regression for the whole graph. Nevertheless, all these data points are situated in region II of severe deoxygenation, according to Venderbosch [89].

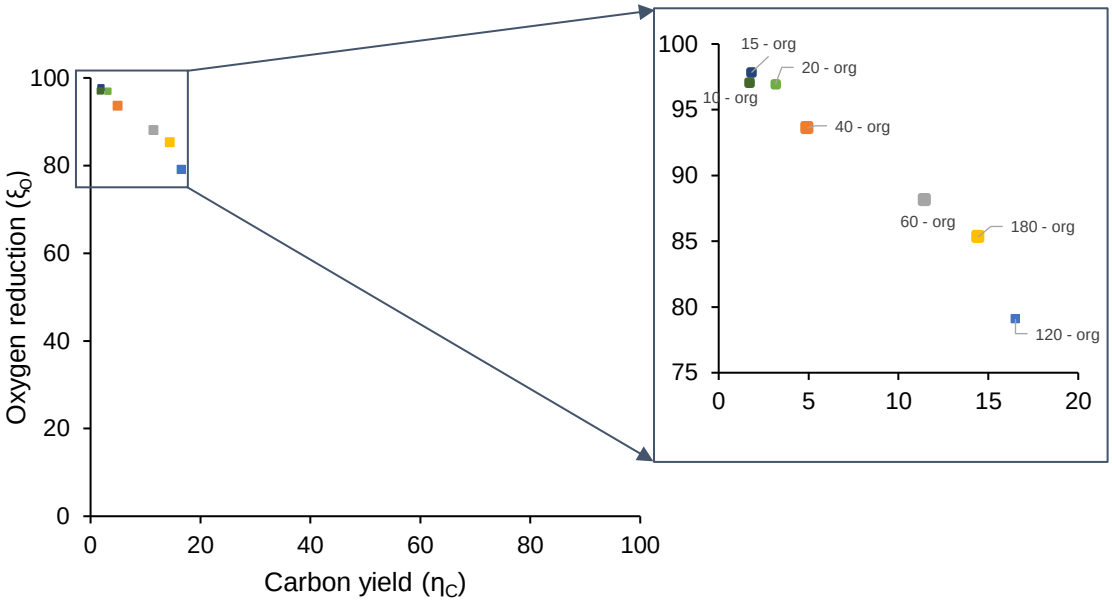

Figure 19: oxygen reduction as a function of carbon yield of the organic phase of catalytic pine wood pyrolysis, on dry feed basis.

There is a relation between the data in figure 18 and figure 19: the ideal mechanism of deoxygenation (so mainly via removal of CO_2) will result in a data point in figure 19 moving to the upper right corner, which is in fact the most beneficial zone to operate in. In that way, a lot of oxygen is removed, while there are still acceptable amounts of carbon present. In practice however, oxygen is eliminated by means of water and CO. In a first phase, there is little deoxygenation taking place when the solid biomass is converted to primary volatiles, char and gas. In fact the elemental composition of the primary volatiles typically is equal (more or less) to that of the original biomass. When more deoxygenation occurs, the major part of carbon already is converted in e.g. gas, char and coke, which also lead to a higher water formation [89].

A trade-off must be made between carbon yield and oxygen reduction, as can be seen in the data points of figure 7 and figure 19. Applying higher TOS can partially overcome the problem of low carbon efficiency, but this comes along with lower oxygen removal and the bio-oil separation will become harder. In that way, liquids will converge in their composition again to bio-oils produced under non-catalytic conditions. Nevertheless, it might shortsighted to be solely fixated on the negative results indicated by this plot. More important to consider is in which compounds and/or functionalities oxygen is incorporated. As Venderbosch also stated, short chain alcohols relatively contain a considerable amount of oxygen but these compounds are considered to be valuable in industry [89]. Regarding the complete pyrolysis liquids, of which the values are listed in addendum A.3, it can roughly be stated that they have similar carbon yields as the organic fraction but they do not score as well in terms of oxygen reduction, since they still contain large quantities water.

5.1.4 Determination of the bio-oil composition

Next to water content determination and elemental analysis, GC/MS was performed for both phases. Due to the use of catalyst, liquid pyrolysis products were easily separated in a more organic fraction (brown to dark, more viscous liquid but still containing a minor amount of water) and an aqueous fraction, which is mainly water mixed with some lighter oxygenated compounds. The higher the TOS, the more difficulties occurred to phase separate the bio-oil.

GC/MS is an appropriate tool to get more insight in the distribution of compounds over time-on-stream. During those analysis, the system was calibrated with a mixture of frequently appearing chemicals in bio-oil, which are listed in the addenda. In that respect, response factors could be determined for those calibrated compounds. Both phases of every liquid sample were dissolved in acetonitrile and also fluoranthene was added as internal standard. According to Eq. (4.15), the wt.% of a certain calibrated compound can be calculated. Addendum A.4 and A.5 give an overview of the most important detected and quantified compounds in the organic and the aqueous phase. Next, the concentration of the organic and the aqueous phase is represented by grouping the individual compounds according to their chemical functionality. These results are presented in figure 20 and 22. For the organic phase, the chemical groups were (mono)aromatics, phenols, polyaromatic hydrocarbons (PAHs), light oxygenates and anhydrosugars. For the aqueous fraction, similar groups were distinguished, except for the aromatic compounds.

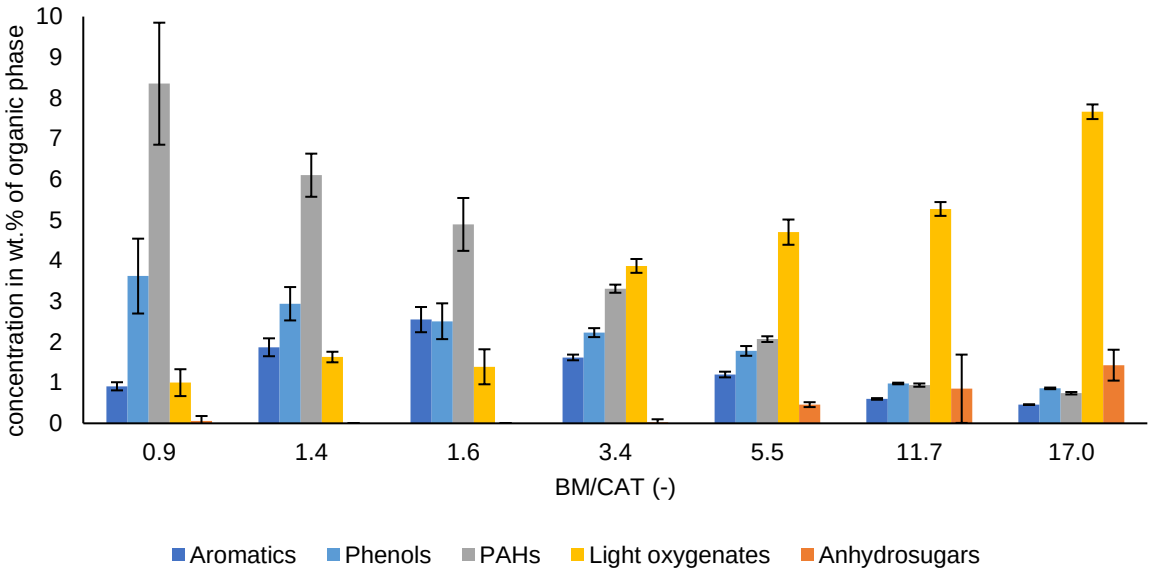

Figure 20: concentration (in wt.%) of different compounds detected in the organic phase of pine wood bio-oil and grouped according to their chemical functionality. Individual concentrations of each quantified chemical are presented in addendum A.4. Compounds attributing to aromatics are: benzene, toluene, o-xylene, m/p-xylene, alkyl- and allyl substituted benzenes and vanillin. Compounds attributing to phenols are: phenol, 2-methoxy-4-methylphenol and alkyl- and allyl substituted phenols. Compounds attributing to PAHs are: naphthalene; 1,2-dihydronaphtalene; alkyl substituted naphthalenes and indene (substitutes). Compounds attributing to light oxygenates are 5-methyl-2-furancarboxyaldehyde; 2,3-butadione; 2,3-pentanedione; acetic acid; propanoic acid; hydroxyacetaldehyde; 1-hydroxy-2-propanone; furfural; 3-methyl-1,2-cyclopentanedione and 2-cyclopenten-1-one and substitutes. The only compound attributing to anhydrosugars is levoglucosan.

In the organic phase, formation of aromatics is desired, as those chemicals can be easily integrated into the current chemical infrastructure. Aromatics originate from all three biopolymers upon catalysis, but mainly from (hemi)cellulose [136]. Lignin does not generate much volatiles (typically less that 10-20 wt.% on d.b.) that can diffuse in the pores of the catalyst [137]. Plotting concentration of aromatics in the organic phase over increasing BM/CAT, a rise can be seen till the value for BM/CAT of 1.6 (20 min.), after which the concentration in aromatics decreases back again. It seemed that in the first 20 min., there is an increase in producing aromatics and this slowly decreases after that time. For the non-calibrated alkyl and allyl substituted benzenes, an estimation of the response factor was made based on calibrated monoaromatics with similar structure. A detailed overview of the composition of these groups is given in addendum A.4. For the substituted benzenes, their concentration changes more slowly over time, with a broader peak concentration around BM/CAT of 1.4 and 3.4.

The highest concentration of detected phenolic compounds was in the first 10 min., corresponding with the BM/CAT of 0.9. With a rising BM/CAT, the concentration of phenols in the organic phase decreases more or less exponentially, starting from 3.62 wt.% to 0.86 wt.%. Lower BM/CAT values (than the ones tested) should be considered to see if the phenol production continues to rise in the lower range of BM/CAT or not. The highest contribution to phenols is by the alkyl substituted phenols, as can be noticed in addendum A.4. Because of the wide diversity in alkyl substituted phenols, they take a significant amount of the total organic yield.

Next to the monoaromatics, PAHs are substantially detected by the GC/MS. From a BM/CAT of 0.9 to 17.0, a remarkably strong decrease in PAHs can be seen, from 8.35 wt.% to 0.86 wt.%. Most abundant chemical here is naphthalene, making up 2.05 wt.% for the lowest BM/CAT tested. The major contribution of the PAHs comes from alkyl substituted naphthalenes which correspond to more than 5 wt.% of the organic phase of the 10 min. experiment. Next to naphthalenes, the other important group of higher aromatics are indenes and indanes. Although indanes have no double bond in their five-ring structure, it is classified under the category of polyaromatics. Other higher aromatics quantified by GC/MS, are phenanthrenes, anthracenes and pyrenes. For those, also no response factor could be determined. Because their peak area was very low, and compared to more abundant compounds which gave already very low yields, these were not taken into account.

Naphthalenes have the highest yield in the organic phase. Those PAHs are known for their slow diffusion in this zeolite type of catalyst. Nevertheless, in the paper of Carlson et al., they speculate that those are formed within the pores and not just on the catalyst surface because of the high pyrolysis temperature (in their case 600 °C), which lowers the energetic barrier [141]. It is also not surprising that the coke yield in the initial phase of pyrolysis is the highest, as this coincides with a peak in PAHs. Because initially, the amount of available active sites relative to the amount of passed pyrolysis vapours is higher, there is also a higher probability that these products undergo further reactions on the catalyst [139].

A fourth category that could be identified, are the light oxygenates. Of these, the most important compounds that could be expected were calibrated for. Here, the highest amount of light oxygenates is identified for the highest BM/CAT. Concentrations in oxygenated molecules range from 1.00 to 7.66 wt.% in the organic phase. Even for the 10, 15 and 20 min. experiment, some compounds like acetic acid, hydroxyacetaldehyde, 1-hydroxy-2-propanone or furfural were not quantified, because they only started to appear at higher BM/CAT.

Finally, also levoglucosan is detected as the only sugar in the organic phase. Surprisingly, for all BM/CAT, except from 1.4 and 1.6, this anhydrosugar could be quantified. Regarding the low concentration and high standard deviation, it cannot be concluded that for the 10 and 40 min. run, whether or not levoglucosan was produced. Although it should be mentioned that with this GC/MS set-up, it is not possible to get a complete overview of all possible sugars present in the bio-oil.

It is a question which BM/CAT results in the best quality bio-oil. Carlson et al. stated that the amount of aromatics can be further increased by making use of higher catalyst-to-feed ratios. In that respect, the 10 min. experiment gives the best result [141]. A lot of studies with varying BM/CAT have been performed with the py-GC/MS technique [114, 136, 139]. Py-GC/MS is an easy tool to test different catalysts and to establish an appropriate BM/CAT, all on microgram scale. It can also help to identify different but still unclear reaction mechanisms occurring during pyrolysis. Most researchers make use of sufficient catalyst (ratios lower than 1) to reduce or to overcome catalyst deactivation. In practice and on larger scale, it is unrealistic to use such high quantities of catalyst compared to the amount of biomass being fed. Another general disadvantage of py-GC/MS is that this technique is not giving a full

representative image of the product obtained with larger scale commercial and industrial set-ups, because e.g. in py-GC/MS the pyrolysis vapours are directly analysed without undergoing a condensation (to bio-oil) step. In that way, comparing results with data obtained of these microgram-scale, analytical set-ups must be done carefully and with a necessary critical mind [131, 142 - 144].

Figure 6 showed the chemical conversion taking place during CFP. The dehydration of cellulose to anhydrosugars is the most important reaction during FP, but with CFP, those sugars are only intermediates, which are further deoxygenated to furans. Further oxygen removal results in a mix of olefins, which can undergo Diels-Alder reactions and subsequent dehydrogenations to form aromatics. Aromatic polymerisation leads to bigger aromatic clusters. These PAHs can be assumed as 'end products' in the reaction scheme proposed by Yildiz et al. [14]. Addendum A.3 also shows the highest concentration for PAHs. Furans are also formed out of hemicellulose and react further to hydrocarbons or coke. Lignin first undergoes a non-catalytic depolymerisation, which yields phenols. Cracking of these products can result in coke or in monoaromatics [2, 14].

Mukarakate et al. (see section 2.5.5) studied the deactivation of the HZSM-5 in a similar way like in this thesis. Making use of a small reactor, BM/CAT varied from 0.05 to 2.50, increasing with steps of 0.05. Roughly, they distinguished three groups of chemical constituents in the bio-oil: group one which contains primarily olefins and aromatics, the second group with furans, phenols and cresols and the last group of furans and lignin primary vapours. Relative concentrations of those groups are presented in figure 21. In the beginning, till a BM/CAT of 0.20 only aromatics and olefins are formed. At that ratio, this first group reaches its top level and the second group starts to appear. Hydrocarbons are collected inside the catalytic pores and after the critical point, they are discharged back into the gas phase. Some hydrocarbons are not released and stay on the catalyst as coke. This carbonaceous material can block the active sites of the zeolite and in that way, compounds of the second group can be formed. At a ratio of 0.60, last group compounds are formed, while the secondary group compounds almost reached their maximum and the hydrocarbons of group one are already decreasing. Around a BM/CAT of 1.60, mainly lignin pyrolysis vapours are formed. Products originating from sugars, like furfural and acetic acid start to breakthrough and their rise converge to concentration found in non-catalytic bio-oils.

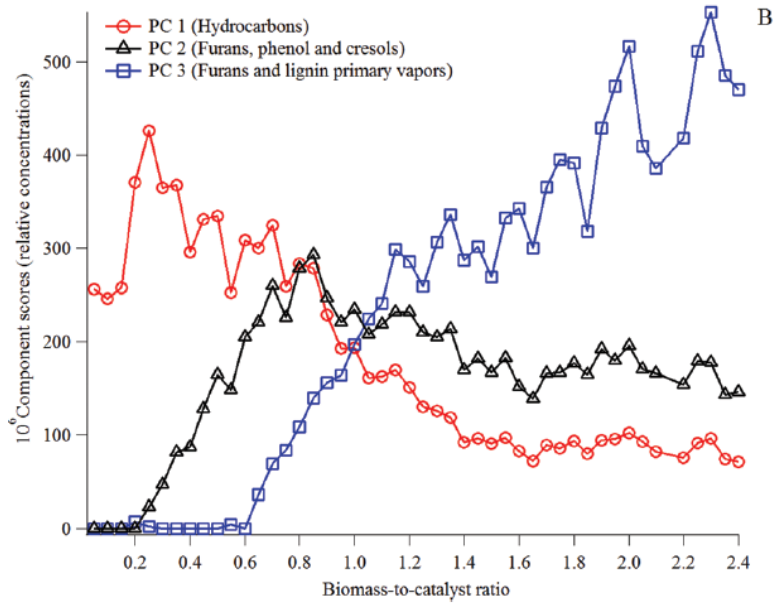

Figure 21: relative concentrations of three groups of compounds as a function of increasing BM/CAT ratio [114].

Figure 22 and addendum A.5 represent the composition of the aqueous phase of the bio-oil. Aqueous phases corresponding with a BM/CAT of 0.9 and 1.4 were not analysed, because the low concentration of dissolved organics would result in a GC response being too low from those short experiments.

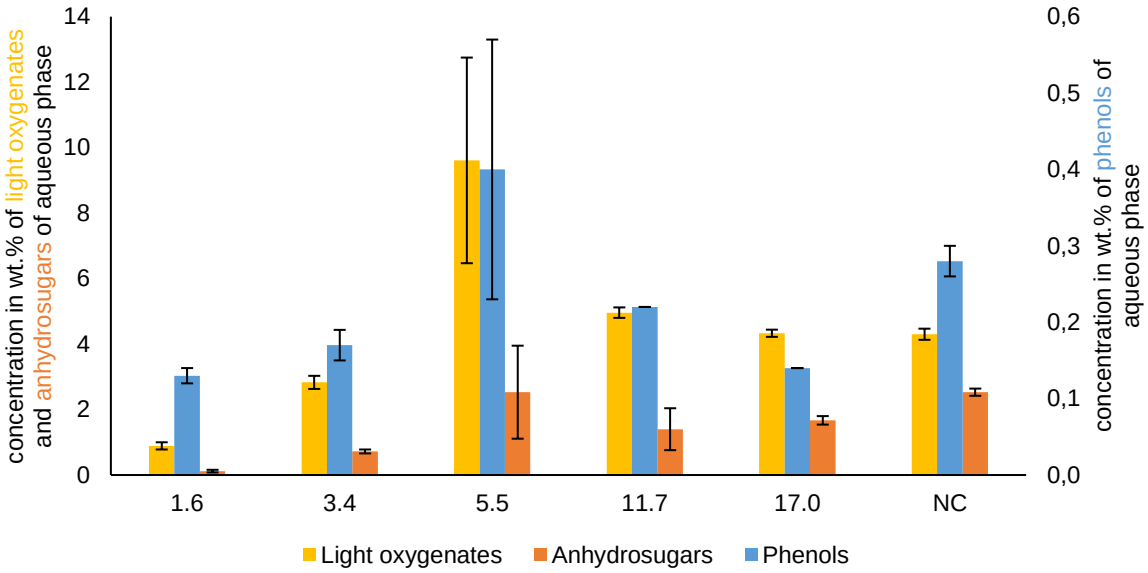

Figure 22: concentration (in wt.%) of different compounds detected in the aqueous phase of pine wood bio-oil and grouped according to their chemical functionality. Individual concentrations of each quantified chemical are presented in addendum A.5. Compounds attributing to light oxygenates are: 5-(hydroxy)methyl-2-furancarboxaldehyde; 2,3-butadione; 2,3-pentanedione; acetic acid; propanoic acid; hydroxyacetaldehyde; 1-hydroxy-2-propanone; furfural; 3-methyl-1,2-cyclopentanedione; 2-cyclopenten-1-one; glycolaldehyde and 1,2-ethanediol monoacetate. Compounds attributing to anhydrosugars are: levoglucosan and other sugars. Compounds attributing to phenols are: phenol, alkyl substituted phenols and hydroquinone.

Just like in the organic phase, phenols were detected. For the organic phase, phenol yield was dropping with higher BM/CAT but for the aqueous phase, a maximum at a BM/CAT of 5.5 can be seen. However, this phenol concentration is still lower than the lowest value achieved in the organic phase. The diversity in phenolic products is also lower, as can be noticed in addendum A.5.

The fraction of light oxygenates is the most important concerning the aqueous fraction of the bio-oil. Similar compounds like the organic phase are detected, supplemented with 5-hydroxymethyl-2-furancarboxaldheyde, hydroxyacetone, 1,2-ethanediol (monoacetate), propanoic acid and 1-hydroxy-2-butanone. In general, all these light oxygenates except furfural follow the same trend as the phenols, with a peak concentration at BM/CAT of 5.5. Chemicals detected in a significant amount are (for 60 min. experiment): hydroxyacetaldehyde (3.07 wt.%), acetic acid (2.53 wt.%) and 1-hydroxy-2-propanone (2.08 wt.%), although these compounds have a large standard deviation for their concentration. The last group are the anhydrosugars, of which levoglucosan is the most important one. Again, the peak concentration is at the BM/CAT of 5.5. Other (anhydro)sugars are not abundant.

If the non-catalytic results are compared to the catalytic ones, it is remarkable that only 41.46 wt.% of the non-catalytic bio-oil is 'characterised'. This is the summation of 7.11 wt.% by py-GC/MS and the other 34.35 wt.% was derived from water, analysed with Karl Fischer titration. In terms of quantified organic fraction, this is much lower than earlier tests, done with the mini-plant. Yildiz et al. published results from non-catalytic experiments with in total 26.23 wt.% of the bio-oil characterised. Nevertheless, it is not fair to judge simply those values, because a more advanced analysis technique (GC x GC-TOF-MS) was used in the work of Yildiz et al.[23].

Just like in the study of Mukarakate et al., a product evolution over increasing BM/CAT based on figure 20 and 22 could be discussed. For the lowest BM/CAT of 0.9, a peak in phenolic and polyaromatic concentration was detected, which starts to decrease after that peak. In that respect, it could be interesting to try lower ratios and see if more PAHs and phenols are formed. There is a rise of benzene (derivatives) continuing till a ratio of 1.6, after which it also starts to decrease. Meanwhile, more and more light oxygenates are formed, with a maximum detected in the organic phase at a ratio of 1.6. From that ratio, also sugar formation started, with a maximum at BM/CAT of 5.5. Further from that ratio, all concentrations are decreasing in the aqueous phase. In the organic phase, light oxygenates and sugars keep on increasing, but that originates from the bio-oil which became harder to separate. Assuming both phases, it can be concluded that the general bio-oil composition converges to non-catalytic bio-oil as the BM/CAT ratio is increased. The authors of the article state that around a ratio of 1, light oxygenates are starting to appear in the product stream, which is confirmed here [114]. To compare their findings with this study, lower BM/CAT must be tested in the future. To make that feasible, more catalyst and/or lowering of the WHSV will be necessary, otherwise there is almost no organic phase to sample for analysis.

5.1.5 Characterisation of the deactivated catalyst

According to Mukarakate and co-workers, coke is formed from polymerisation of aromatic hydrocarbons and/or condensation of unreacted lignin primary vapours. In figure 6, it can be seen that coke formation can come from different reaction steps [14, 114].

Strong acid sites also play an important role in the formation of coke precursors. These precursors undergo condensation reactions to produce large polynuclear aromatic molecules coating the surface of the catalyst. As the used catalyst has a high acidity (SAR of 23), more severe deoxygenation occurs which results in a lower oxygenated liquid product, but nevertheless also in very poor bio-oil yield [100]. Strong acid sites in the used catalyst have been proven to be more active for CO removal instead of CO_2 elimination from oxygenates during CFP. Wang and co-workers also found a perfect correlation between the aromatic yield and catalytically removed CO. They assumed in that way that oxygen products pass over the zeolite and through decarbonylation, these were converted in reaction intermediates that immediately go over into aromatics [135, 145 - 148].

Fresh and the deactivated zeolite were subjected to several analyses, like L.O.I. (loss on ignition, i.e. burning-off the coke-on-catalyst with static air) analysis, elemental analysis and determination of BET surface, acidity and pore volume. Those last three determinations were not done with the spent catalysts during this research, but with spent catalysts obtained from prior experiments conducted under near-identical conditions. Elemental analysis of crushed catalyst samples was done in order to determine how much wt.% of C and H was deposited on the catalyst. The results are shown in addendum A.6 and the H/C ratio is plotted against time-on-stream in figure 23.

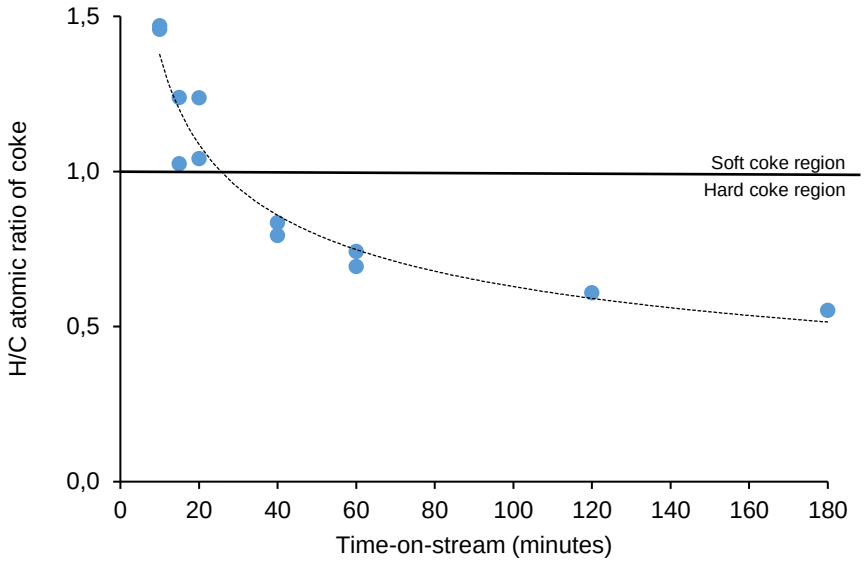

Figure 23: H/C ratio in the coke-on-catalyst of the different catalyst samples collected after fast pyrolysis of pine wood.

For the lowest TOS, there is a clear drop in H/C atomic ratio, which for higher TOS converges to a constant H/C ratio of 0.5. When the exponential trendline exceeds the point of equal hydrogen and carbon, the coke deposited on the catalyst is not called soft coke anymore, but it goes over into hard coke. With lower coke yield, the H/C atomic ratio also declined. Coke rich in hydrogen or type I coke burns at lower temperatures, whereas type II coke burns at higher temperatures [114]. Because the small pores of HZSM-5, coke on this type of catalyst oxidises at higher temperatures than coke on other catalysts [100]. Hernando and co-workers found a H/C ratio from 2.13 to 1.09 as the BM/CAT varies from 1.43 to 10, which slightly differs with results in this thesis [140].

Catalyst acidity was measured by an ammonia - temperature programmed desorption (NH_3 -TPD) method using the Micromeritics Autochem II 2920 Chemisorption analyser. BET surface area and pore volume determinations were conducted using Micromeritics TriStar II surface and a porosity analyser. Results are given in addendum A.7, addendum A.8 and figure 24. The figures are respectively presenting those analyses in function of TOS and coke-on-catalyst. Those analysis were conducted at the Research & Technology Center of Total at Feluy (Belgium).

BET surface area decreased linearly with the coke-on-catalyst, as is represented in figure 24 (R^2 of 0.98). The more coke covers the catalyst, the less surface area is available for further reaction. After 3 hrs. of CFP, the surface area decreased just around 70 % from the initial value. With higher BM/CAT, surface roughness drops and the carbon content of the surface rises due to deposition of a carbonaceous film blocking the pores of the catalyst and deactivates the catalyst as such. Also a decreasing trend in surface area was noticed in the study of Mukarakate et al., although surface area seemed to decrease more rapidly in their study between BM/CAT of 0.4 and 5.0, compared to results of this research. This difference between both studies could be attributed to the smaller scale they worked on and the fact they used an earlier regenerated catalyst which may lost part of its surface area. Mukarakate et al. also did not mention the SAR of their used catalyst, although it is an important parameter [114]. The higher the SAR, the lower the number of active sites which results in an already lower initially acidity [83]. Bartholomew stated that the higher acid strength, the higher the rate and extent of coke formation [100].

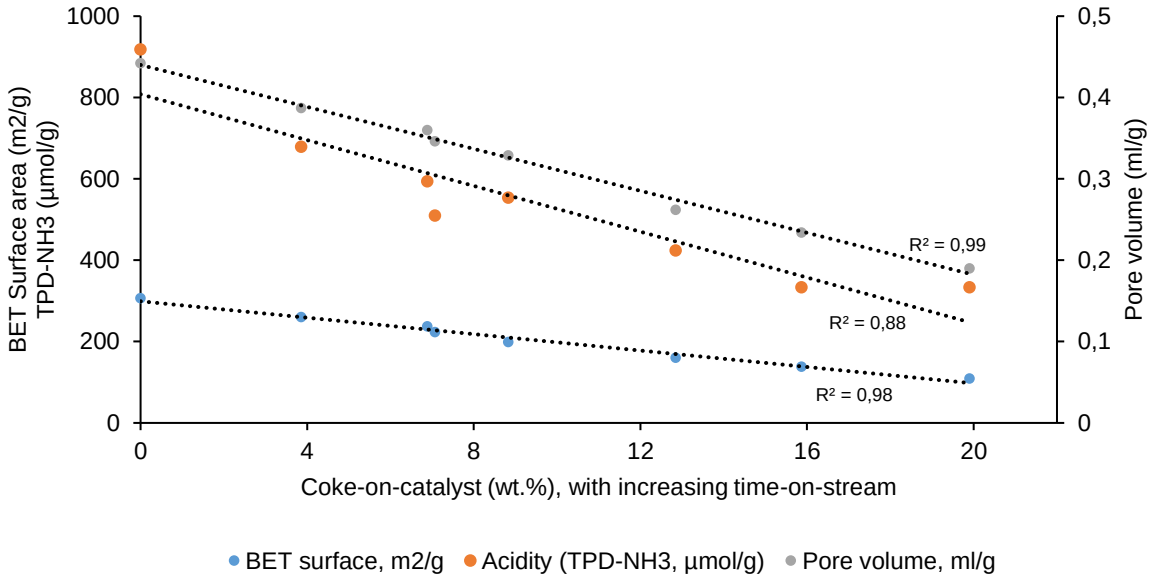

Figure 24: BET surface area, TPD-NH_3 and pore volume in function of coke-on-catalyst of the different catalyst samples collected after fast pyrolysis of pine wood.

Similar decreasing trends (compared to BET surface area) were found for acidity and pore volume. Both properties decreased to respectively 34.64 and 37.10 % of their original value. Acidity, but mainly pore volume declined with a clearly linear trend, shown in figure 24b (R^2 of 0.99). Again, similar observations are reported in the study of Mukarakate et al. [114]. Less pore volume means that less primary vapours can diffuse into the pores and a lower conversion of those vapours to the preferred aromatics will be the result. As the coke is building up in a pore, there is less space available the form additional coke layers, which results in a decreasing coke yield over increasing BM/CAT. Iisa et al. conducted similar acidity analyses for fresh and spent catalysts (a ZSM-5 type, with a SAR of 30, compared to 23 for the extrudates used in this study): initially, the NH_3 desorption was just above 800 mmol/g and this decreased to less than 400 mmol/g as the catalyst was deactivated after a BM/CAT of 1.52. The same conclusions are valid for the acidity: a catalyst with lower acidity has less deoxygenation capacity, which results unavoidably in a bio-oil richer in water, light oxygenates and less (aromatic) hydrocarbons [137].

Studies to determine coking on catalyst were also done on biomass derivates. Zhang et al. completed this for furan as feedstock. As seen in figure 6, furan is an intermediate of the biomass pyrolysis pathway. The loss of the catalyst's activity is associated with coke deposition on the zeolites. Early in the reaction, a higher furan conversion over the zeolites resulted in a higher coking rate. The coking rate seemed to be related to the furan conversion [120].

5.1.6 Conclusion

In this first experimental section, the influence of different BM/CAT in CFP of pine wood was researched in the mini-plant. Due to deactivation of the catalyst, product yields changed with increasing BM/CAT and converged again to the yields of non-catalytic pyrolysis experiments. In the next section, a similar set of experiments was carried out with cellulose, which seemed to be a more promising feedstock to produce high value chemicals in higher concentrations.

5.2 Catalytic fast pyrolysis of cellulose in the mini-plant

5.2.1 Mass balances and product yields

Of the three main constituents of biomass, cellulose appeared the most interesting source to produce high value chemicals [114, 136]. Next to pine wood, also the CFP of cellulose was researched with the mini-plant. Here, only five different BM/CAT were tested, of which all were performed in duplicate, except the first one. Because the very low oil yields, the 10 min. experiment was carried out twice but the liquid of those two experimental runs were collected in one liquid collection vessel. Only the catalyst was renewed during those two experiments, in order to have two samples. Catalytic experiments of more than one hour were not executed because again, pressure problems started to occur when feeding more than six times the amount of biomass over the amount of catalyst. For non-catalytic experiments, already after 30 min., the pipes of the mini-plant are getting blocked by formation of some tarry residue, which could affect the calculations and analysis in a negative way. In order to have a WHSV of around 5, again the biomass flow rate must be set at 200 g/h. For small cellulose pellets, the feedstock conveyor frequency was again determined with a cold flow test and was set at 7.5 Hz.

Concerning the mass balances of the catalytic cellulose experiments, which are all presented in figure 25, they all have a mass balance closure between 92.6 wt.% and 100.2 wt.%. There was one non-catalytic pyrolysis experiment with a lower total yield of 85.9 wt.%, which finally also was taken into account. Again, the catalytic bio-oils were separated in two clear distinctive phases. Unlike with pine wood, the dark organic phase is here on top of the aqueous layer. Addendum B.1 also gives the phase distribution of water and organics over both phases. In terms of product yield, the aqueous phase of bio-oils produced over higher BM/CAT tends to converge more towards the organic phase, which was also the case for pine wood. From 10 to 60 min., the share of organics in the aqueous phase rises from 7.75 wt.% to 37.51 wt.%. The amount of water in the organic phase does not differ that much regardless of the run time, because in all those run time experiments, not more than 3.47 wt.% of water was detected there (see further in table 11).

In the sequence of 20 to 60 min. TOS, the water yield is dropping. This trend was also observable for pine wood. From figure 25 and the data in addendum B.1, again it can be concluded that the organic yield is increasing with longer duration of pyrolysis. Initially, 19.76 wt.% of the liquid was composed of organic constituents, whereas this number increased up till 45.17 wt.% for the 1 hr. experiment. The share of water for a 60 min. catalytic experiment almost equals to that of a non-catalytic run but there are still less organics (in terms of yield in wt.%) being produced.

The increase of liquid yields over higher BM/CAT is observed again with a decrease in gas yields. Compared to fast pyrolysis results without catalyst, there is still a large difference with the highest BM/CAT of 6.2 (24.00 wt.% compared to 8.15 wt.%). Char yield was determined twice, in the way it is described in section 4.2.3.1, and it is assumed to be identical for fast pyrolysis with or without catalyst. The same declining trend in coke yield was observed for cellulose with increasing BM/CAT.

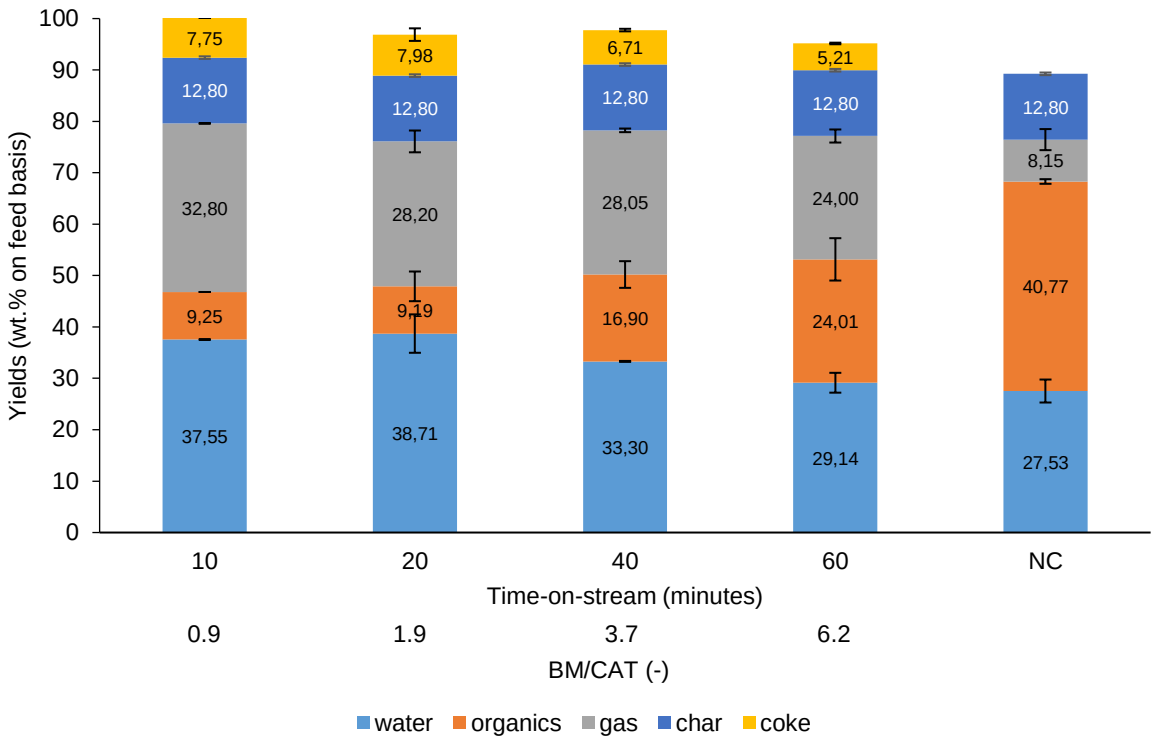

Figure 25: mass balances of the different (catalytic) fast pyrolysis experiments with cellulose in the mini-plant. NC stands for non-catalytic experiment (30 min). Water and organics are present in the aqueous phase as well as in the organic phase.

If cellulose and pine wood are compared for similar BM/CAT, there are resemblances and some differences. In terms of liquid yield, there is not that much difference for similar BM/CAT. With non-catalytic experiments, the biggest difference in total liquid yield was observed, which was on average 4 wt.% in advantage for the cellulose bio-oil (68.3 wt.% and 64.3 wt.% respectively). Nevertheless, with cellulose, 5.68 wt.% water is additionally produced compared to pine, and consequently the organic yield of pine wood yields 1.68 wt.% more organics. Furthermore, if only catalytic results are assumed, there is no significant difference in gas yield for similar ratios. This is in contrast with the non-catalytic experiments: there is a considerable difference in gas yield (14.90 wt.% to 8.15 wt.% for respectively pine wood and cellulose). Also char yield is 3.71 wt.% higher for pine instead of cellulose. Compared with other studies on cellulose pyrolysis, the char yield reported here is still high because of higher vapour residence times. Karanjkar et al. and Yang et al. reported respectively 6 and 7 wt.% char for cellulose pyrolysis [149, 150]. For every pyrolysis temperature, cellulose produces less char than hemicellulose and lignin. For sure this last one is very thermally resistant and lignin originating intermediates have the tendency to repolymerise easily which can explain the high char yield for this biopolymer [135]. Also a comparison in coke yield was done between both feedstocks, which were remarkably higher for cellulose. In total, it can be concluded that fast pyrolysis of cellulose results in a mass balance approximately the same as for pine wood.

5.2.2 Deoxygenation of the bio-oil

When analysing the deoxygenation graph in figure 26, it can be seen that same deoxygenation trends as for pine wood were observed here. Except for the 60 min. experiment, but in all other cases dehydration is the most dominant deoxygenation mechanism. For the non-catalytic experiment, there is almost only deoxygenation via dehydration. Yields of decarboxylation and decarbonylation in the catalytic experiments are slowly converging to the non-catalytic results, but there is already less

dehydration than without use of a catalyst for the two highest BM/CAT. When the BM/CAT of 6.2 is achieved, there is almost no more deoxygenation compared to conditions without catalyst (in total 31.86 wt.% compared to 28.65 wt.%). For pine, this difference was almost 10 wt.% compared at that TOS (in total 39.03 wt.% for the 60 min. with catalyst compared to 29.07 wt.% of the non-catalytic result). This can indicate that the catalyst's lifetime is shorter and hence, deactivates faster, for cellulose experiments instead of pine wood experiments. Nevertheless, it needs to be stated that for that TOS of 60 min. the BM/CAT 6.2 is, compared to 5.5 for pine wood.

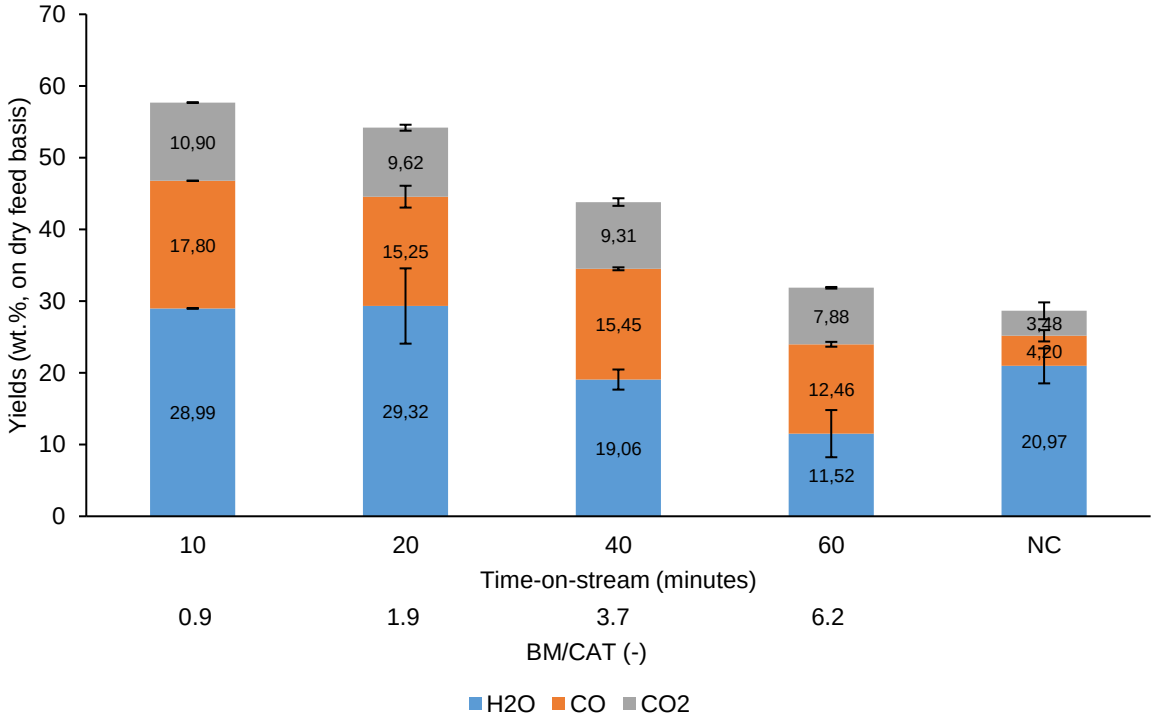

Figure 26: yields of deoxygenation products of the different (catalytic) fast pyrolysis experiments with cellulose in the mini-plant.

As the coke yield is higher for cellulose experiments than for pine wood for similar BM/CAT, it can be assumed that coke is formed due to a significant amount of cellulose-derived pyrolytic intermediates. Wang et al. also mentioned in their paper that catalytic coke mainly is derived from (hemi)cellulose and to a lesser extent of lignin, which has a higher contribution to char formation [135]. When too much dehydration occurs, there will be too less hydrogen left in the vapours, which complicates the creation of aromatics. In addendum B.2, the gas composition (in wt.%) is mentioned of the NCGs produced during CFP and FP of cellulose. Similar trends can be seen in that table as were obtained for pine wood, from which the strong decrease in CO and CO_2 over time is the major observation.

5.2.3 Assessment of the bio-oil quality

Elemental analysis was conducted for the cellulose samples. Because the lack of sample cups, only one analysis (in triplicate) was done for each TOS. Out of the results reported in table 10 and 11, it can be concluded that for the organic-rich phase, there is a lowering of the carbon yield over time, at the expense of oxygen. The aqueous phase on the other hand, shows an opposite trend with increasing carbon content during operating on a higher BM/CAT. Analysing the water content of the aqueous phase, it follows the same trend as for pine wood pyrolysis. Regarding the repeatability of the different analyses, average values of similar BM/CAT experiments differ a lot but the decreasing trend is still observable. Due to the high amount of sample that was necessary to introduce in the Karl Fischer

titrator, water content of the organic phase could not be determined for the very short cellulose experiments. Furthermore, only one analysis was possible for the 40 and 60 min. experiment. To still create a plot of oxygen reduction over carbon yield, the average water content of the four analysed organic phase samples was assumed for 10 and 20 min. experiment. This could be done in this way because they all contain very little amounts of water.

Table 10: elemental analysis of some organic and aqueous phases of the (catalytic) cellulose bio-oils.

		Organic phase, average (± stdev.), on dry basis				Aqueous phase, average (± stdev.), as received basis			
BM/CAT (-)	**TOS (min.)**	**N***	**C**	**H**	**O**	**N***	**C**	**H**	**O**
0.9	10	0.80 (± 0.14)	87.67 (± 1.41)	7.98 (± 0.15)	3.56	0.39 (± 0.55)	3.25 (± 1.19)	9.07 (± 3.55)	87.30
1.9	20	0.80 (± 0.12)	81.64 (± 2.33)	7.56 (± 0.27)	10.00	0.63 (± 0.03)	7.87 (± 0.13)	11.01 (± 0.06)	80.50
3.7	40	0.71 (± 0.19)	78.83 (± 0.03)	7.30 (± 0.03)	13.16	0.35 (± 0.30)	13.13 (± 0.43)	10.23 (± 0.26)	76.29
6.2	60	0.93 (± 0.09)	77.34 (± 1.96)	7.24 (± 0.27)	14.49	0.62 (± 0.07)	17.06 (± 0.58)	10.00 (± 0.23)	72.33
NC	30 (NC)	1.02 (± 0.05)	55.32 (± 0.57)	5.92 (± 0.30)	37.74				

*Table 5 confirmed there is no nitrogen present in the fed cellulose pellets, so the nitrogen that was detected here, can be assumed as an error of the nitrogen analysis.

Table 11: water content of both phases of the (catalytic) cellulose bio-oils.

Experiment code	TOS (min.)	Aq. phase	Org. phase
0.9*	10	92.26 (± 0.83)	2.56
1.9*	20	92.89 (± 0.78) 87.33 (± 1.06)	2.56
3.7**	40	78.91 (± 1.83) 73.50 (± 0.94)	3.12 1.88
6.2**	60	56.87 (± 2.76) 67.60 (± 1.25)	3.47 1.79
NC***	30 (NC)	41.47 39.08	

*For the 10 and 20 min. experiment, there was too little oil left to analyse the water content, it was assumed that their water content was the average of the four other analysis.
**From those short experiments, the amount of water in the organic phase could only be determined once.
***This non-catalytic bio-oil is single-phase, so the water content of the whole liquid is presented in table 11.

Addendum B.3 presents all the η_C and ξ_O values plotted in figure 27. Regarding the organic phase, values for carbon yield do not deviate significantly from those obtained for pine wood. Oxygen reduction decreases more slowly with cellulose (in the series of 10 to 60 min., for cellulose: from 99.55 to 94.57 wt.%, for pine wood: from 96.64 wt.% to 88.13 wt.%), although it may not be forgotten that assumptions were made to determine the water content of the organic phase. All those data points are situated in the same region on figure 27 as for pine wood (see figure 19), indicating that CFP of cellulose results in similar trends in terms of elemental and water content, or more in general a similar deoxygenation trend can be observed for both feedstocks.

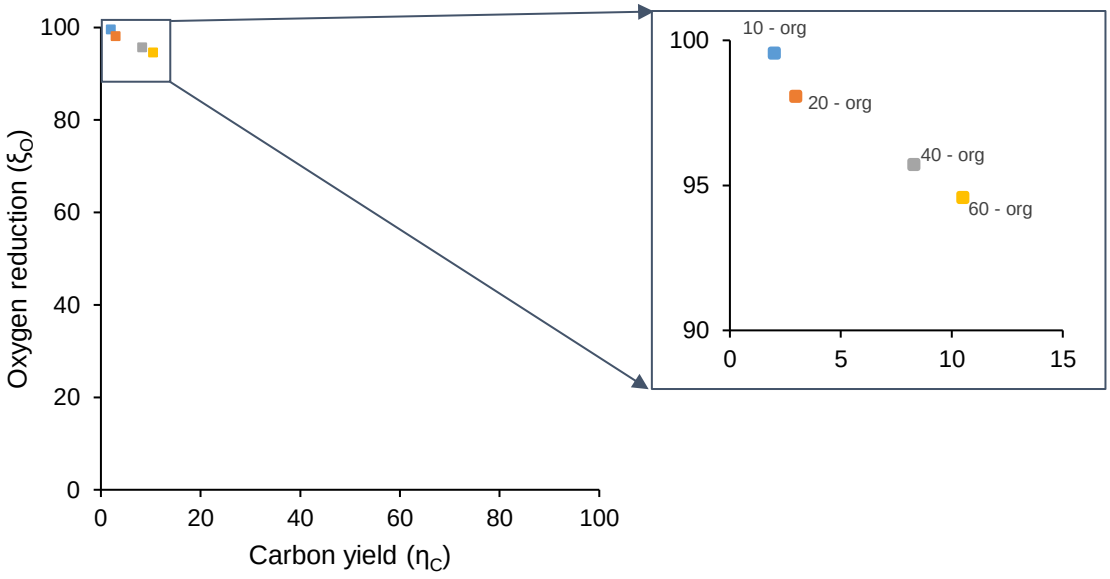

Figure 27: oxygen reduction as a function of carbon yield of the organic phase of catalytic cellulose experiments, on dry feed basis.

Nevertheless, it can be concluded that all observed carbon yields in the tests performed so far are too low (for both pine wood and cellulose lower than 20 %), even for the highest TOS that was tested.

5.2.4 Determination of the bio-oil composition

Addendum B.4 lists the concentration in wt.% of every GC/MS quantified compound in the organic phase, which is visualised in figure 28. In comparison with the composition of the organic pyrolysis liquids from pine wood, the concentration of every chemical group is the same, except there was no levoglucosan detected here. A big discrepancy can be seen in total determined fraction (in wt.%) between the two feedstocks: for pine wood, the summation of all chemical groups for pine wood resulted in a total fraction being quantified between 10 and 15 wt.%. With GC/MS of the organic phase, between 30 and 42 wt.% of the organic fraction is characterised. If the small amount of water found in table 11 is added up to these fractions, then it was possible to assign between 32.91 and 43.58 wt.%. The main reason for this difference between pine wood and cellulose pyrolysis liquids in terms of the quantifiable fraction, is because the cellulose pellets that were used are a single model compound and no interference with other biopolymers or minerals can occur, as would be the case with a real biomass matrix like pine wood [151].

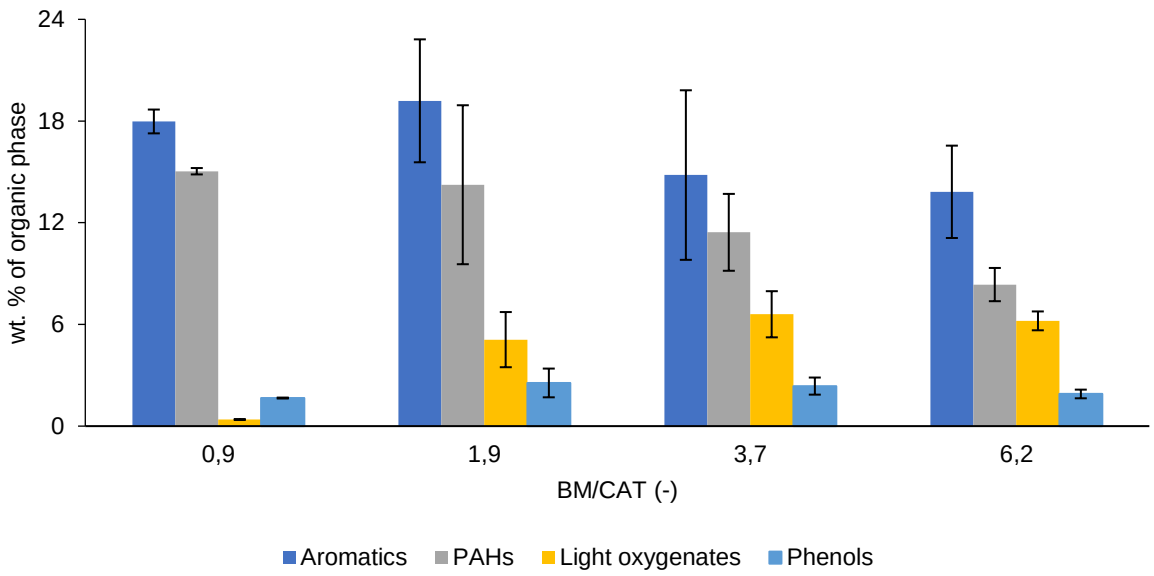

Figure 28: concentration (in wt.%) of different compounds detected in the organic phase of cellulose and grouped according to their chemical functionality. Individual wt.% of each quantified chemical is presented in addendum B.4. Compounds attributing to aromatics are: benzene, toluene, o-xylene, m/p-xylene and alkyl- and allyl substituted benzenes. Compounds attributing to phenols are: phenol and phenol derivatives. Compounds attributing to PAHs are: naphthalene, substituted naphthalenes and indane/indene derivatives. Compounds attributing to light oxygenates are 5-methyl-2-furancarboxyaldehyde, furfural and 3-methyl-1,2-cyclopentanedione.

When examining the concentration of monoaromatics, again the highest production of these MAHs is found at the BM/CAT of 1.9. Except benzene itself, but every (group of) chemicals categorised as aromatics show the same trend: a small increase till a TOS of 20 min., followed by a slow decrease till 60 min. Most of the benzene is formed initially but after a slow decline, it stabilises around 0.30 wt.%. A whole bunch of substituted benzenes are recognised: mono- or disubstituted and alkyl- or allyl substituted, all listed in detail in the appendix. The variation in different MAHs is bigger than for pine wood. Comparing benzene production for both types of biomass, it is clear that cellulose is responsible for the production of a significant amount of MAHs.

Liang et al. tested three cellulose/catalyst-ratios (20/1, 5/1 and 1/1) into a py-GC/MS set-up. The acidity was slightly higher than the catalyst used during this thesis, namely 12.5 instead of 23. Only relative results were shown, but also there, the increase of aromatic hydrocarbons was clearly visible [152].

The second most abundant group of compounds after the monoaromatics, are the PAHs. Although cellulose follows the same continuously decreasing trend with respect to PAH yield with higher BM/CAT ratios, similar to the results obtained with pine, the difference in yield of those polyaromatic compounds is also striking. An initial higher coke yield, which can consist of PAHs, can also declare this discrepancy. Another important thing to mention, is that the standard deviation of cellulose-derived liquids analysis noticeably increased compared to those of pine. Regarding the results in addendum A.4 and B.4, It is clear that cellulose yields aromatic hydrocarbons, which was already confirmed by Wang et al [135].

With cellulose, only three types of light oxygenates were identified in the organic phase: furfural, 3-methyl-1,2-cyclopentanedione and 5-methyl-2-furancarboxaldehyde. Those first two were not detected with the lowest BM/CAT. In the paper of Liang et al., there was a significant increase in peak area with higher BM/CAT [152], although in this research, there was not a significant difference

between the 40 and 60 min. experiment. It was already clear that deoxygenation was very effective during those first 10 min., and here it is confirmed. After 10 min., there is a tremendous breakthrough of furfural, of 3.07 wt.% on average. Furthermore, on average, the phenolic fraction in the organic phase was reduced from 20 min. to 60 min.

The aqueous phase of cellulose, shown in figure 29 and addendum B.5, contains similar compounds compared to pine wood. Here, the total wt.% of compounds determined is respectably increasing from 10 to 60 min. Furthermore, 16.39 wt.% of the organics of the non-catalysed bio-oil are quantified, of which more or less 70.35 % is levoglucosan. Fabbri et al. already found that when a HZSM-5 catalyst is mixed with cellulose, the yield of anhydrosugars is reduced significantly, which can be seen in addendum B.1. When applying a catalyst, levoglucosan is dehydrated, decarbonylated and decarboxylated and ends up as furan derivatives. These pool of furanic compounds undergo also acid-catalysed CO removal and oligomerisations inside the zeolite pores, leading to the formation of aromatics and olefins [135, 152, 153]. After 10 minutes, almost no light oxygenates are formed. These results could not be compared with the results of pine wood, since those were not analysed because of an expected too low response. (which was here in fact also the case). In total, the concentrations of light oxygenates are far under their corresponding pine wood counterpart. The highest amount of a specific compound at 60 min. is glycolaldehyde, with an average concentration of 0.38 wt.%. As the BM/CAT is still increasing, the catalyst is getting deactivated and more and more sugars are formed and not further converted.

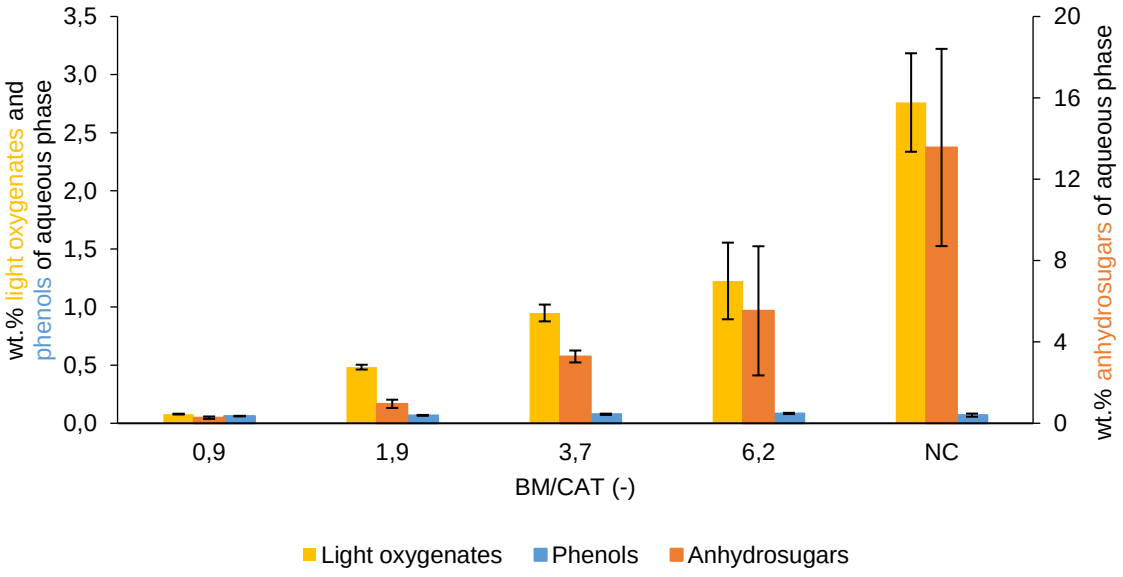

Figure 29: concentration (in wt.%) of different compounds detected in the aqueous phase of cellulose and grouped according to their chemical functionality. Individual wt.% of each quantified chemical is presented in addendum B.5. Compounds attributing to phenols are: phenol, alkyl substituted phenols and hydroquinone. Compounds attributing to light oxygenates are: 5-(hydroxy)methyl-2-furancarboxaldehyde, 2,3-butadione, 2,3-pentanedione, acetic acid, propanoic acid, hydroxyacetaldehyde, 1-hydroxy-2-propanone, furfural, 3-methyl-1,2-cyclopentanedione, 2-cyclopenten-1-one, glycolaldehyde and 1,2-ethanediol, monoacetate. Compounds attributing to anhydrosugars are: levoglucosan and other sugars.

Mukarakate and co-workers already stated that deactivation of cellulose starts around similar BM/CAT than for pine wood. The reason for that is because of the chemical structure of pine: it consists for more or less 63 % of carbohydrates, which produce more primary vapours and it has a lower tendency than lignin to form char [114].

5.2.5 Characterisation of the deactivated catalyst

For the spent catalysts obtained from cellulose experiments, only elemental analysis was executed, in a similar way as was done with pine wood catalyst samples. The results are shown in addendum B.6 and the time-on-stream is plotted over the H/C atomic ratio in figure 30. For all TOS, less carbon was detected, which consequently results in slightly higher H/C atomic ratios. The transition from soft to the heavy coke region is still situated between the 20 min. and 40 min. experiment. Results of the BET surface area, acidity and pore volume were still not done and might be an option to do for later research.

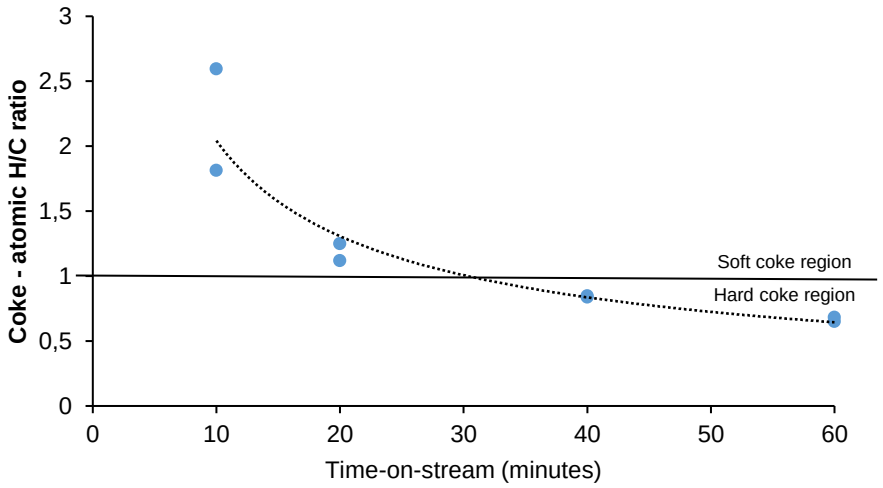

Figure 30: coke-on-catalyst of the different catalyst samples collected after fast pyrolysis of cellulose.

5.2.6 Conclusion

In this second experimental section, the influence of different BM/CAT in CFP of cellulose was researched in the mini-plant. Results in terms of product yield, water content and elemental analysis showed comparable trends as for pine wood. The largest difference was observed in the GC/MS results, where higher concentrations were observed for mono- and polyaromatic hydrocarbons and a higher sugar concentration was obtained for the non-catalytic experiments. Furthermore, it might be interesting to see how hemicellulose and lignin will interact with the catalyst. Therefore, CFP of hemicellulose and lignin in the mini-plant, together with all the catalyst characterisation, would be useful to get more insight in the reaction pathways and of the catalyst deactivation.

In the final part of this chapter, two undervalorised feedstocks namely sugarcane trash and sugarcane bagasse (respectively SCT and SCB) were analysed in an in-situ py-GC/MS equipment. Here the biomass and catalyst were mixed in one sample cup and the BM/CAT was fixed at 0.2. Due to relatively high amount of catalyst and low contact time of the pyrolysis vapours with the catalyst, coke formation due to carbon build-up can be neglected here. Here, the working of the catalyst could be disrupted by the alkali and alkaline earth metals present in biomass. For that reason, the influence of a well-established pretreatment of the feedstocks on CFP was researched in the next section.

5.3 Catalytic pyrolysis of agricultural residues in the py-GC/MS set-up

In the previous sections, catalyst deactivation by coke formation was assumed, but also metals like AAEMs (alkali and alkaline earth metals) present in the biomass could participate in the catalyst deactivation and/or poisoning [111]. In this section, micropyrolysis experiments were done with sugarcane trash (SCT) and sugarcane bagasse (SCB). For this part of the thesis, SCT and SCB were pretreated in order to have their minerals removed prior to the actual pyrolysis. In that way, potential deactivation of the catalyst by biomass-derived minerals is reduced. Both types of sugarcane residues are pyrolysed with a fixed BM/CAT of 0.2 (300 µg BM/1500 µg catalyst). The influence of the catalyst, as well as the influence of fixed demineralisation pretreatment was investigated. Leaching SCB as well as SCT in 0.5 M citric acid (CA), for 1 h at 25 °C came out as the best solution compared to other inorganic acids and different tested concentrations, as was found in previous research [132]. Table 12 demonstrates significant reductions of these minerals after pretreatment with citric acid, but similar for SCT and SCB. The initial Si concentration of SCT is rather high, although this element, not belonging to the AAEMs, is not that active [91]. This may be attributed to a higher deposition of silica (SiO_2) in leaves and inflorescences of the crop [154, 155]. It is also possible that SCT especially, was contaminated with soil (clay and silt) particles, which remained attached on the epidermis of SCT during processing. The concentration of Si just decreased by half for both feedstocks upon pretreatment, but still remains rather high [123]. Using py-GC/MS, the biomass is pyrolysed and the vapours separated in the GC column are analysed by the MS detector. The 75 most abundant identified compounds were selected and divided in different groups, according to their chemical functionality. For SCT as well as for SCB, the experimental plan was to have four different results: the influence of pretreatment, the influence on catalyst and finally the influence of pretreatment and catalyst. All those analyses were done in triplicate, to check to repeatability of these experiments.

Table 12: inorganic composition (mg/kg, on dry basis) of SCT and SCB samples being untreated and leached with citric acid solution of 0.5 M, at 25 °C during 1 h [123].

	SCT			SCB		
	Untreated	**CA-treated**	**Reduction (%)**	**Untreated**	**CA-treated**	**Reduction (%)**
K	2300.0	17.6	99.23	1800.0	17.0	99.06
Al	216.0	78.0	63.89	279.0	131.0	53.04
Fe	245.0	104.6	57.31	327.0	123.0	62.39
Si	13400.0	6300.0	52.99	8600.0	4400.0	48.84
Mg	492.0	29.6	93.98	287.0	68.1	76.27
Na	56.8	< 5.0	91.20	32.1	< 5.0	84.42
Total	16709.8	6534.8	60.89	11325.1	4744.1	58.11

Addendum C.1 gives an overview of the thirty most abundant compounds detected in the py-GC/MS experiments for each experimental set-up. This table was provided in the appendix to show the reader there is a large abundance and variation in detected compounds.

5.3.1 Sugarcane trash micropyrolysis experiments

In contrast to figures 20, 22, 28 and 29, in figure 31 and addendum C.2, the py-GC/MS results are reported as GC/MS response per mg biomass (with standard deviation) for each sample. The method of reporting is done because, as opposed to GC/MS analysis of liquid sample, py-GC/MS cannot be calibrated as such. The summation of the peak area is divided by the sample weight to give an estimate of the production of a certain compound in the pyrolysis-GC/MS experiments. Subsequently, this value is divided by a factor 10^{10}, to get a response below 10. This way of assessment is by no means fully quantitative but enables comparison between different biomass samples that were pyrolysed under identical conditions.

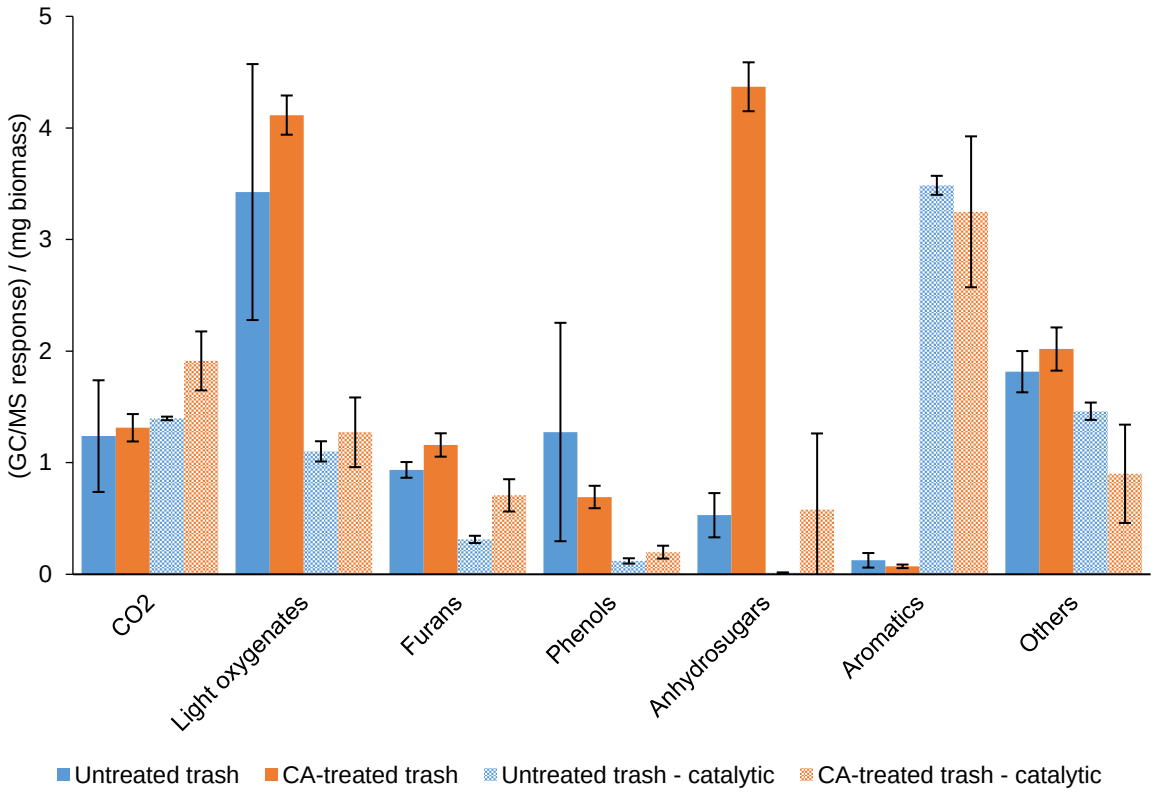

Figure 31: comparison of catalytic and non-catalytic fast pyrolysis of untreated and CA-treated SCT, expressed in GC/MS response per mg biomass. Light oxygenates include carboxylic acids, aldehydes, ketones and alcohols), whereas aromatics include mono- and polyaromatic hydrocarbons. Others include N-compounds, ethers and esters.

Influence of pretreatment

A substantial increase in the production of anhydrosugars can be noticed if the non-catalytic pyrolysis of untreated SCT is compared to the CA SCT (0.53 respectively 4.37). This clearly shows the effect of the pretreatment. Minerals (mainly AAEMs) adsorbing on cellulose of sugarcane will induce ring scission of the glucose units, yielding compounds like hydroxyacetaldehyde, formic acid, 1-hydroxy-2-propanone, 2-furaldehyde and 5-hydroxymethylfurfural which contribute to the light oxygenates. Although unexpected, there is no significant difference in light oxygenates of both non-catalytic results. On average, there is even a higher response per mg biomass for the CA SCT compared to untreated SCT, with respectively 4.11 (± 0.18) and 3.43 (± 1.15). A reason for this strange behavior could be that ash removal, calculated with Eq. (2.6), is not that efficient for SCT as for SCB, with the same pretreatment conditions. With SCB, 48.4 % of the ash is removed, using a 0.5 M solution of CA, whereas for SCT only 38.9 % is removed. SCT had also around 2.8 times higher initial ash content compared to SCB (respectively 0.053 and 0.019 g/g d.b.) [123].

Without the presence of minerals, glycosidic bond cleavages can reduce the chain length and the anhydrosugar levoglucosan is formed instead [156]. Yang and co-workers predicted that K and Ca are two promotors of homolytic scission of several bonds in the pyranose ring, resulting in the production of more light oxygenates such as glycolaldehyde and 1-hydroxy-2-propanone [157]. Due to the competition of both pathways, more anhydrosugars are formed with pretreated SCT and SCB or more light oxygenates are formed without pretreatment [91].

Furthermore, no remarkable difference is found in CO_2, phenolic and aromatic yields. Besides, there are slightly more furans produced with the treated SCT (0.94 compared to 1.16), which can be possible

due to the higher amount of anhydrosugars produced, which are the precursor for these furanic compounds, which is approved in figure 6 [14].

Influence of catalyst

Here, significant differences can be observed in addendum C.2 and figure 31 for light oxygenates, furans, phenols, anhydrosugars and aromatics. Those first four groups are typical products that can be obtained with normal fast pyrolysis. Anhydrosugars and furans are the main dehydration products of respectively cellulose and hemicellulose, as can be seen in figure 6 [14]. Due to the low BM/CAT and low contact time of the pyrolysis vapours with the catalyst, deactivation by coke formation can be excluded, which declares the high aromatic yield. In general, the catalyst increases the gas yield, as was confirmed in figure 17, due to deoxygenation via water and NCGs. The slightly higher CO_2 peak areas (on average) for the catalytic results can be assigned to the higher decarboxylation capacity with use of a catalyst, resulting in more products like CO_2.

As expected, the GC/MS response for aromatics is much higher for the catalytic runs, as well for the pretreated and the untreated biomass. (untreated: 3.49 over 0.13, CA-treated: 3.25 over 0.07). Together with this elevation in aromatics, there is a decrease in light oxygenates, furans and phenols for catalytic results. Those last three group of compounds are products appearing during deactivation of the catalyst. A negligible small amount of anhydrosugars are detected for the untreated biomass with catalyst, which was expected, since both untreated biomass and catalytic pyrolysis are not conducive to yield sugars.

Influence of pretreatment and catalyst

It is not very clear which effect (presence of catalyst or pretreatment) predominates. Although there is catalyst present, which normally eliminates the presence of anhydrosugars, with pretreatment there is on average a response of anhydrosugars of 0.58 (± 0.68). Because of the high standard deviation, it cannot be concluded with certainty that anhydrosugars are formed or this was a detection problem. The use of pretreated SCT together with catalyst has no significant difference in aromatic yield (3.49 for untreated SCT compared to 3.25 for CA SCT).

In summary, it can be stated that if aromatics are preferred, it does matter if the SCT is treated or not, as in the long term the catalyst will poison in the presence of the minerals from biomass. However, it seems to be less important which type of intermediate is formed in pyrolysis which is catalysed into aromatics. Whether it is levoglucosan or other oxygenates, both are equally efficient converted into aromatics. In that way, the pretreatment does not make sense to perform. The GC/MS response of aromatics does not change significantly for untreated or CA treated catalyst. If anhydrosugars are preferred, pretreatment can be useful, because more anhydrosugars are detected after the feedstock was leached using a citric acid solution. If aromatics like BTX are targeted, demineralising the feedstock before pyrolysis does not yield an advantage in terms of aromatics yield.

5.3.2 Sugarcane bagasse micropyrolysis experiments

In a similar way, SCB was pyrolysed and analysed. Figure 32 and addendum C.3 show the GC/MS response per mg biomass, together with their standard deviation, given for each sample.

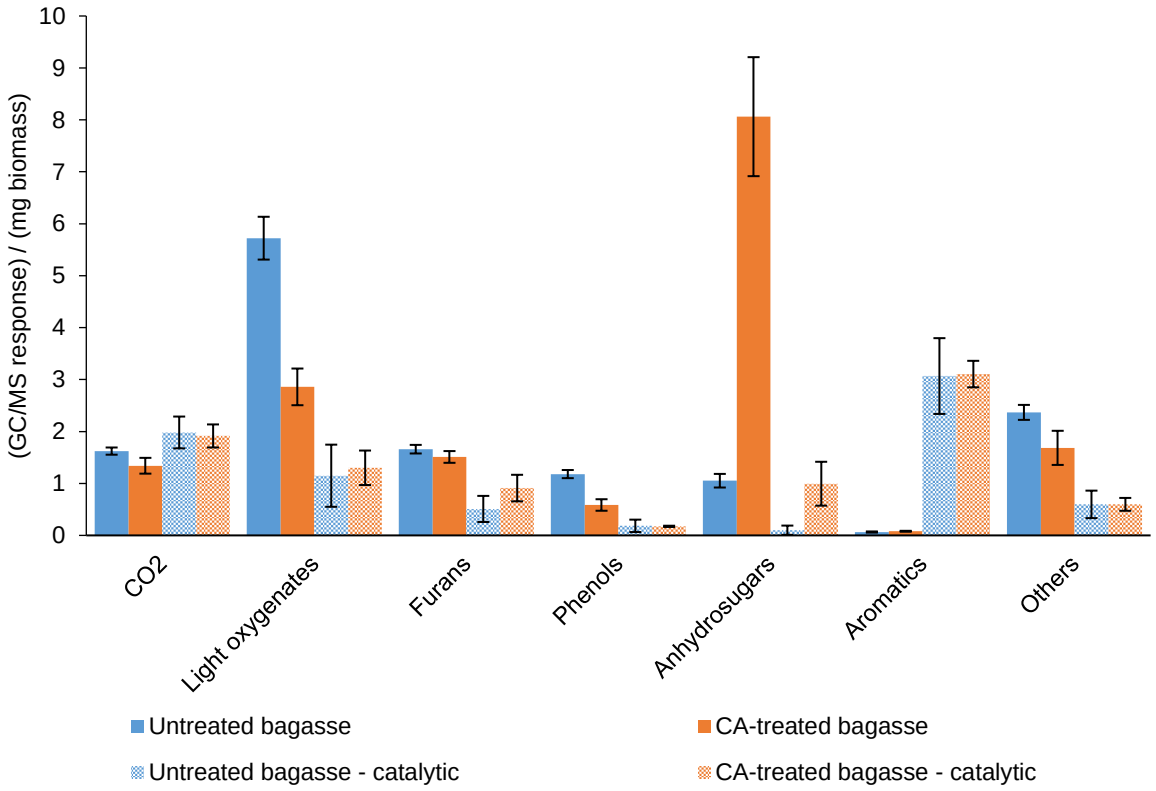

Figure 32: comparison of catalytic and non-catalytic fast pyrolysis of untreated and CA-treated SCB, expressed in GC/MS response per mg biomass. Compounds are sorted similarly like in figure 31.

Influence of pretreatment

Also here, a spectacular rise of anhydrosugars can be seen if citric acid pretreated SCB is used instead of untreated SCB (1.05 compared to 8.06). For the untreated SCB, there are twice as much light oxygenates quantified compared to the CA-treated SCB, which is more logical and in accordance with the findings of Yildiz et al. that minerals adsorbing on cellulose of SCB will induce ring scission of the glucose units, yielding light oxygenates [111]. Again, no significant difference in CO_2, furans and aromatics are noticed here. More phenols are detected in the untreated sample, which was also the case for SCT.

Influence of catalyst

Comparable values and similar trends can be found for the aromatics and anhydrosugars, as for SCT. Although there is enough catalyst, there are some light oxygenates. Compounds attributing to these oxygenates are e.g. acetone, acetic acid and (hydroxy)acetaldehyde, as can be deduced in addendum C.1. Phenols also follow a decreasing trend just like for SCT. Furthermore, it can be noticed that product composition over both catalytic results, CA-treated or not pretreated, the differences are rather small. This lack of difference can come from too short contact times of the pyrolysis vapours with the catalyst in this type of configuration. Further ex-situ experiments could accept or reject this hypothesis.

Influence of pretreatment and catalyst

Aromatic yield is still high for the CA-treated and catalysed SCB, and equals to the response of untreated and catalysed SCB. Here there is no effect of the catalyst on the anhydrosugar yield after pretreatment (1.05 for untreated non-catalytic SCB compared to 1.00 for CA-treated catalytic SCB). This effect could also be seen for SCT, so it means that the combination of pretreatment and catalyst not result in a lowering of the anhydrosugar content.

5.3.3 Conclusion

Despite the higher amount of light oxygenates in the untreated and non-catalysed SCB, there are no differences in trends or observations between SCB and SCT. If anhydrosugars are desired, it is better to work with the non-catalysed but pretreated SCB instead of SCT, because the response for SCB is 1.84 as high as for SCT. The highest response for aromatics was obtained with untreated SCT with use of catalyst, but the difference with SCB under the same conditions is not significant (3.49 (± 0.09) for SCT compared to 3.07 (± 0.73) for SCB).

It might be interesting for the future to do the same experimental plan in the ex-situ mode, described in section 4.3.1. In- and ex situ experiments with cellulose or levoglucosan might also be useful to see which effect predominates with a model compound. This potentially can confirm or disprove aforementioned ideas and hypotheses.

Out of the results, it cannot be decided which feedstock, SCT or SCB, gives the best result. Although SCT yields slightly more aromatics, production of anhydrosugars can be optimised using SCB. SCB is a very sugar-rich product and in fact it is the waste stream after sugar extraction. It needs to be considered that the applications of the most abundant sugar, namely levoglucosan, are rather restricted and the price for SCB is approximately € 7.3/ton, whereas for SCT, this is around € 2.0/ton, which could give the advantage to SCT [162].

6. Conclusion

This thesis consists of three main parts. In the first section, ex-situ CFP of pine wood was conducted in the mini-plant. Initially, using fresh catalyst resulted in a lot of water, NCGs and coke but all those product yields decreased significantly with higher TOS, in favour of the organic yield. The higher the BM/CAT (biomass-to-catalyst ratio), the more resemblance the product distribution showed towards non-catalytic conditions (which indicated catalyst deactivation). Preferred deoxygenation pathway was found to be in this order: dehydration > decarbonylation > decarboxylation. With increasing TOS, less carbon and more oxygen are present in the organic phase, while the opposite occurs for the aqueous phase. Water yield in the organic phase also raises with the length of an experiment and decreased for the aqueous phase. Concerning product distribution, the two phases are moving to each other with higher BM/CAT. For the lowest BM/CAT, mainly aromatics and phenols were detected in the organic phase, while towards higher run times, more light oxygenates and anhydrosugars start to appear, at the expense of those aromatic hydrocarbons. The aqueous phase showed an optimal production of light oxygenates at 60 min. of reaction, after which the yield drops back to non-catalytic results. Due to the use of catalyst, less levoglucosan is quantified in the aqueous phase.

Analysis of the catalyst showed a decreasing coke yield over time, together with a lower H/C atomic ratio and decreased BET surface area, pore volume and lower acidity. Coke is formed because of the high acidity and consequently high reactive zeolite. Compounds that are dependent for the coke formation are phenols, furans and MAHs, which act as CFP intermediates.

Out of literature review, it seemed that cellulose was the most promising compound to elevate the production of aromatics and olefins. It is also the most abundant biopolymer present in pine wood, namely around 40 %. A similar set-up of experiments was done with this biopolymer. Basically, same trends could be observed in terms of mass balance and elemental and water content analysis. Coke yield was slightly higher, because production of aromatics is favoured with cellulose, and these are known as coke precursors. Furthermore, cellulose yields more anhydrosugars, although for non-catalytic FP. In contrary to pine wood pyrolysis oil, the organic phase has a lighter density than the aqueous phase. As was expected, higher aromatic yields were obtained here, but after a BM/CAT-ratio of 1.9, their maximum concentration was already reached. Between 30 and 40 wt.% of the organic layer could be allocated to the right chemicals. Furthermore, GC/MS results showed less variation in product distribution.

Py-GC/MS results of both sugarcane residues showed a high response for anhydrosugars, with CA-treated biomass. As the AAEMs are removed, less conversion of anhydrosugars to light oxygenates is attained. Because the catalyst is not limiting here, also large amounts of aromatics were formed here, but pretreatment has no direct added value in the production of aromatic hydrocarbons, although presence of the AAEMs could deactivate the catalyst over a longer term.

7. Future outlook and own perspectives

Catalytic fast pyrolysis with ex-situ operation mode (vapour phase upgrading over a fixed bed of catalyst) resulted in the favoured production of olefins and monoaromatics. Those compounds could be mixed with gasoline or could be used as direct substitutes of the fossil fuel based aromatics. Unfortunately, yields of those products were very low, which was confirmed during this research.

The catalyst used throughout this thesis was a HZSM-5 zeolite. This is the most widely reported type of heterogeneous catalyst for CFP research. Due to its optimal trade-off between pore size, coke formation is as much as possible avoided, but aromatic (coke) precursors can still diffuse through the zeolite. This zeolite has a good deoxygenation capacity, but nevertheless results in low carbon yields. Venderbosch demonstrated this in a visual way, plotting carbon yield vs. oxygen reduction data available from literature, presented in figure 7. Similar calculations were done as well in the framework of this thesis (see figure 19 and 27), which confirmed earlier conclusions. Energetic yields of all the plotted results were between 10 and 25 %.

During this thesis, the focus was directed to the evolution of catalytic products during catalyst deactivation. Due to this highly reactive catalyst, coke formation is favoured and predominates the formation of desirable products such as monoaromatics. In that way, the catalyst must be regenerated at regular time intervals, possibly leading to other problems or technical challenges, like downtime of the reactor, additional energy cost of regeneration or complete and irreversible activity loss after multiple regeneration cycles.

As the catalyst deactivates over time, the chemical composition of the bio-oil will also change. Initially, severe deoxygenation of pyrolysis vapors results in the production of preferred aromatics. But, as more pyrolysis vapours are passing over the catalyst, the catalyst starts to lose its activity. It will act as an inert material resulting in an oxygenated product stream (e.g. (methoxy)phenols, indenols, naphtols, levoglucosan…) converging to non-catalysed FP bio-oil in terms of composition.

Following sections give an overview of some recent (upgrading) techniques improving the whole fast pyrolysis concept including hydrotreating, co-processing of bio-oil and carbon-carbon coupling reactions.

Iisa et al. proposed partial but targeted deoxygenation of the bio-oil. In that respect, around 20 wt.% of oxygen is still kept in the bio-oil, which in a following step can be subjected to downstream processing to upgrade the pyrolysis liquid. Remaining oxygenates, in the form of furans, ketones, aldehydes can react together, resulting in higher-value compounds with additional formation of CO_2 and water [158].

Hydrotreating, explained in detail in section 2.4.1, removes the oxygen out of the bio-oil in presence of a catalyst and high hydrogen pressures. Other reactions happening here at the same time are cracking, repolymerisation and saturation of aromatics and olefins. Here again, the catalyst can be deactivated by coke formation originating from thermally induced polymerisation of reactive oxygenates. At low temperature, these aldehydes, ketones and others can be hydrogenated, resulting in less active alcohols. This is proposed as a first milder hydrotreating step, before the coke inducing reactions like polymerisation can be overcome in a second more intensive hydrotreating step. Nevertheless, optimal process conditions still need to be further researched and hydrogen consumption must be limited, in order to keep the cost at reasonable levels [158]. Mante et al. already achieved promising results with CFP coupled to HDO, resulted in an oxygen content from initially 19.5

wt.% after CFP, to 0.5 – 11.0 wt.% after hydrotreating and a carbon yield of 80 – 93 wt.% in the liquid, which had a lower overall yield between 17 and 32 wt.% [159].

Another option that recently received more attention, was co-processing bio-oil in a standard petroleum refinery. This seemed as an ideal solution to elevate the use of renewable carbon by replacing (part) of the finite fossil fuel carbon source. (Partially) upgraded bio-oil could be co-processed in a fluid catalytic cracking (FCC) system, which converts long chain paraffins to shorter hydrocarbons. This solution instead of upgrading by means of HDO has mainly an economical advantage [158].

As the bio-oil (aqueous phase) is rich in light oxygenates, it might be interesting to react those compounds to yield more fuel-range molecules. Several possible reactions are aldol condensations, ketonisations, (trans)alkylations and Diels Alder reactions. These carbon-carbon coupling reactions are more effective if they are applied after CFP instead of ordinary fast pyrolysis. For certain couplings, an extra type of catalyst might be necessary, and for some reactions, water and/or CO_2 are released [158].

Iisa et al. finally concluded that there is still a large necessity for fundamental studies of catalyst structure (mainly focusing in activity and selectivity) and kinetics of pyrolysis and its pathways. CFP experiments should be conducted on a scale that is big enough to collect sufficient bio-oil for subsequent upgrading [158].

Techno-economic analysis

Techno-economic analysis are important studies, because they can judge, in advance, the feasibility of a potential (pyrolysis) plant. They can also study the coupling of existing pyrolysis installations to an additional upgrading step. It is clear that making assumptions of some variables will be required, but the more assumptions are made, the more the conclusions with respect to techno-economic feasibility of a proposed installation could deviate from the reality. Such studies are not (yet) available for CFP. For that reason, two techno-economic analysis from fast pyrolysis installations were scrutinised. Some of those findings or assumptions could be directly translated from the bench-scale which was used during this thesis, to a more industrial scale of installation.

Both analyses are applying fast pyrolysis without ex-situ vapour upgrading, which was the used upgrading technique during this thesis. In the first analysis of Brown et al., bio-oil at a production rate of 2 000 tonnes/day will be produced in a fluidised bed reactor. Upgrading of only the aqueous phase (obtained after liquid/liquid extraction) was done by a two stage hydrotreating (respectively over a Ru/C and Pt/C catalyst) and FCC over a HZSM-5 catalyst. With these upgrading techniques, production of commodity chemicals is aimed for [160].

Only the aqueous phase was valorised here, because it is a carbohydrate-rich product which after catalyst interaction, leads to higher aromatic and olefin yields. The other products were partially sold or partially combusted to recover some energy. Brown et al. researched four different liquid yields, ranging from 52 to 70 wt.%. This clearly affects the economic viability of this process. The internal rate of return (IRR) was calculated for each of those four yields and ranged from 4.27 % to 14.32 %, with increasing bio-oil yield. This value is still below 25 %, which can be assumed as the lowest return necessary to invest in a new technology [160].

Nevertheless, there are some doubts and questions that arise about possible simplifications of this proposed fast pyrolysis system: for the moment, there is no plant operating of that size that produces such high amounts of bio-oil. It is also a question how long they can operate without interrupting the process for cleaning or unplugging. Is this down time considered or not? They also do not mention how the organic phase will be fractionated into olefins and aromatics. This practical issue can come together

with an additional cost and also lower product yields. Based upon that IRR, Brown et al. finally concluded that integrated catalytic processing of fast pyrolysis products is not lucrative.

In a second example, conducted by Herregods, fast pyrolysis of willow, SCT and SCB in a proposed fluidised bed reactor was researched, with prior acid pretreatment of biomass. The assimilation capacity of this plant was estimated at 78 000 tonnes of biomass/year. Here, the purpose is to use the obtained pyrolysis liquid as a fuel which can be applied in boilers, turbines or furnaces [161]. Using a mix of valid data and assumptions, a discounted cash flow analysis (DCF) was made to determine the IRR. It was already found that pretreatment takes 45.12 % of the total cost per ton of bio-oil, which can be assumed as too high for just a pretreatment [161]. The question can be asked if it is not more beneficial to use a feedstock at a higher price, but one which has no need to be pretreated. Although use of unvalorised feedstocks is more preferred, excessive amounts of acid for pretreatment makes this process not cleaner in total. Another option is to research if lower acid concentrations have a sufficient effect, but that gives than a trade-off between acid consumption and bio-oil quality.

According to its calculation, the break-even selling price of the pyrolysis oil from willow, SCT and SCB would be respectively € 367/ton, € 274/ton and € 264/ton. Compared to the selling price of € 330 (related to the price of fossil fuels), for SCT and SCB, they are lower. It needs to be considered that for that price, more than 20 years of pay-off time is required. This pay-off time and general profit can be reduced by increasing the selling price. Demand of bio-oil will also be dependent on fossil fuel prices, which are currently low, but increasing use of those will also raise their price. The final decision will be made after comparison of all positive and negative aspects of biomass and fossil fuel feedstocks, but it is still questionable if these positive aspects could balance the extra cost of biomass. Although producers and consumers more and more become aware of sustainability, both parties do not want to take on the additional cost [161].

The last part of this discussion contains a simple and maybe rough calculation, which will help to reach a final conclusion. The following case can be assumed:

Table 13a gives an overview of all the calculations of following paragraph. Assume we want to use CFP of cellulose (like it was done in this research) to isolate the fraction of BTX out of the organic phase of the bio-oil. The highest production of BTX appear at a BM/CAT of 1.9, corresponding with a TOS of 20 min (see addendum B.4). The organic phase contained on average 15.20 wt.% BTX. Figure 25 stated that after 20 min., the share of organics in the mass balance is 9.19 wt.%. Multiplying both values result in a yield of 1.40 wt.% BTX on biomass basis. So of all the biomass that was converted during those first 20 min, 1.40 % of the biomass weight ended up as BTX. For the 20 min. experiment, with a BM/CAT of 1.9, we have fed 76 g of cellulose. This can be stated like this: to produce 1.06 g of BTX, 76 g of cellulose will be necessary, or to produce 1 kg BTX, 71.43 kg of cellulose will be required. Similar calculations can be done for (substituted) naphthalenes and for pine wood, and are listed in table 13a.

In the paper of Lange, some price assumptions were made: the price of lignocellulose feedstocks can vary from \$ 0.05 - \$ 0.10 $kg^{-1,}$ whereas the price for commodity chemicals could range from \$ 1.00 - \$ 2.00 kg^{-1} [163]. With 418.43 kg pine wood, 1 kg BTX and 2.73 kg naphthalenes could be formed, whereas with 153.17 kg pine wood, 0.36 kg BTX and 1 kg naphthalenes could be produced. Now, with those price intervals, the profit of each case was quickly determined in table 13b.

Table 13a: calculations to analyse the possibility of scaling-up the used set-up during this thesis.

	cellulose (wt.%)	BM/CAT	organics (wt.%)	g product	g cellulose	kg cellulose for 1 kg product
BTX	15.2	1.9	9.19	1.06	76	71.59
naphthalenes	11.32	0.9	9.25	0.38	36	95.50

	pine wood (wt.%)	BM/CAT	organics (wt.%)	g product	g pine wood	kg pine wood for 1 kg product
BTX	1.98	1.6	12.07	0.15	64	418.43
naphthalenes	7.19	0.9	9.08	0.24	36	153.17
Total product for 418.4 kg pine wood				1 kg BTX + 2.73 kg naphthalenes = 3.73 kg product		
Total product for 153.2 kg pine wood				0.36 kg BTX + 1 kg naphthalenes = 1.36 kg product		

Table 13b: estimations of the profit on producing commodity chemicals from lignocellulosic biomass (in $).

		lignocellulose (418.4 kg pine wood)		lignocellulose (153.2 kg pine wood)	
	$/kg	**0.05**	**0.10**	**0.05**	**0.10**
commodity chemicals	**1**	-17.19	-38.11	-6.30	-11.59
	2	-13.46	-34.38	-4.94	-7.86

There is a loss in each of the above cases, and this is even without addition of investment costs or processing costs taken into account. Table 14 lists some advantages and drawbacks of a more commercial process as calculated above.

Table 14: overview of the most important advantages and disadvantages linked related to upscaling CFP.

ADVANTAGES
+ only two fractions (BTX and naphthalenes) are assumed while there are more other valuable chemicals in the organic phase
+ besides, also the char, NCGs and aqueous phase of the bio-oil can be (partially) sold or recovered. In that respect, this CFP plant will have less waste streams to handle
+ not only cellulose can yield aromatics, but these can also come from hemicellulose and lignin
DRAWBACKS
- price of the used cellets (cellulose) is rather high (approximately € 250/kg), but 'ordinary' cellulose costs between € 1 and 2/kg
- can CFP of cellulose be realised with a feeding rate of 2000 tonnes/day?
- how can an automated catalyst regeneration system be integrated into CFP on this scale?
- the higher the BM/CAT, the more organics are produced, but less aromatics are obtained
- how will the industrial fractionation be done into an organic and aqueous phase?

Although this calculation is very simplistic, it already demonstrates that it is almost impossible that CFP directly can take over the production of the most important industrial aromatics. With the current prices of the fossil fuel industry, it is very hard to compete with lignocellulosic biomass and to produce an economical benefit. Finally it can be concluded that, based upon results of this thesis, observations from other techno-economic processes and this rudimentary calculation that bio-oil in its whole has the potential to be valorised. Nevertheless, it is difficult to extract one or more compounds out of the aqueous or organic phase. Currently, it still seems better to research applications where the entire bio-oil can be used, which was already stated by Czernik and Bridgwater (see section 2.3.2) [33].

In the way CFP was conducted in this thesis, some further research might be interesting: the behavior of the other two model compounds, namely hemicellulose and lignin can be researched, to state their effect on catalyst deactivation. With additional analysis techniques, further insights might gained on the catalyst deactivation during CFP. Because of the lack of time and the unforeseen long period in which the py-GC/MS was out of order, ex-situ catalytic experiments with SCB and SCT have to be conducted in the future, as well as with levoglucosan, to get a better understanding of all the reactions biomass vapours undergo in the presence of a catalyst.

8. Bibliography

[1] Prins, W., & Ronsse, F. (2017). Thermochemische conversie van biomassa. Academic year 2016-2017. Ghent: Ghent University.

[2] Beeckman, J., & Minnaert, B. (2017). Duurzame energie en rationeel energiegebruik. Academiejaar 2016-2017 Ghent: Ghent University.

[3] Herregods-Van De Pontseele, K. (2016). Snelle pyrolyse van voorbehandelde agrarische residuen.

[4] Kan, T., Strezov, V., & Evans, T. J. (2016). Lignocellulosic Biomass Pyrolysis: A Review of Product Properties and Effects of Pyrolysis Parameters. *ChemInform, 47*(28).

[5] Zhu, X., & Lu, Q. (2010). Production of Chemicals from Selective Fast Pyrolysis of Biomass. Biomass.

[6] Wooten, J. B., Seeman, J. I., & Hajaligol, M. R. (2004). Observation and Characterisation of Cellulose Pyrolysis Intermediates by ^{13}C CPMAS NMR. A New Mechanistic Model. *Energy & Fuels*, 18(1), 1-15.

[7] Lin, Y.C. et al. (2009). Kinetics and mechanism of cellulose pyrolysis. *Journal of Physical Chemistry C*, 113, 20097-20107.

[8] Piskorz, J., Radlein, D., & Scott, D. S. (1986). On the mechanism of the rapid pyrolysis of cellulose. *Journal of Analytical and Applied Pyrolysis*, 9(2), 121-137.

[9] Radlein, D., Piskorz, J. & Scott, D.S. (1991). Fast pyrolysis of natural polysaccharides as a potential Industrial-process. *Journal of Analytical and Applied Pyrolysis*, 19, 41-63.

[10] Bridgwater, A. (2012). Review of fast pyrolysis of biomass and product upgrading. *Biomass and Bioenergy, 38*, 68-94.

[11] Venderbosch, R., & Prins, W. (2010). Fast pyrolysis technology development. *Biofuels, Bioproducts and Biorefining, 4*(2), 178-208.

[12] Mohan, D., Pittman, C. U., & Steele, P. H. (2006). Pyrolysis of Wood/Biomass for Bio-oil: A Critical Review. *Energy & Fuels, 20*(3), 848-889.

[13] Dynamotive. (2007). Bio-oil Production at Dynamotive's Guelph plant: cellulose based bio-oil aimed at industrial fuel markets and input to BTL plants. *ThermalNet Newsletter*, 5.

[14] Yildiz, G., Ronsse, F., & Prins, W. (2017). Catalytic Fast Pyrolysis Over Zeolites. *Green Chemistry Series Fast Pyrolysis of Biomass,* 200-230.

[15] Ronsse, F. (2017). Pyrolyse, bio-energie en biochemicaliën: een stand van zaken. ODE studiedag, Presentaties. Presented at the ODE studiedag: Groene warmte, nieuwe kansen voor energie uit biomassa.

[16] Zhang, H. et al. (2013). Catalytic fast pyrolysis of straw biomass in an internally interconnected fluidized bed to produce aromatics and olefins: Effect of different catalysts. *Bioresource Technology,* 137, 82-87

[17] Jensen, P. A. (2013). Liquid Fuel Production by Fast Pyrolysis of Biomass. DTU International Energy Conference 2013, Lyngby, Denmark, 10/09/2013, *http://www.natlab.dtu.dk/Energikonferencer/DTU_International_Energy_Conference_2013*.

[18] Rotating cone reactor technology. *http://www.btgworld.com/en/rtd/technologies/fast-pyrolysis* Accessed on 20/04/2018.

[19] Yildiz, G., Ronsse, F., & Prins, W. (2015). Catalytic fast pyrolysis of biomass: from lab-scale research to industrial applications. Thermochemical Conversion Science, 4th International conference, Abstracts. Presented at the 4th International conference on Thermochemical Conversion Science (TcBiomass 2015).

[20] Liaw, S. et al. (2012). Effect of pyrolysis temperature on the yield and properties of bio-oils obtained from the auger pyrolysis of Douglas Fir wood. *Journal of Analytical and Applied Pyrolysis*, 93, 52-62.

[21] Brown, J., & Brown, R. (2012). Process optimisation of an auger pyrolyser with heat carrier using response surface methodology. *Bioresource Technology*, 103(1), 405-414.

[22] Auger reactor technology. *https://www.bioliq.de/english/64.php* Accessed on 15/05/2018.

[23] Yildiz, G. et al. (2013). Validation of a new set-up for continuous catalytic fast pyrolysis of biomass coupled with vapour phase upgrading. *Journal of Analytical and Applied Pyrolysis*, 103, 343-351.

[24] Brassard, P., Godbout, S., & Raghavan, V. (2017). Pyrolysis in auger reactors for biochar and bio-oil production: A review. *Biosystems Engineering*, 161, 80-92.

[25] Oasmaa, A., & Peacocke, C. (2001). A guide to physical property characterisation of biomass derived fast pyrolysis liquids. Espoo: VTT Technical Research Centre of Finland.

[26] Meier, D., Oasmaa, A., & Peacocke, G. V. (1997). Properties of Fast Pyrolysis Liquids: Status of Test Methods. *Developments in Thermochemical Biomass Conversion,* 391-408.

[27] Soltes, J., & Lin, S. K. (1984). Hydroprocessing of Biomass Tars for Liquid Engine Fuels. *Progress in Biomass Conversion,* 1-68.

[28] Bridgwater, A. V. (2011). Upgrading Fast Pyrolysis Liquids. *Thermochemical Processing of Biomass*, 157-199.

[29] Westerhof, R.J.M., et al. (2008). Effect of condenser operation on the biomass fast pyrolysis oil. *16th European Conference & Exhibition Proceedings*. 1095-1099.

[30] Elliott, D. C. (1994). Water, alkali and char in flash pyrolysis oils. *Biomass and Bioenergy, 7*(1-6), 179-185.

[31] Diebold, J. P. (1999). A review of the chemical and physical mechanisms of the storage stability of fast pyrolysis bio-oils.

[32] Elliott, D. C. et al. (2012). Results of the IEA Round Robin on Viscosity and Stability of Fast Pyrolysis Bio-oils. *Energy & Fuels*, 26(6), 3769-3776.

[33] Czernik, S., & Bridgwater, A. V. (2004). Overview of Applications of Biomass Fast Pyrolysis Oil. *Energy & Fuels,* 18(2), 590-598.

[34] Solantausta, Y. et al. (1993). Wood-pyrolysis oil as fuel in a diesel-power plant. *Bioresource Technology,* 46(1-2), 177-188.

[35] Solantausta, Y., Nylund, N., & Gust, S. (1994). Use of pyrolysis oil in a test diesel engine to study the feasibility of a diesel power plant concept. *Biomass and Bioenergy,* 7(1-6), 297-306.

[36] Ikura, M., Slamak, M., Sawatzky, H. (1998). Pyrolysis Liquid-in-Diesel Oil Microemulsions. U.S. Patent 5,820,640.

[37] Baglioni, P. et al. (2008). Bio-Crude-Oil/Diesel Oil Emulsification: Main Achievements of the Emulsification Process and Preliminary Results of Tests on Diesel engine. *Progress in Thermochemical Biomass Conversion,* 1525-1539.

[38] Freel, B., Graham, R. G. (2002). Bio-oil Preservatives. U.S. Patent 6,485,841.

[39] Meier, D. et al. (2001). Preliminary Study on Fungicide and Sorption Effects of Fast Pyrolysis Liquids Used as Wood Preservative. *Progress in Thermochemical Biomass Conversion,* 1550-1563.

[40] Cheng, S. et al. (2012). Synthesis of biobased phenolic resins/adhesives with methylolated wood-derived bio-oil. *Journal of Applied Polymer Science*, 126(S1).

[41] Stradal, J. A., Underwood, G. (1995). Process for producing hydroxyacetaldehyde. U.S. Patent 5,393,542.

[42] Majerski, P., Piskorz, J., Radlein, D. (2001). Production of glycolaldehyde by hydrous thermolysis of sugars, PCT/CA01/01562.

[43] Oehr, K. H., Scott, D. S., Czernik, S. (1993). Method of producing calcium salts from biomass. U.S. Patent 5,264,623.

[44] Dobele, G. et al. (2001). Levoglucosenone — A Product of Catalytic Fast Pyrolysis of Cellulose. *Progress in Thermochemical Biomass Conversion,* 1500-1508.

[45] Chemat, F., & Cravotto, G. (2017). Green Solvents and Sustainable Processes. *Reference Module in Food Science*.

[46] Sherwood, J. et al. (2014). Dihydrolevoglucosenone (Cyrene) as a bio-based alternative for dipolar aprotic solvents. *Chem. Commun*., 50(68), 9650-9652.

[47] Pavlath, A. E., & Gregorski, K. S. (1988). Carbohydrate Pyrolysis. II. Formation of Furfural and Furfuryl Alcohol during the Pyrolysis of Selected Carbohydrates with Acidic and Basic Catalysts. *Research in Thermochemical Biomass Conversion,* 155-163.

[48] Pinho, A. D. et al. (2015). Co-processing raw bio-oil and gasoil in an FCC Unit. *Fuel Processing Technology*, 131, 159-166.

[49] Fogassy, G. et al. (2012). The fate of bio-carbon in FCC co-processing products. *Green Chemistry*, 14(5), 1367.

[50] Diebold, J. P., & Czernik, S. (1997). Additives to Lower and Stabilize the Viscosity of Pyrolysis Oils during Storage. *Energy & Fuels*, 11(5), 1081-1091.

[51] Butler, E. et al. (2011). A review of recent laboratory research and commercial developments in fast pyrolysis and upgrading. *Renewable and Sustainable Energy Reviews, 15*(8), 4171-4186.

[52] Huber, G. W., & Dumesic, J. A. (2006). An overview of aqueous-phase catalytic processes for production of hydrogen and alkanes in a biorefinery. *Catalysis Today*, 111(1-2), 119-132.

[53] Cortright, R. D., Davda, R. R., & Dumesic, J. A. (2002). Hydrogen from catalytic reforming of biomass-derived hydrocarbons in liquid water. *Nature*, 418(6901), 964-967.

[54] Huber, G. W., Cortright, R. D., & Dumesic, J. A. (2004). Renewable Alkanes by Aqueous-Phase Reforming of Biomass-Derived Oxygenates. *Angewandte Chemie International Edition*, 43(12), 1549-1551.

[55] Gollakota, A. R. et al. (2016). A review on the upgradation techniques of pyrolysis oil. *Renewable and Sustainable Energy Reviews*, 58, 1543-1568.

[56] Czernik, S., Wang, D., & Chornet, E. (1998). Production of hydrogen from biomass by catalytic steam reforming of fast pyrolysis oil.

[57] Hu, X., & Lu, G. (2010). Bio-oil steam reforming, partial oxidation or oxidative steam reforming coupled with bio-oil dry reforming to eliminate CO_2 emission. *International Journal of Hydrogen Energy*, 35(13), 7169-7176.

[58] Medrano, J. et al. (2011). Hydrogen from aqueous fraction of biomass pyrolysis liquids by catalytic steam reforming in fluidized bed. *Energy*, 36(4), 2215-2224.

[59] Rennard, D. et al. (2010). Production of synthesis gas by partial oxidation and steam reforming of biomass pyrolysis oils. *International Journal of Hydrogen Energy*, 35(9), 4048-4059.

[60] He, Z., & Wang, X. (2013). Hydrodeoxygenation of model compounds and catalytic systems for pyrolysis bio-oils upgrading. *Catalysis for Sustainable Energy,* 28-52.

[61] Graça, I. et al. (2013). Bio-oils Upgrading for Second Generation Biofuels. *Industrial & Engineering Chemistry Research,* 52(1), 275-287.

[62] Mortensen, P. et al. (2011). A review of catalytic upgrading of bio-oil to engine fuels. *Applied Catalysis A: General,* 407(1-2), 1-19.

[63] Yang, Y., Gilbert, A., & Xu, C. (2009). Hydrodeoxygenation of bio-crude in supercritical hexane with sulfided CoMo and CoMoP catalysts supported on MgO: A model compound study using phenol. *Applied Catalysis A: General,* 360(2), 242-249.

[64] Jacobson, K., Maheria, K. C., & Dalai, A. K. (2013). Bio-oil valorisation: A review. *Renewable and Sustainable Energy Reviews, 23*, 91-106.

[65] Junming, X. et al. (2008). Bio-oil upgrading by means of ethyl ester production in reactive distillation to remove water and to improve storage and fuel characteristics. *Biomass and Bioenergy, 32*(11), 1056-1061.

[66] Zhang, Q. et al. (2007). Review of biomass pyrolysis oil properties and upgrading research. *Energy Conversion and Management*, 48(1), 87-92.

[67] Elliott, D. C., & Neuenschwander, G. G. (1997). Liquid Fuels by Low-Severity Hydrotreating of Biocrude. *Developments in Thermochemical Biomass Conversion*, 611-621.

[68] Brown, R.C., & Holmgren, J. (2006). Fast Pyrolysis and Bio-oil Upgrading Distributed Biomass and Diesel. *http://www.ascension-publishing.com/BIZ/HD50.pdf*. Accessed on 21/04/2018.

[69] Pindoria, R. V. et al. (1997). Structural characterisation of biomass pyrolysis tars/oils from eucalyptus wood waste: Effect of H_2 pressure and sample configuration. *Fuel*, 76(11), 1013-1023.

[70] Marker, T. L. et al. (2011). Integrated hydropyrolysis and hydroconversion (IH^2) for the direct production of gasoline and diesel fuels or blending components from biomass, part 1: Proof of principle testing. *Environmental Progress & Sustainable Energy*, 31(2), 191-199.

[71] Marker, T. L. et al. (2013). Integrated hydropyrolysis and hydroconversion ($IH^{2®}$) for the direct production of gasoline and diesel fuels or blending components from biomass, Part 2: Continuous testing. *Environmental Progress & Sustainable Energy*, 33(3), 762-768.

[72] Linck, M. et al. (2014). Integrated biomass hydropyrolysis and hydrotreating: a brief review. *Energy & Environmental Science*, 3, 575-581.

[73] Van Der Voort, P. (2016). Heterogeneous Catalysis. Academic year 2015-2016. Ghent: Ghent University.

[74] Lin, Y., & Huber, G. W. (2009). The critical role of heterogeneous catalysis in lignocellulosic biomass conversion. *Energy & Environmental Science,* 2(1), 68-80.

[75] Morris, M. (2011). Production of bio-oils via catalytic pyrolysis. *Handbook of Biofuels Production,* 349-389.

[76] Mante, O. D., Agblevor, F., & Mcclung, R. (2013). A study on catalytic pyrolysis of biomass with Y-zeolite based FCC catalyst using response surface methodology. *Fuel,* 108, 451-464.

[77] Kersten, S., & Garcia-Perez, M. (2013). Recent developments in fast pyrolysis of ligno-cellulosic materials. *Current Opinion in Biotechnology,* 24(3), 414-420.

[78] Scott, D. S. et al. (1988). The role of temperature in the fast pyrolysis of cellulose and wood. *Industrial & Engineering Chemistry Research,* 27(1), 8-15.

[79] Hayes, D. J. (2013). Biomass Composition and Its Relevance to Biorefining. *The Role of Catalysis for the Sustainable Production of Bio-fuels and Bio-chemicals,* 27-65.

[80] Jacobson, K., Maheria, K. C., & Dalai, A. K. (2013). Bio-oil valorisation: A review. *Renewable and Sustainable Energy Reviews,* 23, 91-106.

[81] Bartholomew, C. H., & Farrauto, R. J. (2006). Fundamentals of Industrial Catalytic Processes. Wiley Interscience, Hoboken.

[82] Morris, M. (2011). Production of bio-oils via catalytic pyrolysis. *Handbook of Biofuels Production,* 349-389.

[83] Engtrakul, C. et al. (2016). Effect of ZSM-5 acidity on aromatic product selectivity during upgrading of pine pyrolysis vapors. *Catalysis Today*, 269, 175-181.

[84] Karg, H. G., Hunger, M., & Beyer, H. K. (1999). Characterisation of zeolites. *Catalysis and Zeolites: Fundamentals and applications,* 198–326.

[85] Hansch, C. (1953). The dehydrocyclisation reaction. *Chemical Review*, 53(3), 353-396.

[86] Zhang, H. et al. (2011). Catalytic conversion of biomass-derived feedstocks into olefins and aromatics with ZSM-5: The hydrogen to carbon effective ratio. *Energy & Environmental Science,* 4(6), 2297.

[87] Qiang, L., et al. (2009). Analytical pyrolysis–gas chromatography/mass spectrometry (Py–GC/MS) of sawdust with Al/SBA-15 catalysts. *Journal of Analytical and Applied Pyrolysis,* 84(2), 131-138.

[88] Stefanidis, S.D. et al. (2011). In-situ upgrading of biomass pyrolysis vapors: Catalyst screening on a fixed bed reactor. *Bioresource Technology*. 102(17), 8261-8267.

[89] Venderbosch, R. H. (2015). A Critical View on Catalytic Pyrolysis of Biomass. *ChemSusChem*, 8(8), 1306-1316.

[90] Nik-Azar, M., et al. (1997). Mineral matter effects in rapid pyrolysis of beech wood. *Fuel Processing Technology*, 51(1-2), 7-17.

[91] Mahadevan, R. et al. (2016). Effect of Alkali and Alkaline Earth Metals on in-Situ Catalytic Fast Pyrolysis of Lignocellulosic Biomass: A Microreactor Study. *Energy & Fuels*, 30(4), 3045-3056.

[92] Blasi, C. D., Branca, C., & Galgano, A. (2008). Thermal and catalytic decomposition of wood impregnated with sulfur- and phosphorus-containing ammonium salts. *Polymer Degradation and Stability,* 93(2), 335-346.

[93] Yaman, S. (2004). Pyrolysis of biomass to produce fuels and chemical feedstocks. *Energy Conversion and Management*, 45(5), 651-671.

[94] Zheng, Y. et al. (2014). Pretreatment of lignocellulosic biomass for enhanced biogas production. *Progress in Energy and Combustion Science,* 42, 35-53.

[95] Erlich, C. et al. (2006). Pyrolysis and gasification of pellets from sugar cane bagasse and wood. *Fuel,* 85(10-11), 1535-1540.

[96] Schultz, T. P., Biermann, C. J., & Mcginnis, G. D. (1983). Steam explosion of mixed hardwood chips as a biomass pretreatment. *Industrial & Engineering Chemistry Product Research and Development,* 22(2), 344-348.

[97] Yu, Y. et al. (2013). Improving the conversion of biomass in catalytic fast pyrolysis via white-rot fungal pretreatment. *Bioresource Technology,* 134, 198-203.

[98] Stevens, C., & D'hooghe, M. (2013). Bio-organic chemistry. Academic year 2016-2017. Ghent: Ghent University.

[99] Tan, H. T., & Lee, K. T. (2012). Understanding the impact of ionic liquid pretreatment on biomass and enzymatic hydrolysis. *Chemical Engineering Journal,* 183, 448-458.

[100] Bartholomew, C. H. (2010). Mechanisms of Catalyst Deactivation. *Applied Catalysis A: general,* 212(27), 17-60.

[101] Yu, Y. et al. (2012). The role of shape selectivity in catalytic fast pyrolysis of lignin with zeolite catalysts. *Applied Catalysis A: General,* 447-448, 115-123.

[102] Aguayo, A. et al. (2005). Regeneration of a HZSM-5 zeolite catalyst deactivated in the transformation of aqueous ethanol into hydrocarbons. *Catalysis Today,* 107-108, 410-416.

[103] Fogassy, G., et al. (2011). From biomass to bio-gasoline by FCC co-processing: Effect of feed composition and catalyst structure on product quality. *Energy & Environmental Science,* 4(12), 5068-5076.

[104] Du, S. et al. (2016). Coke formation of model compounds relevant to pyrolysis bio-oil over ZSM-5. *Applied Catalysis A: General,* 513, 67-81.

[105] Ibarra, Á. Et al. (2016). Dual coke deactivation pathways during the catalytic cracking of raw bio-oil and vacuum gasoil in FCC conditions. *Applied Catalysis B: Environmental,* 182, 336-346.

[106] Ngoye, F. et al. (2014). Mitigating coking during methylcyclohexane transformation on HZSM-5 zeolites with additional porosity. *Journal of Catalysis,* 320, 118-126.

[107] Guisnet, M., & Magnoux, P. (1997). Deactivation by coking of zeolite catalysts. Prevention of deactivation. Optimal conditions for regeneration. *Catalysis Today,* 36(4), 477-483.

[108] Cerqueira, H. S., & Ribeiro, F. R. (2011). Deactivation and Regeneration of FCC Catalysts. *Deactivation and Regeneration of Zeolite Catalysts Catalytic Science Series,* 235-251.

[109] Triantafillidis, C. S., et al. (2001). Effect of the degree and type of the dealumination method on the structural, compositional and acidic characteristics of H-ZSM-5 zeolites. *Microporous and Mesoporous Materials,* 47(2-3), 369-388.

[110] Zhang, B. et al. (2015). Catalytic upgrading of fast pyrolysis biomass vapors over fresh, spent and regenerated ZSM-5 zeolites. *Fuel Processing Technology*, 138, 430-434.

[111] Yildiz, G. et al. (2015). Effect of biomass ash in catalytic fast pyrolysis of pine wood. *Applied Catalysis B: Environmental*, 168-169, 203-211.

[112] Jia, L. Y. et al. (2017). Catalytic fast pyrolysis of biomass: Superior selectivity of hierarchical zeolites to aromatics. *Green Chemistry,* 19(22), 5442-5459.

[113] Williams, P. T., & Nugranad, N. (2000). Comparison of products from the pyrolysis and catalytic pyrolysis of rice husks. *Energy,* 25(6), 493-513.

[114] Mukarakate, C. et al. (2014). Real-time monitoring of the deactivation of HZSM-5 during upgrading of pine pyrolysis vapors. *Green Chemistry,* 16(3), 1444-1461.

[115] Corma, A. (2003). State of the art and future challenges of zeolites as catalysts. *Journal of Catalysis,* 216(1-2), 298-312.

[116] Adjaye, J., & Bakhshi, N. (1995). Production of hydrocarbons by catalytic upgrading of a fast pyrolysis bio-oil. Part I: Conversion over various catalysts. *Fuel Processing Technology, 45*(3), 161-183.

[117] Adjaye, J., & Bakhshi, N. (1995). Production of hydrocarbons by catalytic upgrading of a fast pyrolysis bio-oil. Part II: Comparative catalyst performance and reaction pathways. *Fuel Processing Technology, 45*(3), 185-202.

[118] Vitolo, S., et al. (2001). Catalytic upgrading of pyrolytic oils over HZSM-5 zeolite: Behaviour of the catalyst when used in repeated upgrading–regenerating cycles. *Fuel, 80*(1), 17-26.

[119] Vitolo, S. et al. (1999). Catalytic upgrading of pyrolytic oils to fuel over different zeolites. *Fuel, 78*(10), 1147-1159.

[120] Zhang, H. et al. (2013). Characterisation of Coke Deposition in the Catalytic Fast Pyrolysis of Biomass Derivates. *Energy & Fuels*, 28(1), 52-57.

[121] Das, P., Ganesh, A., & Wangikar, P. (2004). Influence of pretreatment for deashing of sugarcane bagasse on pyrolysis products. *Biomass and Bioenergy, 27*(5), 445-457.

[122] Obernberger, I., & Brunner, T. (2014). Advanced characterisation methods for solid biomass fuels. *IEA Bioenergy Task 32.*

[123] Rodríguez-Machín, L. et al. (2018). Effect of citric acid leaching on the demineralisation and thermal degradation behavior of sugarcane trash and bagasse. *Biomass and Bioenergy*, 108, 371-380.

[124] Patwardhan, P. R. (2010). Understanding the product distribution from biomass fast pyrolysis. Iowa State University.

[125] J.M. Perez, J.M., Duda, J.L., Schobert, H.H. (1998). A review of current fuels, fuel chemistry, and fuel trends. Pennsylvania State University.

[126] Larba, R., et al. (2013). Citric acid as an alternative lixiviant for zinc oxide dissolution. *Hydrometallurgy*, 134-135, 117-123.

[127] Vasconcelos, S. M., et al. (2013). Diluted phosphoric acid pretreatment for production of fermentable sugars in a sugarcane-based biorefinery. *Bioresource Technology*, 135, 46-52.

[128] Carrier, M., et al. (2012). Influence of Chemical Pretreatment on the Internal Structure and Reactivity of Pyrolysis Chars Produced from Sugar Cane Bagasse. *Energy & Fuels*, 26(7), 4497-4506.

[129] Yadegary, M. et al. (2013). Citric Acid Production from Sugarcane Bagasse through Solid State Fermentation Method Using *Aspergillus niger* Mold and Optimisation of Citric Acid Production by Taguchi Method. *Journal of Microbiology*, 6(9).

[130] Kumar, D., Jain, V., Shanker, G., & Srivastava, A. (2003). Citric acid production by solid state fermentation using sugarcane bagasse. *Process Biochemistry*, 38(12), 1731-1738.

[131] Yildiz, G. et al. (2014). Catalytic Fast Pyrolysis of Pine Wood: Effect of Successive Catalyst Regeneration. *Energy & Fuels*, 28(7), 4560-4572.

[132] Feys, J. et al. (2017). Valorisation of sugarcane bagasse and straw to liquid fuels by means of demineralisation and fast pyrolysis. Ghent: Ghent University.

[133] Tan, S. et al. (2013). Recent progress of catalytic pyrolysis of biomass by HZSM-5. *Chinese Journal of Catalysis, 34*(4), 641-650.

[134] Vercruysse, J. et al. (2013). Valorisation potential of natural low HCT poplar mutants in catalytic fast pyrolysis. Proceedings EU BC&E 2013: 21th European biomass conference and exhibition (pp. 506–510). Presented at the 21th European Biomass conference and exhibition (EU BC&E 2013), Florence, Italy: ETA-Florence Renewable Energies.

[135] Wang, K., Kim, K. H., & Brown, R. C. (2014). Catalytic pyrolysis of individual components of lignocellulosic biomass. *Green Chem*., 16(2), 727-735.

[136] Howe, D. et al. (2015). Field-to-Fuel Performance Testing of Lignocellulosic Feedstocks: An Integrated Study of the Fast Pyrolysis–Hydrotreating Pathway. *Energy & Fuels*, 29(5), 3188-3197.

[137] Iisa, K. et al. (2016). In Situ and ex Situ Catalytic Pyrolysis of Pine in a Bench-Scale Fluidized Bed Reactor System. *Energy & Fuels*, 30(3), 2144-2157.

[138] Hernando, H. et al. (2016). Assessing biomass catalytic pyrolysis in terms of deoxygenation pathways and energy yields for the efficient production of advanced biofuels. *Catalysis Science & Technology*, 6(8), 2829-2843.

[139] Paasikallio, V. et al. (2016). Catalytic Fast Pyrolysis: Influencing Bio-Oil Quality with the Catalyst-to-Biomass Ratio. *Energy Technology*, 5(1), 94-103.

[140] Hernando, H. et al. (2016). Assessing biomass catalytic pyrolysis in terms of deoxygenation pathways and energy yields for the efficient production of advanced biofuels. *Catalysis Science & Technology*, 6(8), 2829-2843.

[141] Carlson, T. R. et al. (2009). Aromatic Production from Catalytic Fast Pyrolysis of Biomass-Derived Feedstocks. *Topics in Catalysis*, 52(3), 241-252.

[142] Torri, C. et al. (2010). Investigation on catalytic pyrolysis of pine sawdust: Catalyst screening by Py-GC-MIP-AED. *Journal of Analytical and Applied Pyrolysis*, 88(1), 7-13.

[143] Mihalcik, D. J., Mullen, C. A., & Boateng, A. A. (2011). Screening acidic zeolites for catalytic fast pyrolysis of biomass and its components. *Journal of Analytical and Applied Pyrolysis*, 92(1), 224-232.

[144] Carlson, T. R. et al. (2011). Production of green aromatics and olefins by catalytic fast pyrolysis of wood sawdust. *Energy Environ. Sci*., 4(1), 145-161.

[145] Corma, A. et al. (2007). Processing biomass-derived oxygenates in the oil refinery: Catalytic cracking (FCC) reaction pathways and role of catalyst. *Journal of Catalysis*, 247(2), 307-327.

[146] Dao, L. H. et al. (1988). Reactions of Model Compounds of Biomass-Pyrolysis Oils over ZSM—5 Zeolite Catalysts. *ACS Symposium Series Pyrolysis Oils from Biomass*, 328-341.

[147] Horne, P. A., & Williams, P. T. (1996). Reaction of oxygenated biomass pyrolysis model compounds over a ZSM-5 catalyst. *Renewable Energy*, 7(2), 131-144.

[148] Cheng, Y., & Huber, G. W. (2011). Chemistry of Furan Conversion into Aromatics and Olefins over HZSM-5: A Model Biomass Conversion Reaction. *ACS Catalysis*, 1(6), 611-628.

[149] Karanjkar, P. U. et al. (2014). Production of aromatics by catalytic fast pyrolysis of cellulose in a bubbling fluidized bed reactor. *AIChE Journal*, 60(4), 1320-1335.

[150] Yang, H. et al. (2017). The effects of contact time and coking on the catalytic fast pyrolysis of cellulose. *Green Chemistry*, 19(1), 286-297.

[151] Cellets. http://www.cellets.com/ Accessed on 19/05/2018.

[152] Liang, T. et al. (2011). Catalytic Fast Pyrolysis of Cellulose with HZSM-5. *Advanced Materials Research*, 347-353, 2459-2463.

[153] Fabbri, D., Torri, C., & Baravelli, V. (2007). Effect of zeolites and nanopowder metal oxides on the distribution of chiral anhydrosugars evolved from pyrolysis of cellulose: An analytical study. *Journal of Analytical and Applied Pyrolysis*, 80(1), 24-29.

[154] Savant, N. K. et al. (1999). Silicon nutrition and sugarcane production: A review. *Journal of Plant Nutrition*, 22(12), 1853-1903.

[155] Lanning, F. C., & Eleuterius, L. N. (1987, 10). Silica and Ash in Native Plants of the Central and Southeastern Regions of the United States. *Annals of Botany*, 60(4), 361-375.

[156] Patwardhan, P. R. et al. (2010). Influence of inorganic salts on the primary pyrolysis products of cellulose. *Bioresource Technology*, 101(12), 4646-4655.

[157] Yang, C. et al. (2006). TG-FTIR Study on Corn Straw Pyrolysis-influence of Minerals. *Chemical Research in Chinese Universities*, 22(4), 524-532.

[158] Iisa, K. et al. (2018). Improving biomass pyrolysis economics by integrating vapor and liquid phase upgrading. *Green Chemistry*, 20(3), 567-582.

[159] Mante, O. D. et al. (2016). Integration of catalytic fast pyrolysis and hydroprocessing: A pathway to refinery intermediates and “drop-in” fuels from biomass. *Green Chemistry*, 18(22), 6123-6135.

[160] Bridgwater, A. (1996). Production of high grade fuels and chemicals from catalytic pyrolysis of biomass. *Catalysis Today*, 29(1-4), 285-295.

[161] Brown, T. R. et al. (2012). Techno-economic analysis of biobased chemicals production via integrated catalytic processing. *Biofuels, Bioproducts and Biorefining*, 6(1), 73-87.

[162] Herregods-Van De Pontseele, K. (2017). Snelle pyrolyse van biomassa met voorbehandeling: techno-economische evaluatie.

[163] Lange, J. (2016). Catalysis for biorefineries – performance criteria for industrial operation. *Catalysis Science & Technology*, 6(13), 4759-4767.

9. Appendix

Appendix A: catalytic fast pyrolysis of pine wood in the mini-plant

Addendum A.1: phase distributions of the different bio-oils of the CFP experiments with pine wood in the mini-plant.

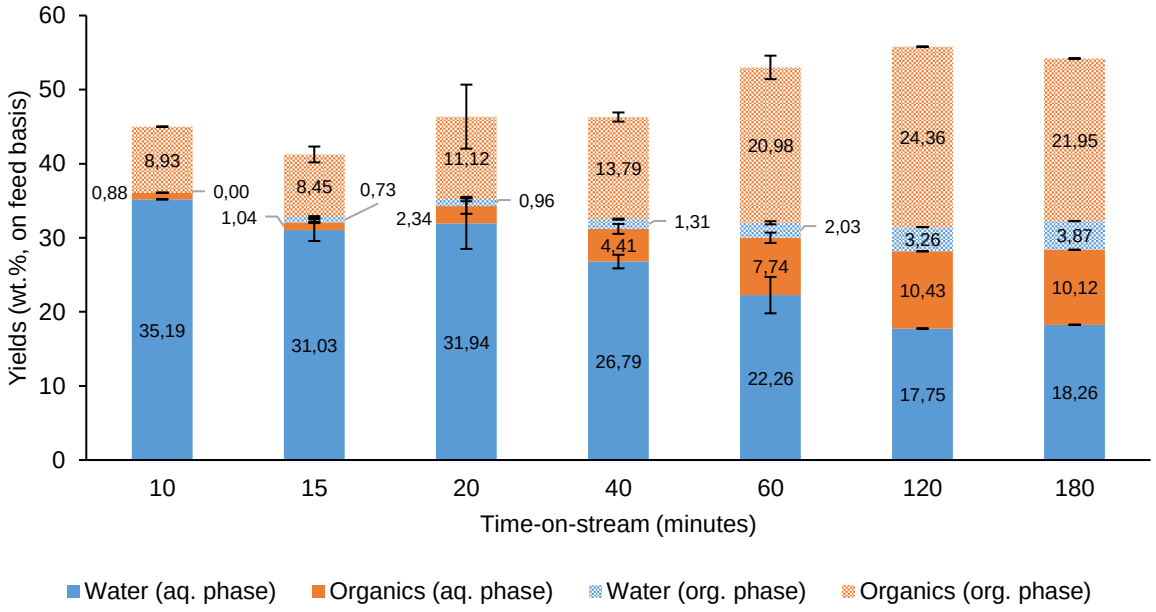

Addendum A.2: average (± st.dev.) wt.% of each non-condensable gas produced during CFP of pine wood.

BM/CAT (-)	TOS (min.)	H_2	CH_4	CO	CO_2	C_2H_4	C_2H_6	C_3H_6/C_3H_8	Total
0.9	10	0.20 (± 0.03)	1.72 (± 0.03)	17.19 (± 0.09)	10.63 (± 0.57)	1.72 (± 0.03)	0.34 (± 0.01)	2.04 (± 0.07)	33.84 (± 0.59)
1.4	15	0.18 (± 0.03)	1.58 (± 0.11)	15.65 (± 0.82)	9.65 (± 0.77)	1.47 (± 0.07)	0.30 (± 0.02)	1.72 (± 0.12)	30.55 (± 1.14)
1.6	20	0.20 (± 0.01)	1.60 (± 0.17)	16.11 (± 0.88)	10.14 (± 0.71)	1.50 (± 0.09)	0.31 (± 0.01)	1.81 (± 0.10)	31.66 (± 1.15)
3.4	40	0.16 (± 0.01)	1.59 (± 0.17)	14.63 (± 1.32)	8.93 (± 0.55)	1.14 (± 0.11)	0.27 (± 0.02)	1.36 (± 0.10)	28.08 (± 1.45)
5.5	60	0.14 (± 0.01)	1.37 (± 0.06)	12.28 (± 0.46)	7.52 (± 0.42)	0.86 (± 0.01)	0.23 (± 0.01)	1.08 (± 0.02)	23.48 (± 0.63)
11.7	120	0.12	1.23	10.68	6.66	0.67	0.18	0.82	20.38
17.0	180	0.13	1.31	10.99	7.15	0.62	0.18	0.73	21.12
NC	NC	0.08 (± 0.01)	1.08 (± 0.13)	8.16 (± 1.01)	4.93 (± 0.61)	0.29 (± 0.04)	0.10 (± 0.01)	0.25 (± 0.03)	14.87 (± 1.19)

Addendum A.3: values of carbon yield and oxygen reduction for the organic phase as well as the complete bio-oil of catalytic pine wood experiments. The values for the organic phase are plotted in figure 19.

BM/CAT	TOS	Organic phase		Complete bio-oil	
(-)	(min.)	η_C	ξ_O	η_C	ξ_O
0.9	10	1.73	97.04		
1.4	15	1.82	97.83		
1.6	20	3.16	96.64	5.89	30.43
3.4	40	4.94	93.62	7.42	40.31
5.5	60	11.46	88.13	13.85	39.33
11.7	120	16.51	79.09	18.76	39.98
17.0	180	14.43	85.33	16.69	43.02

Addendum A.4, A.5, B.4 and B.5 present an overview of the most abundant compounds present in the (catalytic) bio-oils of pine wood and cellulose, expressed as concentration (in wt.%) of organic/aqueous phase. Bold compounds were calibrated and their response factor has been calculated. For the other chemicals, an estimation of the response factor was made of similar calibrated compounds. For those without mentioned average value and standard deviation, they were respectively below 0.005 wt.%. Sometimes, substituted chemicals were calculated together. Compounds present in such a group are listed above the table, and position of substituted structures are numbered by x, y and z, which can vary from 1 – 4

Addendum A.4: overview of different chemicals detected in the **organic phase** of the (catalytic) bio-oils of pine wood, expressed as concentration (in wt.%) of organic phase. ***Benzene, alkyl/allyl substituted**: (x)-ethyl-(y)-methyl-, (x,y,z)-trimethyl-, ethyl- and 1-propenylbenzene, styrene and 2,4-dimethylstyrene. * **Phenol, alkyl substituted**: (x)-methyl-, (x,y)-dimethyl-, (x,y,z)-trimethyl-, (x)-ethyl-, (x)-ethyl-(y)-methyl- and (x)-methyl-(y)-propylphenol ***Phenol, alkyl/allyl substituted:** 2-allylphenol and 2-allyl-4-methylphenol ***Naphthalene, alkyl substituted:** (x)-methyl-, (y)-ethyl-, (x,y)-dimethyl- and (x,y,z)-trimethylnapthalene. ***Indene and substitutes:** (2,3-dihydro)-1H-indenol, 2,3-dimethyl-(4-methyl)-1H-indene, indene, 1-methylindan…

BM/CAT	0.9	1.4	1.6	3.4	5.5	11.7	17.0
TOS (min)	10	15	20	40	60	120	180
BENZENES	**0.91** (± 0.10)	**1.87** (± 0.22)	**2.55** (± 0.31)	**1.62** (± 0.07)	**1.20** (± 0.07)	**0.60** (± 0.02)	**0.46**
Benzene	0.01 (± 0.01)	0.07 (± 0.01)	0.11 (± 0.03)	0.06	0.05	0.02	0.00
Toluene	0.28 (± 0.04)	0.82 (± 0.20)	1.34 (± 0.30)	0.62 (± 0.06)	0.43 (± 0.04)	0.19 (± 0.02)	0.13
o-Xylene	0.20 (± 0.05)	0.32 (± 0.04)	0.43 (± 0.04)	0.27 (± 0.01)	0.19 (± 0.02)	0.09 (± 0.01)	0.06
m/p-Xylene	0.03 (± 0.01)	0.07 (± 0.01)	0.10 (± 0.01)	0.05 (± 0.01)	0.04	0.02	0.01
Benzene, alkyl/allyl substituted*	0.38 (± 0.08)	0.59 (± 0.08)	0.57 (± 0.08)	0.53 (± 0.04)	0.42 (± 0.05)	0.26	0.21
Vanillin	0.00	0.00	0.00	0.08	0.07 (± 0.01)	0.04	0.06
PHENOLS	**3.62** (± 0.92)	**2.94** (± 0.41)	**2.51** (± 0.44)	**2.23** (± 0.11)	**1.78** (± 0.12)	**0.98** (± 0.02)	**0.86** (± 0.02)
Phenol	0.69 (± 0.17)	0.63 (± 0.07)	0.55 (± 0.11)	0.42 (± 0.04)	0.30 (± 0.03)	0.14 (± 0.01)	0.12
2-Methoxy-4-methylphenol	0.11 (± 0.02)	0.10 (± 0.01)	0.07 (± 0.02)	0.07 (± 0.01)	0.07 (± 0.01)	0.05	0.04
Phenol, alkyl substituted*	2.59 (± 0.90)	1.95 (± 0.40)	1.73 (± 0.42)	1.50 (± 0.10)	1.20 (± 0.11)	0.67 (± 0.02)	0.59 (± 0.02)
Phenol, alkyl/allyl substituted*	0.25 (± 0.01)	0.25 (± 0.05)	0.16 (± 0.06)	0.23 (± 0.01)	0.21 (± 0.02)	0.13	0.11 (± 0.01)
PAHs	**8.35** (± 1.50)	**6.10** (± 0.53)	**4.89** (± 0.65)	**3.31** (± 0.10)	**2.07** (± 0.07)	**0.94** (± 0.04)	**0.74** (± 0.03)
Naphtalene	2.05 (± 0.60)	1.63 (± 0.19)	1.38 (± 0.31)	0.96 (± 0.08)	0.59 (± 0.04)	0.27 (± 0.02)	0.21 (± 0.01)
1,2-dihydronaphthalene	0.15 (± 0.03)	0.13 (± 0.01)	0.11 (± 0.03)	0.08 (± 0.01)	0.05	0.02	0.01
Naphtalene, alkyl substituted*	5.14 (± 1.36)	3.28 (± 0.48)	2.62 (± 0.52)	1.64 (± 0.08)	1.03 (± 0.04)	0.48 (± 0.03)	0.38 (± 0.02)
Indene and substitutes*	1.00 (± 0.18)	1.04 (± 0.12)	0.77 (± 0.24)	0.62 (± 0.04)	0.40 (± 0.04)	0.16 (± 0.01)	0.13 (± 0.02)
LIGHT OXYGENATES	**1.00** (± 0.33)	**1.63** (± 0.13)	**1.39** (± 0.43)	**3.87** (± 0.17)	**4.70** (± 0.31)	**5.27** (± 0.17)	**7.66** (± 0.18)
5-Methyl-2-furancarboxaldehyde	0.08 (± 0.10)	0.30 (± 0.04)	0.25 (± 0.14)	0.51 (± 0.08)	0.46 (± 0.04)	0.23 (± 0.01)	0.20
2,3-Butanedione	0.00	0.00	0.00	0.29 (± 0.03)	0.32 (± 0.04)	0.30	0.29 (± 0.02)
Acetic acid	0.00	0.00	0.00	0.34 (± 0.07)	0.64 (± 0.17)	0.69 (± 0.05)	1.14 (± 0.13)
Hydroxyacetaldehyde	0.00	0.00	0.00	0.27 (± 0.05)	0.73 (± 0.20)	1.46 (± 0.16)	2.94 (± 0.08)
1-hydroxy-2-propanone	0.00	0.00	0.00	0.65 (± 0.03)	0.88 (± 0.09)	1.36 (± 0.01)	1.86 (± 0.09)
Furfural	0.00	0.00	0.00	1.12 (± 0.10)	0.99 (± 0.08)	0.68 (± 0.01)	0.63 (± 0.02)
3-Methyl-1,2-cyclopentanedione	0.03 (± 0.05)	0.16 (± 0.03)	0.10 (± 0.06)	0.22 (± 0.01)	0.22 (± 0.02)	0.15 (± 0.02)	0.17 (± 0.02)
2-Cyclopenten-1-one	0.89 (± 0.31)	1.17 (± 0.12)	1.03 (± 0.40)	0.47 (± 0.05)	0.43 (± 0.04)	0.30 (± 0.02)	0.35 (± 0.02)
2,3-Pentanedione	0.00	0.00	0.00	0.00	0.03 (± 0.07)	0.11	0.10 (± 0.01)
ANHYDROSUGARS (levoglucosan)	**0.06** (± 0.12)	**0.00**	**0.00**	**0.03** (± 0.07)	**0.46** (± 0.06)	**0.85** (± 0.84)	**1.43** (± 0.38)
TOTAL WT.% DETERMINED	**14.00** (± 1.80)	**12.54** (± 0.71)	**11.34** (± 0.95)	**11.06** (± 0.25)	**10.21** (± 0.35)	**8.64** (± 0.86)	**11.15** (± 0.42)

Addendum A.5: overview of different chemicals detected in the **aqueous phase** of the (catalytic) bio-oils of **pine wood**, expressed as concentration (in wt.%) of aqueous phase. ***Phenol, alkyl substituted**: (x)-methyl-, (x,y)-dimethyl- and (x)-ethyl-(y)-methylphenol. ***Other sugars**: D-allose, 1,4:3,6-dianhydro-α-D-glucopyranose and methyl-α-D-ribo-furanoside.

BM/CAT	**1.6**	**3.4**	**5.5**	**11.7**	**17.0**	**NC**
TOS (min)	**20**	**40**	**60**	**120**	**180**	**120**
PHENOLS	**0.13** (± 0.01)	**0.17** (± 0.02)	**0.40** (± 0.17)	**0.22**	**0.14**	**0.28** (± 0.02)
Phenol	0.07	0.06 (± 0.01)	0.12 (± 0.08)	0.05	0.04	0.03
Phenol, alkyl substituted*	0.05 (± 0.01)	0.08 (± 0.01)	0.21 (± 0.14)	0.15	0.08	0.24 (± 0.02)
Hydroquinone	0.01	0.03 (± 0.01)	0.07 (± 0.05)	0.02	0.02	0.00 (± 0.01)
LIGHT OXYGENATES	**0.89** (± 0.11)	**2.83** (± 0.20)	**9.61** (± 3.14)	**4.96** (± 0.16)	**4.33** (± 0.11)	**4.30** (± 0.17)
5-Methyl-2-furan-carboxaldehyde	0.00	0.01 (± 0.08)	0.04 (± 0.04)	0.03	0.01	0.14 (± 0.01)
5-Hydroxymethyl-2-furan-carboxaldehyde	0.00	0.03 (± 0.01)	0.09 (± 0.06)	0.02 (± 0.01)	0.02 (± 0.01)	0.04 (± 0.04)
2-Cyclopenten-1-one	0.06 (± 0.02)	0.19 (± 0.04)	0.55 (± 0.41)	0.06 (± 0.01)	0.04	0.28 (± 0.08)
2,3-Butanedione	0.05	0.09 (± 0.02)	0.24 (± 0.22)	0.17 (± 0.01)	0.09 (± 0.06)	0.08 (± 0.12)
Glycolaldehyde	0.20 (± 0.05)	0.79 (± 0.03)	3.07 (± 1.88)	1.88 (± 0.13)	1.80 (± 0.09)	0.35 (± 0.01)
Furfural	0.00	0.00	0.00	0.12	0.08	0.19 (± 0.01)
Acetic acid	0.33 (± 0.07)	0.83 (± 0.13)	2.53 (± 1.89)	1.13 (± 0.06)	1.07	1.23 (± 0.07)
Hydroxyacetone	0.17 (± 0.06)	0.59 (± 0.11)	2.08 (± 1.54)	1.01 (± 0.07)	0.92 (± 0.01)	1.26 (± 0.02)
1,2-Ethanediol, monoacetate	0.04 (± 0.02)	0.16 (± 0.01)	0.53 (± 0.36)	0.31 (± 0.02)	0.11	0.42 (± 0.01)
2,3-Pentadione	0.02	0.02	0.06 (± 0.03)	0.03	0.03	0.00
Propanoic acid	0.01 (± 0.01)	0.06 (± 0.02)	0.18 (± 0.15)	0.08	0.06	0.08 (± 0.02)
3-Methyl-1,2-cyclopentane-dione	0.01 (± 0.01)	0.05 (± 0.02)	0.14 (± 0.11)	0.11	0.07 (± 0.01)	0.16 (± 0.04)
1-Hydroxy-2-butanone	0.00	0.03 (± 0.01)	0.11 (± 0.01)	0.02	0.02	0.09 (± 0.01)
ANHYDROSUGARS	**0.12** (± 0.04)	**0.72** (± 0.06)	**2.53** (± 1.42)	**1.40** (± 0.64)	**1.67** (± 0.13)	**2.53** (± 0.11)
Levoglucosan	0.09 (± 0.03)	0.70 (± 0.06)	2.45 (± 1.38)	1.36 (± 0.64)	1.63 (± 0.13)	2.21 (± 0.10)
Other sugars*	0.03 (± 0.02)	0.02	0.08 (± 0.05)	0.05 (± 0.02)	0.04	0.32 (± 0.04)
TOTAL WT.% DETERMINED	**1.12** (± 0.12)	**3.72** (± 0.21)	**12.49** (± 3.45)	**6.55** (± 0.66)	**6.11** (± 0.17)	**7.11** (± 0.20)

Addendum A.6: elemental analysis of the coked catalyst samples of the catalytic pine wood experiments.

BM/CAT (-)	TOS (min)	Average (± stdev.) C	H	BM/CAT (-)	TOS (min)	Average (± stdev.) C	H
0.9	10	5.89 (± 0.18)	0.72 (± 0.03)	3.4	40	11.61 (± 0.65)	0.77 (± 0.05)
		5.80 (± 0.35)	0.71 (± 0.01)			11.44 (± 0.23)	0.80 (± 0.02)
1.4	15	8.00 (± 0.76)	0.68 (± 0.05)	5.5	60	15.17 (± 0.26)	0.88 (± 0.00)
		6.52 (± 0.16)	0.67 (± 0.03)			14.38 (± 0.17)	0.89 (± 0.06)
1.6	20	8.01 (± 1.29)	0.70 (± 0.06)	11.7	120	17.84 (± 0.05)	0.91 (± 0.00)
		7.85 (± 0.38)	0.81 (± 0.10)	17	180 (2x 90)	19.96 (± 1.39)	0.92 (± 0.02)

Addendum A.7: values of BET surface area, TPD-NH3 and pore volume of the spent catalysts of pine wood experiments. Values given in parentheses are the percentage of remaining surface, acidity and volume compared with the fresh catalyst.

TOS (min.)	Theor. BM/CAT	Coke (wt.%)	BET surface (m^2/g) (% of originial)	TPD-NH_3 (µmol/g) (% of original)	Pore volume (ml/g) (% of original)
0	0	0.00	307 (100.00 %)	918 (100.00 %)	0.442 (100.00 %)
5	0.4	3.86	260 (84.69 %)	679 (73.97 %)	0.387 (87.56 %)
10	0.8	6.88	237 (77.20 %)	594 (64.71 %)	0.360 (81.45 %)
15	1.3	7.06	223 (72.64 %)	510 (55.56 %)	0.346 (78.28 %)
20	1.7	8.83	199 (64.82 %)	554 (60.35 %)	0.329 (74.43 %)
40	3.3	12.85	160 (52.12 %)	424 (46.19 %)	0.262 (59.28 %)
60	5.0	15.86	138 (44.12 %)	333 (36.27 %)	0.234 (52.94 %)
120	10.0	19.90	109 (35.50 %)	333 (36.27 %)	0.190 (42.99 %)
180	15.0	21.09	92 (29.97 %)	318 (34.64 %)	0.164 (37.10 %)

Addendum A.8: BET surface area, TPD-NH_3 and pore volume in function of time-on-stream of the different catalyst samples collected after fast pyrolysis of pine wood.

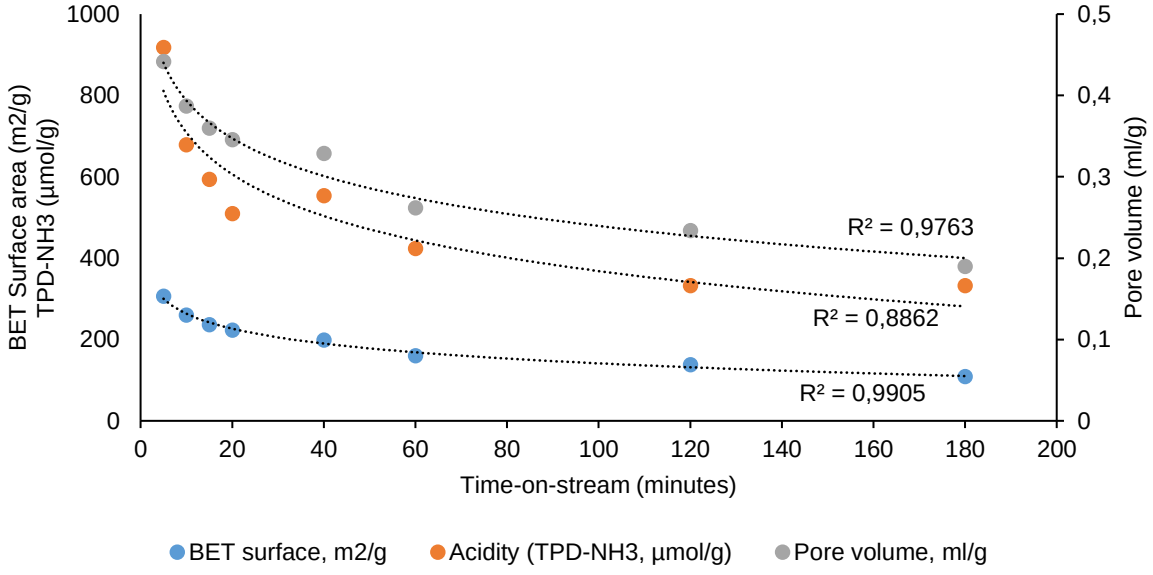

Appendix B: catalytic fast pyrolysis of cellulose in the mini-plant

Addendum B.1: phase distributions of the different bio-oils of the CFP experiments with cellulose in the mini-plant.

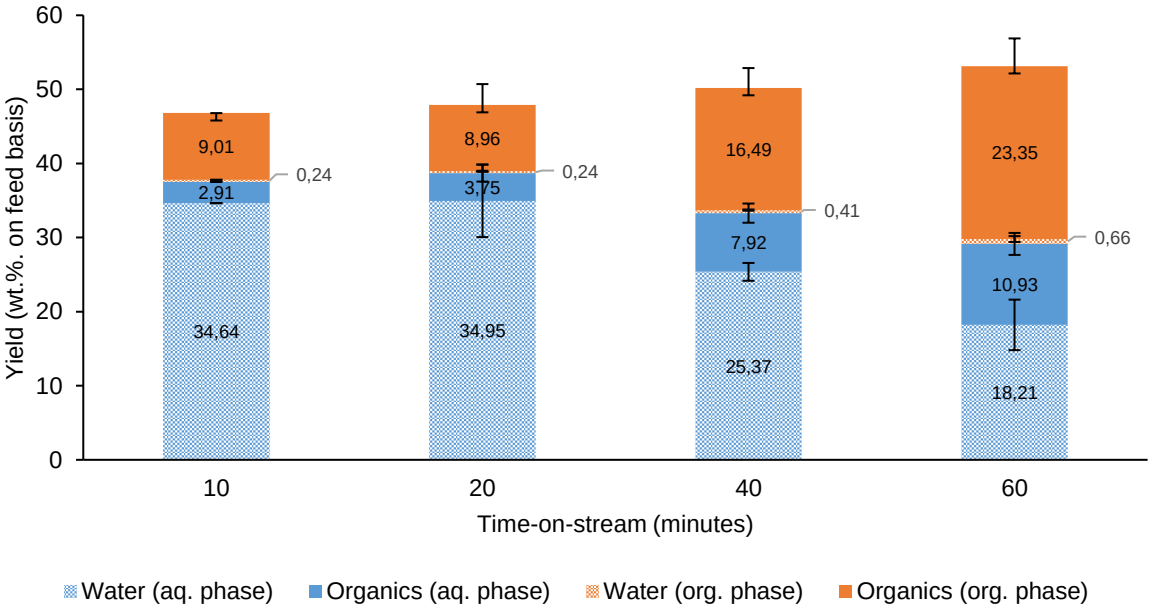

Addendum B.2: average wt.% of each non-condensable gas produced during CFP of cellulose.

	H_2	CH_4	CO	CO_2	C_2H_4	C_2H_6	C_3H_6/C_3H_8	Total
10	0.20	0.62	18.07	10.65	1.64	0.20	1.43	32.42
20	0.17 (± 0.01)	0.54 (± 0.05)	15.28 (± 1.32)	9.61 (± 0.30)	1.33 (± 0.06)	0.08 (± 0.12)	1.20 (± 0.08)	28.22 (± 1.36)
40	0.15 (± 0.01)	0.59 (± 0.02)	14.78 (± 1.14)	8.92 (± 1.08)	1.11 (± 0.01)	0.08 (± 0.12)	1.20 (± 0.08)	26.83 (± 1.58)
60	0.13 (± 0.03)	0.50 (± 0.06)	12.28 (± 1.69)	7.77 (± 1.13)	0.82 (± 0.11)	0.13 (± 0.02)	0.78 (± 0.09)	22.40 (± 2.04)
NC	0.09 (± 0.03)	0.15 (± 0.02)	4.18 (± 0.63)	3.45 (± 1.03)	0.11 (± 0.02)	0.03	0.12 (± 0.02)	8.14 (± 1.21)

Addendum B.3: values of carbon yield and oxygen reduction for the organic phase as well as the complete bio-oil of catalytic cellulose experiments. The values for the organic phase are plotted in figure 27.

BM/CAT	TOS	Organic phase		Complete bio-oil	
(-)	(min.)	η_C	ξ_O	η_C	ξ_O
0.9	10	2.02	99.55	4.91	35.35
1.9	20	2.99	98.06	9.69	41.21
3.7	40	8.30	95.71	14.50	45.86
6.2	60	10.51	94.57	16.18	51.35

Addendum B.4: overview of different chemicals detected in the **organic phase** of the (catalytic) bio-oils of cellulose, expressed as concentration (in wt.%) of organic phase. ***Benzene, substituted***: (x,y,z)-trimethyl-, (x)-ethyl-(y)-methyl-, (x)-ethyl-, 1-methyl-2-cyclopropen-1-yl, 1-methyl-4-(2-propenyl)-, (x)-propenyl-, (x)-methyl-(y)-propenyl-, (x)-ethenyl)-(y)-methyl-, 1-methylpenta-1,3-dienyl-, (x)-propyl- and 1-methylpropyl- ***Phenol, derivatives***: (x)-methyl-, (x,y)-dimethyl- and ethylphenol ***Naphtalene, substituted***: (x)-methyl-, (x,y)-dimethyl-, 1,2-dihydro-, (x)-ethyl-, 2-(1-methylethyl)-, (x,y,z)-trimethyl- and (x)-propylnapthalene ***Indane/indene derivatives***: 1-methylene-1H-, 2,3-dimethyl-1H-,2,3-dihydro-5-methyl-1H-,3-methyl-1H-indene, indene, indane, 2,3-dihydro-1H-inden-1-one…

BM/CAT	**0.9**	**1.9**	**3.7**	**6.2**
TOS (min)	**10**	**20**	**40**	**60**
BENZENES	**17.98** (± 0.46)	**19.19** (± 2.09)	**14.81** (± 2.84)	**13.82** (± 1.41)
Benzene	0.49	0.35 (± 0.17)	0.23 (± 0.22)	0.27 (± 0.14)
Toluene	5.31 (± 0.09)	5.60 (± 1.10)	3.78 (± 2.16)	3.90 (± 0.87)
o-Xylene	2.09 (± 0.03)	2.24 (± 0.50)	1.82 (± 0.55)	1.50 (± 0.22)
m/p-Xylene	6.29 (± 0.17)	7.01 (± 1.55)	5.70 (± 1.69)	5.12 (± 0.75)
Benzene, substituted*	3.80 (± 0.42)	3.99 (± 0.70)	3.28 (± 0.47)	3.03 (± 0.78)
PHENOLS	**1.66** (± 0.03)	**2.55** (± 0.64)	**2.36** (± 0.38)	**1.90** (± 0.21)
Phenol	0.47	0.83 (± 0.28)	0.79 (± 0.17)	0.66 (± 0.10)
Phenol, derivatives*	1.19 (± 0.03)	1.71 (± 0.57)	1.57 (± 0.34)	1.24 (± 0.19)
PAHs	**15.04** (± 0.40)	**14.24** (± 3.29)	**11.43** (± 1.62)	**8.35** (± 1.05)
Naphtalene	3.13 (± 0.15)	2.96 (± 1.02)	2.32 (± 0.43)	1.60 (± 0.14)
Naphtalene, substituted*	8.19 (± 0.28)	8.34 (± 3.04)	6.59 (± 1.52)	4.89 (± 0.79)
Indane/indene derivatives*	3.71 (± 0.24)	2.95 (± 0.74)	2.52 (± 0.35)	1.86 (± 0.68)
LIGHT OXYGENATES	**0.39**	**5.10** (± 1.13)	**6.60** (± 0.95)	**6.21** (± 0.38)
5-Methyl-2-furancarboxaldehyde	0.39	1.83 (± 0.60)	2.51 (± 0.52)	2.30 (± 0.22)
Furfural	0.00	3.07 (± 0.95)	3.82 (± 0.79)	3.65 (± 0.31)
3-Methyl-1,2-cyclopentanedione	0.00	0.21 (± 0.07)	0.27 (± 0.05)	0.26 (± 0.04)
TOTAL WT.% DETERMINED	**35.07** (± 0.61)	**41.08** (± 4.11)	**35.20** (± 3.43)	**30.28** (± 1.81)

Addendum B.5: overview of different chemicals detected in the **aqueous phase** of the (catalytic) bio-oils of **cellulose**, expressed as concentration (in wt.%) of aqueous phase. ***Phenol, alkyl substituted**: (x)-methylphenol ***Other sugars**: D-allose, D-mannose, 1,6-anhydro-α-D-galactofuranose and 1,4:3,6-dianhydro-α-D-glucopyranose

BM/CAT	**0.9**	**1.9**	**3.7**	**6.2**	**NC**
TOS (min)	**10**	**20**	**40**	**60**	**30**
PHENOLS	**0.06**	**0.07**	**0.08**	**0.08**	**0.07** (± 0.01)
Phenol	0.04	0.04	0.04	0.04	0.04 (± 0.01)
Phenol, alkyl substituted*	0.01	0.01	0.02	0.02	0.02
Hydroquinone	0.01	0.02	0.02	0.02	0.01 (± 0.01)
LIGHT OXYGENATES	**0.08**	**0.49** (± 0.02)	**1.04** (± 0.05)	**1.66** (± 0.18)	**2.76** (± 0.33)
5-Methyl-2-furancarboxaldehyde	0.00	0.02	0.04 (± 0.01)	0.05 (± 0.02)	0.06 (± 0.01)
5-Hydroxymethyl-2-furancarboxaldehyde	0.00	0.00 (± 0.01)	0.04	0.11 (± 0.05)	0.16 (± 0.07)
2-Cyclopenten-1-one	0.06	0.20 (± 0.01)	0.31 (± 0.03)	0.35 (± 0.06)	0.19 (± 0.05)
2,3-butadione	0.01	0.03	0.05 (± 0.01)	0.07 (± 0.03)	0.04 (± 0.04)
Glycolaldehyde	0.00	0.09 (± 0.01)	0.24 (± 0.04)	0.38 (± 0.14)	1.35 (± 0.30)
Furfural	0.00	0.00	0.00	0.27 (± 0.05)	0.27 (± 0.07)
Acetic acid	0.01	0.09 (± 0.01)	0.15 (± 0.01)	0.16 (± 0.03)	0.19 (± 0.04)
Hydroxyacetone	0.00	0.04	0.10 (± 0.01)	0.14 (± 0.03)	0.24 (± 0.02)
1,2-Ethanediol, monoacetate	0.00	0.00	0.00	0.01	0.02
Propanoic acid	0.00	0.02	0.05	0.06 (± 0.02)	0.09 (± 0.02)
3-Methyl-1,2-cyclopentanedione	0.00	0.00	0.05 (± 0.01)	0.05 (± 0.02)	0.13 (± 0.06)
1-Hydroxy-2-butanone	0.00	0.00	0.01	0.01 (± 0.01)	0.02 (± 0.01)
ANHYDROSUGARS	**0.28** (± 0.05)	**0.96** (± 0.18)	**3.28** (± 0.34)	**5.53** (± 2.84)	**13.56** (± 4.08)
Levoglucosan	0.25 (± 0.05)	0.81 (± 0.18)	2.77 (± 0.31)	4.79 (± 2.82)	11.53 (± 3.99)
Other sugars*	0.03 (± 0.01)	0.14 (± 0.03)	0.51 (± 0.14)	0.74 (± 0.35)	2.03 (± 0.87)
TOTAL WT.% DETERMINED	**0.42** (± 0.05)	**1.52** (± 0.18)	**4.40** (± 0.34)	**7.27** (± 2.85)	**16.39** (± 4.09)

Addendum B.6: elemental analysis of the coked catalyst samples of the catalytic cellulose experiments.

	TOS (min)	Average (± stdev.) C	H		TOS (min)	Average (± stdev.) C	H
0.9	10	3.10 (± 0.23)	0.67 (± 0.03)	**3.7**	40	9.79 (± 0.80)	0.68 (± 0.02)
		4.46 (± 0.21)	0.67 (± 0.02)			9.62 (± 0.60)	0.68 (± 0.02)
1.9	20	7.18 (± 0.32)	0.67 (± 0.02)	**6.2**	60	13.24 (± 0.35)	0.75 (± 0.02)
		5.94 (± 0.94)	0.62 (± 0.05)			12.90 (± 1.52)	0.70 (± 0.02)

Appendix C: PY-GC/MS of catalytic SCT and SCB

Addendum C.1: overview of the 30 most abundant compounds for each experimental set-up. +++: absolute peak area was higher than 10^{10}, ++: absolute peak area was higher than 10^{9} and +: absolute peak area was higher than 10^{8}. The higher the retention time (RT), the more the compounds shift over that retention time.

		SCT				SCB			
		non-cat.		cat.		non-cat.		cat.	
	RT	untr.	CA tr.	untr.	CA tr.	untr.	CA tr.	untr.	CA tr.
CO_2	4.0	++	++	++	++	++	++	++	++
LIGHT OXYGENATES									
1,3-dioxolane-4,5-dione	4.1	+	++			++	++		
acetaldehyde	4.4	+	+	+	+	+	+	+	+
methanol	4.6	+	+	+	+	+	+		+
1-methylcyclopropanemethanol	5.3			+				+	
acetone	5.4			+	+			+	+
2,3-butanedione	7.2	+	+			+			
hydroxyacetaldehyde	8.4	++	++			++	++	+	
acetic acid	9.5	++	++	+	+	++	++	++	++
1-hydroxy-2-propanone	10.8	++	+	+		++	+		
2-oxo-3-cyclopentene-1-acetaldehyde	16.3			+					
acetyloxyacetic acid	18.0					++			
2-hydroxy-2-cyclopenten-1-one	19.9	+	+			+	+		
3-methyl-1,2-cyclopentanedione/ 2-hydroxy-3-methyl-2-cyclopenten-1-one	23.1	+	+			+	+		
cyclopropyl carbinol	27.8	+	+			+			
D-(+)-ribonic acid-γ-lactone	31.0	+					++		
3-heptanol	34.2		+				+		
2,3,4,5-tetrahydroxypentanal	34.8		++						
4-hydroxybenzaldehyde	37.9					+			
1,4-dioxaspiro[2,4]heptan-5-one	43.1					+			
FURANS									
furan	5.0			+	+			+	+
2-methylfuran	6.4			+	+			+	+
furfural	16.3	+	+		+	+	+	+	+
2-furanmethanol	17.7	+							
2(5H)-furanone	21.9	+	+		+	+	+		+
2,5-dimethyl-4-hydroxy-3(2H)-furanone	24.6		+						
2,3-dihydrobenzofuran	31.3	++	++	+	+	++	++		+
5-hydroxymethyl-2-furancarboxaldehyde	32.4		+			+	+	+	

PHENOLS									
phenol	24.0	+		+	+				+
2-methoxyphenol	24.6	+				+	+		
2-methoxy-4-vinylphenol	31.4	+	++		+	++		+	
(Z)-2-methoxy-4-(1-propenyl)-furancarboxaldehyde	32.4					+			
2,6-dimethoxyphenol	32.8	+				+	+		
2,6-dimethoxy-4-(2-propenyl)phenol	41.2					+	+		
4-((1E)-3-hydroxy-1-propenyl)-2-methoxyphenol	43.7					+			
ANHYDROSUGARS									
2,3-anhydro-d-galactosan	30.3						+		
1,3-di-O-acetyl-α-D-ribopyranose	33.1		+				++		+
methyl-α-D-ribofuranoside	34.7	+	++		+	+	+		+
1,6-anhydro-α-D-glucopyranose	40.6	+	+++		+	++	+++	+	++
1,6-anhydro-α-D-galactofuranose	43.1		+				+		
AROMATICS									
benzene	7.8			+	+			+	+
toluene	11.0			++	++			++	++
ethylbenzene	14.2			+	+			+	+
m/p-xylene	14.5			++	++			++	++
o-xylene	15.5			+	+			+	+
1-ethyl-4-methylbenzene	17.6			+	+			+	+
1,2,3-trimethylbenzene	18.8			+				+	
1-ethenyl-2-methylbenzene/indane/ 2-propenylbenzene	20.5			+	+			+	+
indene	21.4			+	+			+	+
2,3-dihydro-4-methyl-1H-indene	23.7			+					
1,2-methanoindan	24.6			+	+			+	+
1,4-dihydronaphthalene	25.0			+					
naphthalene/azulene	26.4			+	+			+	++
1/2-methylnaphtalene	29.5			+	+			+	+
benzocycloheptatriene	30.0				+				+
1,7-dimethylnaphthalene	32.4							+	
2,6-dimethylnaphthalene	32.4			+	+			+	+
1,2,4-trimethoxybenzene	35.1						+		
OTHERS									
cyclopropane	4.1			++					
2-butene	4.2			++	+			+	+
chloromethane	4.2	+							
hydrogen azide/ acetic anhydride	5.6	+	++		+	++	+	+	+
acetonitrile	6.1			+	+				+
propanoic acid, anhydride	7.6	+				+			
1,2-ethanediol, monoacetate/ acetic acid, methyl ester	14.3	+	+				+	+	
(S)-methyloxirane/1-nitro-2-propanone/ acetohydroxamic acid	15.8	++	+	+		++	+	+	
1,2-ethanediol, diacetate	18.0	+							
1-methylcyclopropylurea	20.3	+							
2-methyliminoperhydro-1,3-oxazine	22.4	+	++			+	++		
N-(aminocarbonyl)-2-propenamide	20.9		+				+		
2-methylbutyloxirane/ 5-(2-propopynyloxy)-2-pentanol	30.0		+				+		

Addendum C.2: GC/MS responses (average ± standard deviation) per mg biomass of four different SCT samples.

	untr. SCT - non-cat.	CA SCT - non-cat.	untr. SCT - cat.	CA SCT - cat.
CO_2	1.24 (± 0.50)	1.31 (± 0.12)	1.40 (± 0.02)	1.91 (± 0.26)
Light oxygenates	3.43 (± 1.15)	4.11 (± 0.18)	1.10 (± 0.09)	1.27 (± 0.31)
Furans	0.94 (± 0.07)	1.16 (± 0.10)	0.31 (± 0.03)	0.71 (± 0.14)
Phenols	1.27 (± 0.98)	0.69 (± 0.10)	0.12 (± 0.02)	0.20 (± 0.06)
Anhydrosugars	0.53 (± 0.20)	4.37 (± 0.22)	0.01 (± 0.00)	0.58 (± 0.68)
Aromatics	0.13 (± 0.07)	0.07 (± 0.02)	3.49 (± 0.09)	3.25 (± 0.68)
Others	1.82 (± 0.18)	2.02 (± 0.19)	1.46 (± 0.08)	0.90 (± 0.44)
Total	9.36 (± 1.62)	13.73 (± 0.39)	7.89 (± 0.16)	8.82 (± 1.14)

Addendum C.3: GC/MS responses (average ± standard deviation) per mg biomass of four different SCB samples.

	untr. SCB - non-cat.	CA SCB - non-cat.	untr. SCB - cat.	CA SCB - cat.
CO_2	1.62 (± 0.07)	1.34 (± 0.15)	1.98 (± 0.31)	1.92 (± 0.22)
Light oxygenates	5.72 (± 0.41)	2.86 (± 0.35)	1.15 (± 0.60)	1.30 (± 0.33)
Furans	1.66 (± 0.08)	1.51 (± 0.11)	0.51 (± 0.25)	0.79 (± 0.26)
Phenols	1.18 (± 0.08)	0.59 (± 0.11)	0.18 (± 0.12)	0.17 (± 0.01)
Anhydrosugars	1.05 (± 0.13)	8.06 (± 1.15)	0.10 (± 0.09)	1.00 (± 0.42)
Aromatics	0.06 (± 0.01)	0.08 (± 0.01)	3.07 (± 0.73)	3.11 (± 0.26)
Others	2.37 (± 0.14)	1.69 (± 0.33)	0.60 (± 0.26)	0.60 (± 0.12)
Total	13.66 (± 0.47)	16.13 (± 1.27)	7.59 (± 1.07)	8.89 (± 0.70)